A Time Domain Damage Identification Technique for Building Structures under Arbitrary Excitation

Dissertation Advisor :   Prof. Mita, Akira

Keio University
Graduate School of Science and Technology
School of Science for Open and Environmental Systems
March 2008

Qian, Yuyin

ABSTRACT

Structural Health Monitoring (SHM), a field inaugurated in aerospace engineering in the late 20th century through mechanical engineering towards civil engineering communities. As the process of implementing a damage detection strategy, SHM has received increasingly attention and interest in the civil engineering with prominent technology development and promising economic attraction. Even as research on SHM chugs along, challenges remain before they can be applied to civil engineering structures.

This dissertation includes damage identification of structures using pattern classification and direct identification of structural parameters from dynamic responses, though the latter would be stressed.

In the case of structural identification, damage is usually described as the decrease in structural parameters such as the stiffness of structural members. Effective pattern classification or interpretation of the changes in structural response or dynamic properties due to damage is a critical task.

The fundamental idea of the pattern classification approach is to use training data to determine the classifier referred to as training the classifier and according to the classifier to evaluate the category of the test data. However, a very large database is required to store training data for as many damage cases as one may wish to consider. In general, damage cases of single-damage and multiple-damage with different and/or the same damage extents should be considered.

This research presents a possible solution for damage identification of structures using pattern classification methods. The damage identification process is divided into two steps. The damage location is identified in the first step using Parzen-window approach, while the corresponding damage degree is estimated in the second step using feed-forward back-propagation neural network.

In order to implement the theory in practical applications, a series of vibration experiments for

a 5-story shear frame structure were performed to verify the performance of the approach. The results show that for shear buildings, damage degree and extent can be determined through measuring the frequency change.

The backbone of this dissertation is the direct identification of structural parameters from dynamic responses. An evaluation approach for building structures under earthquakes is proposed to provide damage alarm and detailed damage information. It is a time-domain evaluation procedure capable of alarming, localizing and quantifying damage using limited acceleration measurements. The technique is a combination of the damage detection based on acceleration-based emulator neural network (AENN) and the system identification using the particle swarm optimization (PSO).

To implement the concept, a two-phase approach is proposed.

In the first phase, the AENN used for emulating the structural response is tuned to properly model the hysteretic nature of building response. To facilitate the most realistic monitoring system using accelerometers, the acceleration streams at the same location but at different time steps are utilized. The prediction accuracy can be raised by the increment of number of acceleration streams at different time steps. Damage occurrence alarm can be obtained practically and economically only using readily available acceleration time histories in this phase.

After knowing the damage occurrence, the next phase is necessary to be performed to determine the damage location and quantity. Most currently available damage localization approaches are mostly based on pattern recognition methods to classify the different damage location. However, such approaches need analytical data for all damage case situations, which can be computationally expensive and even impossible. Therefore, the system identification is utilized for damage determination. In this paper the system identification problem is formulated as an optimization problem using the PSO.

A series of experiments was conducted using two experimental structures. A five-story structure was initially healthy with all original columns intact. Two columns of one floor were then replaced by weak columns (of the same material and integrity with healthy columns, but with

smaller cross-sectional area) to simulate single-damage case. The double-damage case was simulated by replacing the columns of two different floors. Under the basement of the structure, there were some bearings so that the structure could have a ground motion. Another steel structure on shake-table was utilized to verify the proposed method. It was also a five-story frame structure, with height 5m and floor plate 3m x 2m. The damages were introduced by re moving the splices at different location, loosing the bolts and damaging the beams. The verification of the proposed approach is provided as well by application to a real building.

ACKNOWLEDGEMENTS

Many thanks to Professor Akira Mita, my advisor, for his constant encouragement and guidance. Without his consistent illuminating instruction and broad-ranging professional view, this dissertation could not have reached its present form. The positive attitude to face problems and dauntless courage to overcome difficulties, enlightened by his persistent determination and true benevolence, are most valuable treasures in the research work and in my life. Thanks, sensei, more than I can say.

Many thanks to Professor Songtao Xue at Tongji University, who led me into this field of structural health monitoring, for his great kindness, high responsibility and continual support in the past seven years.

Many thanks to the students at Mita Laboratory and friends at Keio University who gave me countless warm help and friendship.

Many thanks to the international course of Keio University for the financial support through MONBUKAGAKUSHO scholarship during the four and a half years on pursuing my master and doctor degrees.

And finally never enough thanks to my beloved family for their loving considerations and great confidence all through these years.

CONTENTS

I

Figures

Tables

CHAPTER 1

Introduction

1.1 Perspective

This research falls into the family of Structural Health Monitoring (SHM), a field inaugurated in aerospace engineering in the late 20th century through mechanical engineering towards civil engineering communities. As the process of implementing a damage detection strategy, SHM has received increasingly attention and interest in the civil engineering with prominent technological development and promising economic attraction. A new area has been taking shape before our eyes in the few decades beyond academia to industry.

SHM passes damage information masked by outward appearance on to human's cognition with a deep pool of mixed knowledge: economic analysis, statistical theory, intelligent optimization, etc. for operational evaluation; excitation methods, MEMS technology, material science and technology, data transmission, etc. for data acquisition and signal processing; structural mechanics, control theories, system identification, etc. for feature extraction; and information condensation, pattern classification, intelligence diagnosis, statistical learning theories, etc. for statistical discrimination of features for damage detection.

A great deal of energy and production are devoted to sensor network progress constructively and pragmatically because sensor is a vital driveshaft of the SHM system, transmitting the state of structural health into storable and operable signal. Along with the sensor/sensor network technology development rising to stratospheric levels, damage identification algorithm attracts

plenty of efforts, turning abstract signal into substantial damage information.

SHM system handles much more active terms about its strategy summing up all components to ultimately reduce life cycle cost.

1.2 Damage in civil engineering structures

Compared with the damage in the aerospace and mechanics engineering, the damage in civil engineering structures occurs in more ambiguous and intractable ways.

In the most general terms, damage can be defined as changes introduced into a system that adversely affects its performance (Farrar et al. 1995). As for civil engineering structures, changes in materials, connections, boundary conditions, etc., which result in deteriorated performance of the structure, can be defined as damage. It can be caused in various ways. Corrosion, aging, and daily activities cause damage to buildings. Bridges can be damaged due to traffic, wind loads and collisions by boats. These loads also torture offshore structures, plus wave loading and corrosion due to seawater. Moreover, there are damage sources emerging not frequently but consequentially catastrophic, like tornados, hurricanes, and earthquakes, which can potentially cause terrible damage in civil engineering structures.

The importance of SHM has been especially underlined and exposed to the public by many recent occurrences of structural failure. In July 2007 alone, Japan was struck by a major earthquake in the Niigata region that destroyed wooden structures and caused fire in a nuclear power plant, New York suffered from the explosion of an 83-year-old steam pipe, and Americans were horrified to see a bridge filled with commuter traffic collapse across the Mississippi River.

Detecting the damage in civil engineering structures faces an interlocking set of existential questions from which all its once and future challenges flow: Is there damage in the structure? Where is the damage in the structure? What kind of damage is present? How severe is the damage? How much useful life remains?

1.3 Challenge

Even as SHM chugs along, challenges remain before they can be applied to civil engineering structures. Most currently available damage detection methods are global in nature, i.e., the dynamic properties (natural frequencies and mode shapes) are obtained for the entire structure from the input–output data using global structural analyses e.g., (Doebling, et al. 1996). However, natural frequencies and mode shapes are not sensitive to minor damage and local damage.

The techniques using time-domain dynamic responses are appealing and promising. Furthermore, the dynamic responses of structures under environmental excitation or small-scale earthquakes are very economical information for structural identification and health monitoring, especially in the place where small-scale earthquakes occur frequently. Some information about structural parameters and dynamic properties can be identified by the direct use of these time-domain response. Krishnan et al. (2006) proposed a damage detection and localization algorithm based on time series modeling. And there is an approach by using dynamic responses directly in time series without extraction of dynamic properties proposed by Xu et al. (2003), where acceleration, velocity and displacement time histories were used as the input to the emulator neural network. These methods are effective for damage detection determining damage existence; however, there are various problems in damage localization and quantification. Most currently available damage localization approaches are mostly based on pattern recognition methods to classify the different damage location. However, such approaches need analytical data for all damage case situations, which can be computationally expensive and even impossible.

1.4 Contents

This dissertation includes damage identification of structures using pattern classification and direct identification of structural parameters from dynamic responses, though the latter would be stressed.

1.4.1   Damage identification of structures using pattern classification

In general, damage identification for health monitoring involves the comparison of the changes in structural properties or response, and it can be viewed as a pattern classification problem. In the case of structural identification, damage is usually described as the decrease in structural parameters such as the stiffness of structural members. Effective pattern classification or interpretation of the changes in structural response or dynamic properties due to damage is a critical task.

The fundamental idea of the pattern classification approach is to use training data to determine the classifier referred to as training the classifier and according to the classifier to evaluate the category of the test data. However, a very large database is required to store training data for as many damage cases as one may wish to consider. In general, damage cases of single-damage and multiple-damage with different and/or the same damage extents should be considered.

This research presents a possible solution for damage identification of structures using pattern classification methods (Qian et al. 2007). The damage identification process is divided into two steps. The damage location is identified in the first step using Parzen-window approach, while the corresponding damage degree is estimated in the second step using feed-forward back-propagation neural network.

A series of numerical simulations are performed to verify the performance of our proposed approach. The measured structural vibration response data always contain noise. The output inevitably has some errors when the data with noise is input into the classifiers network. The approach was thus enhanced to have stability against such noise by considering variations in signals. The results of numerical simulations show that by the approach the structural damage can be identified and identification accuracy can be improved by randomness injected. An appropriate range of random ratio is proposed corresponding to modal parameters with various noise ratios.

In order to implement the theory in practical applications, a series of vibration experiments for 5-story shear frame structure were performed to verify the performance of the approach. The results show that for shear buildings, damage degree and extent can be determined through

measuring the frequency change.

1.4.2   Direct identification of structural parameters from dynamic responses

The backbone of this dissertation is the direct identification of structural parameters from dynamic responses. An evaluation approach for building structures under earthquakes is proposed to provide damage alarm and detailed damage information. It is a time-domain evaluation procedure capable of alarming, localizing and quantifying damage using limited acceleration measurements. The technique is a combination of the damage detection based on acceleration-based emulator neural network (AENN) and the system identification using the particle swarm optimization (PSO).

To implement the concept, a two-phase approach is used.

In the first phase, the AENN used for emulating the structural response is tuned to properly model the hysteretic nature of building response. To facilitate the most realistic monitoring system using accelerometers, the acceleration streams at the same location but at different time steps are utilized. The prediction accuracy can be raised by the increment of number of acceleration streams at different time steps. Damage occurrence alarm can be obtained practically and economically only using readily available acceleration time histories in this phase.

After knowing the damage occurrence, the next phase is necessary to be performed to determine the damage location and quantity. Most currently available damage localization approaches are mostly based on pattern recognition methods to classify the different damage location. However, such approaches need analytical data for all damage case situations, which can be computationally expensive and even impossible. Therefore, the system identification scheme is utilized for damage determination. In this paper the system identification problem is formulated as an optimization problem in terms of the PSO.

The proposed approach is briefly described in Fig. 1.1.
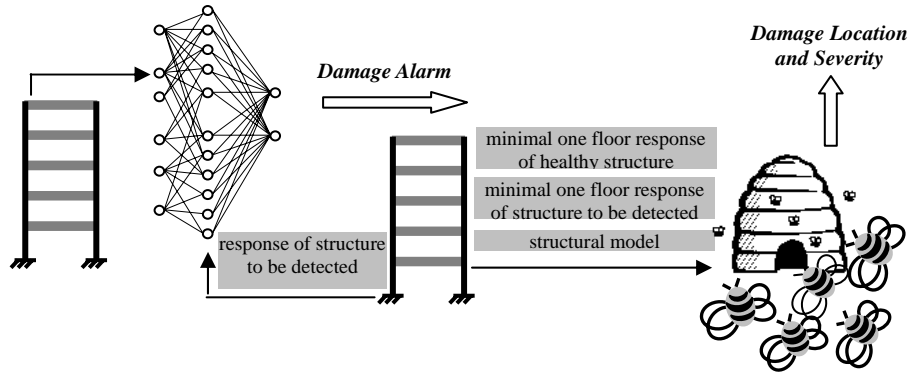
Figure 1.1 Two-phase damage evaluation approach

1.4.3   Overview of dissertation

Chapter 1 exhibits the big picture of field of SHM and research of this dissertation.

Chapter 2 reviews previous research on statistical discrimination of features for damage detection and time series-based damage identification techniques.

Chapter 3 presents acceleration-based damage occurrence alarm for building structures using AENN. The progress improving AENN using displacement, velocity and acceleration as inputs to AENN using acceleration alone is explained in detail. The approach is further modified by using the acceleration at later time steps as the output of the neural network to obtain the better damage occurrence index, followed by searching for necessary number of acceleration stream and appropriate time delay of ground acceleration. Discussion on multi-input AENN is considered with the goal of higher flexibility with the approach.

Chapter 4 presents acceleration-based damage localization and quantification of structures. The identification problem is understood as an optimization problem in which the error between the actual physical measured response of a structure and the simulated response of a numerical model is viewed as objective fit function to be minimized. The PSO is introduced to perform optimization where the result is compared with the ones from Genetic Analysis (GA) and

Simulated Annealing (SA). Both cases for full output information and partial output information are considered in this chapter.

Chapter 5 presents experimental verifications. A five-story structure was initially healthy with all original columns intact. Two columns of one floor were then replaced by weak columns (of the same material and integrity with healthy columns, but with smaller cross-sectional area) to simulate single-damage case. The double-damage case was simulated by replacing the columns of two different floors. Under the basement of the structure, there were some bearings so that the structure could have a ground motion. Another steel structure on shake-table was used to verify the proposed method. It was also a five-story frame structure, with height 5m and floor plate 3m x 2m. The damages were introduced by re-moving the splices at different location, loosing the bolts and damaging the beams. The verification of the proposed approach is provided as well by application to a real building.

Finally, Chapter 6 summarizes in this dissertation and its contribution, and presents possible directions for future research.

$$CHAPTER\ 2$$

Review of Existing Methods

This chapter provides a review of a typical damage localization and quantification approach using pattern classification methods. In addition, a brief review of some of the existing direct identification of structural parameters from dynamic responses is presented.

2.1 Statistical discrimination of features for damage detection

In general, structural identification for health monitoring involves the comparison of the changes in structural properties or response, and it can be viewed as a pattern classification problem. In the case of structural identification, damage is usually described as the decrease in structural parameters such as the stiffness of structural members. Effective pattern classification or interpretation of the changes in structural response or dynamic properties due to damage is a critical task. The fundamental idea of the pattern classification approach is to use training data obtained from simulation calculation to determine the classifier referred to as training the classifier and according to the classifier to evaluate the category of the test data. However, a very large database is required to store training data for as many damage cases as one may wish to consider. In general, damage cases of single-damage and multiple-damage with different and/or the same damage extents should be considered.

A possible solution for this problem dividing the damage identification process into two steps is presented. The damage location is identified in the first step using non-parametric probability

function estimation, in particular, using Parzen-window approach, while the corresponding damage degree is estimated in the second step using feed-forward back-propagation neural network. The output inevitably has some errors when the data with noise is inputted into the classifiers network. The approach was thus enhanced to have stability against such noise by considering variations in signals. A series of numerical simulations are performed to verify the performance of our proposed approach

2.1.1 Damage Location Identification Using Parzen-Windows Approach

Parzen-windows approach belongs to nonparametric techniques (Duda et al. 2001). Nonparametric procedures can be used with arbitrary distributions and without the assumption that the forms of the underlying densities are known. Because of this property, nonparametric techniques are selected to identify the damage location.

The most fundamental techniques of estimating an unknown probability density function rely on the fact that the probability P that a vector $\mathbf{x}$ will fall in a region $\Re$ is given by

$$P = \int_{\Re} p(\mathbf{x}') d\mathbf{x}' \tag{2-1}$$

Thus P is a smoothed or averaged version of the density function $p(\mathbf{x})$, and we can estimate this smoothed value of p by estimating the probability P. Suppose that n samples $\mathbf{x}_1, \ldots, \mathbf{x}_n$ are drawn independently and identically distributed (i.i.d.) according to the probability law $p(\mathbf{x})$. Clearly, the probability that k of these n fall in $\Re$ is given by the binomial law

$$P_k = \binom{n}{k} P^k (1-P)^{n-k} \tag{2-2}$$

and the expected value for k is

$$\varepsilon[k] = nP \tag{2-3}$$

Moreover, this binomial distribution for k peaks very sharply about the mean, so that we expect that the ratio k/n will be a very good estimate for the probability P, and hence for the smoothed density function. This estimate is especially accurate when n is very large. If we now assume that $p(\mathbf{x})$ is continuous and that the region $\Re$ is so small that p does not vary appreciably within it, we can write

$$\int_{\Re} p(\mathbf{x}')d\mathbf{x}' \cong p(\mathbf{x})V \tag{2-4}$$

where $\mathbf{x}$ is a point within $\Re$ and V is the volume enclosed by $\Re$. Combining Eqs. (2-1), (2-3), and (2-4), we arrive at the following obvious estimate for $p(\mathbf{x})$,

$$p(\mathbf{x}) \cong \frac{k/n}{V} \tag{2-5}$$

There are several problems that remain---some practical and some theoretical. If we fix the volume V and take more and more training samples, the ratios k/n will converge (in probability) as desired, but then we have only obtained an estimate of the space-average value of $p(\mathbf{x})$,

$$\frac{P}{V} = \frac{\displaystyle\int_{\Re} p(\mathbf{x}')d\mathbf{x}'}{\displaystyle\int_{\Re} d\mathbf{x}'} \tag{2-6}$$

If we want to obtain $p(\mathbf{x})$ rather than just an average version of it, we must be prepared to let V approach zero. However, if we fix the number n of samples and let V approach zero, the region will eventually become so small that it will enclose no samples, and our estimate $p(\mathbf{x}) = 0$ will be useless. On the other hand, if by chance one or more of the training samples coincide at $\mathbf{x}$, the estimate diverges to infinity, which is equally useless.

From a practical standpoint, we note that the number of samples is always limited. Thus, the volume V cannot be allowed to become arbitrarily small. If this kind of estimate is to be used, one will have to accept a certain amount of variance in the ratio k/n and a certain amount of averaging of the density $p(\mathbf{x})$.

From a theoretical standpoint, it is interesting to ask how these limitations can be circumvented if an unlimited number of samples is available. Suppose we use the following procedure. To estimate the density at $\mathbf{x}$, we form a sequence of regions $\Re_1, \Re_2, \ldots$, containing $\mathbf{x}$ ---the first region to be used with one sample, the second with two, and so on. Let V_n be the volume of $\Re_n$, k_n be the number of samples falling in $\Re_n$, and $p_n(\mathbf{x})$ be the n th estimate for $p(\mathbf{x})$:

$$p_n(\mathbf{x}) = \frac{k_n/n}{V_n} \tag{2-7}$$

If $p_n(\mathbf{x})$ is to converge to $p(\mathbf{x})$, three conditions appear to be required:

$$\lim_{n \to \infty} V_n = 0$$
$$\lim_{n \to \infty} k_n = \infty$$
$$\lim_{n \to \infty} k_n/n = 0$$

The first condition assures us that the space averaged P/V will converge to $p(\mathbf{x})$, provided that the regions shrink uniformly and that $p(\cdot)$ is continuous at $\mathbf{x}$. The second condition, which only makes sense if $p(\mathbf{x}) \neq 0$, assures us that the frequency ratio will converge (in probability) to the probability P. The third condition is clearly necessary if $p_n(\mathbf{x})$ given by Eq. (2-7) is to converge at all. It also says that although a huge number of samples will eventually fall within the small region $\Re_n$, they will form a negligibly small fraction of the total number of samples.

There are two common ways of obtaining sequences of regions that satisfy these conditions. One is to shrink an initial region by specifying the volume V_n as some function of n, such as $V_n = 1/\sqrt{n}$. It then must be shown that the random variables k_n and k_n/n behave properly or, more to the point, that $p_n(\mathbf{x})$ converges to $p(\mathbf{x})$. This is basically the Parzen-window estimation method. The second method is to specify k_n as some function of n, such as $k_n = \sqrt{n}$. Here the volume V_n is grown until it encloses k_n neighbors of $\mathbf{x}$. This is the k_n-nearest-neighbor estimate method. Both of these methods do in fact converge, although it is difficult to make meaningful statements about their finite-sample behaviour.

The Parzen-window approach (Duda et al. 2001) to estimating densities can be introduced by temporarily assuming that the region $\Re_n$ is a d-dimensional hypercube. If h_n is the length of an edge of that hypercube, then its volume is given by

$$V_n = h_n^d \tag{2-8}$$

We can obtain an analytic expression for k_n, the number of samples falling in the hypercube, by defining the following window function:

$$\varphi(\mathbf{u}) = \begin{cases} 1 & |u_j| \le 1/2 \\ 0 & otherwise \end{cases} \qquad j = 1,\ldots,d \qquad (2\text{-}9)$$

Thus, $\varphi(\mathbf{u})$ defines a unit hypercube centered at the origin. It follows that $\varphi\big((\mathbf{x} - \mathbf{x}_i)/h_n\big)$ is equal to unity if $\mathbf{x}_i$ falls within the hypercube of volume V_n centered at $\mathbf{x}$, and is zero otherwise. The number of samples in this hypercube is therefore given by

$$k_n = \sum_{i=1}^{n} \varphi\left(\frac{\mathbf{x} - \mathbf{x}_i}{h_n} \right) \qquad (2\text{-}10)$$

and when we substitute this into Eq. (2-7) we obtain the estimate

$$p_n(\mathbf{x}) = \frac{1}{n} \sum_{i=1}^{n} \frac{1}{V_n} \varphi\left(\frac{\mathbf{x} - \mathbf{x}_i}{h_n} \right) \qquad (2\text{-}11)$$

This equation suggests a more general approach to estimating density functions. Rather than limiting ourselves to the hyper cube window function of Eq. (2-9), suppose we allow a more general class of window functions. In such a case, Eq. (2-11) expresses our estimate for $p(\mathbf{x})$ as an average of functions of $\mathbf{x}$ and the samples $\mathbf{x}_i$. In essence, the window function is being used for interpolation---each sample contributing to the estimate in accordance with its distance from $\mathbf{x}$ shown in Figure 2.1.
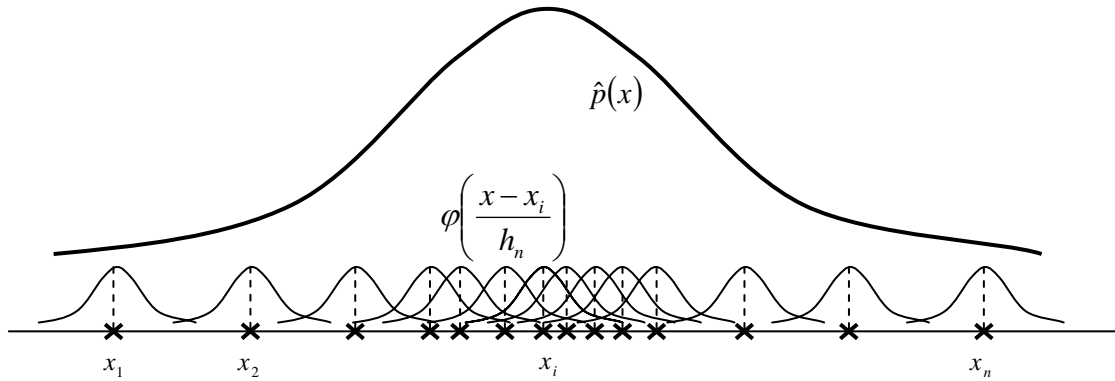
Figure 2.1. Each Sample Contributing to the Estimate

It is natural to ask that the estimate $p_n(\mathbf{x})$ be a legitimate density function, that is, that it be nonnegative and integrative to one. This can be assured by requiring the window function itself be a density function. To be more precise, if we require that

$$\varphi(\mathbf{x}) \geq 0 \tag{2-12}$$

and

$$\int \varphi(\mathbf{u})d\mathbf{u} = 1 \tag{2-13}$$

and if we maintain the relation $V_n = h_n^d$, then it follows at once that $p_n(\mathbf{x})$ also satisfies these conditions.

Most pattern recognition methods can be implemented in a parallel fashion that trades space complexity (amount of memory) for time complexity (cost of calculation time). These implementations are naturally represented as artificial neural networks. The Parzen-window

method can be implemented as a neural network known as a Probabilistic Neural Network (PNN) (Duda et al. 2001).
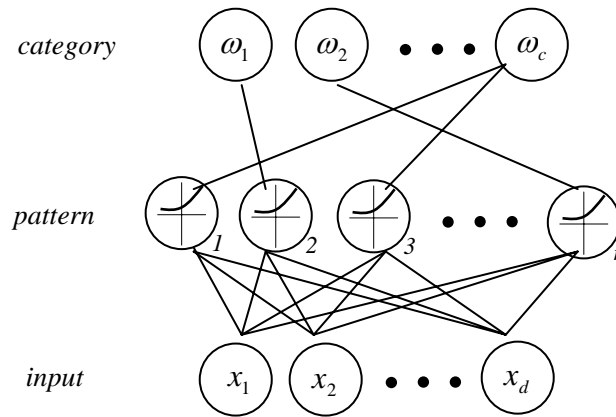
Figure 2.2. Probabilistic Neural Network

Suppose we wish to form a Parzen estimate based on n patterns, each of which is d-dimensional, randomly sampled from c classes. The PNN for this case consists of d dimensional input units comprising the input layer, where each unit is connected to each of the n pattern units; each pattern unit is, in turn, connected to one and only one of the c category units. The connections from the input to pattern units represent modifiable weights, which will be trained. Each category unit computes the sum of the pattern units connected to it.

The PNN is trained in the following way. First, each pattern $\mathbf{x}$ of the training set is normalized to have unit length---that is, is scaled so that $\sum_{i=1}^{d} x_i^2 = 1$. Training step 1, the first normalized training pattern is placed on the input units, step 2, the modifiable weights linking the input units and the first pattern unit are set such that $\mathbf{w}_1 = \mathbf{x}_1$. (Note that because of the normalization of $\mathbf{x}_1$, $\mathbf{w}_1$ is normalized too.) Then, step 3, a single connection from the first pattern unit is made to the category unit corresponding to the known class of that pattern. Step 4,

the process is repeated with each of the remaining training patterns, setting the weights to the successive pattern units such that $\mathbf{w}_k = \mathbf{x}_k$ for $k = 1, 2, \ldots, n$. After such training we have a network that is fully connected between input and pattern units, and sparsely connected from pattern to category units.

The trained network is then used for classification in the following way. A normalized test pattern $\mathbf{x}$ is placed at the input units. Each pattern unit computes the inner product to yield the net activation or simply net,

$$net_k = \mathbf{w}_k^t \mathbf{x} \tag{2-14}$$

and emits a nonlinear function of net_k; each output unit sums the contributions from all pattern units connected to it. The nonlinear function is $e^{(net_k-1)/\sigma^2}$, where σ is a parameter set by the user and determines the width of the effective Gaussian window. This activation function or transfer function, here must be an exponential to implement the Parzen windows algorithm. To see this, consider an (unnormalized) Gaussian window centered on the position of one of the training pattern $\mathbf{w}_k$. We work backwards from the desired Gaussian window function to infer the nonlinear activation function that should be employed by the pattern units. That is, if we let our effective width h_n be a constant, the window function is

$$
\begin{aligned}
\varphi\left(\frac{\mathbf{x} - \mathbf{w}_k}{h_n}\right) &\propto \overbrace{e^{-(\mathbf{x}-\mathbf{w}_k)^t(\mathbf{x}-\mathbf{w}_k)/2\sigma^2}}^{\text{desired Gaussian}} \\
&= e^{-(\mathbf{x}^t\mathbf{x}+\mathbf{w}_k^t\mathbf{w}_k-2\mathbf{x}^t\mathbf{w}_k)/2\sigma^2} = \underbrace{e^{(net_k-1)/\sigma^2}}_{\substack{\text{activation} \\ \text{function}}}
\end{aligned}
\tag{2-15}
$$

where we have used our normalization conditions $\mathbf{x}^t\mathbf{x} = \mathbf{w}_k^t\mathbf{w}_k = 1$. Thus each pattern unit contributes to its associated category unit a signal equal to the probability the test point was

generated by a Gaussian centered on the associated training point. The sum of these local estimates (computed at the corresponding category unit) gives the discriminant function $g_i(\mathbf{x})$ ---the Parzen-window estimate of the underlying distribution. The $\max_i g_i(\mathbf{x})$ $i = 1, 2, \cdots, c$ operation gives the desired category for the test point.

One of the benefits of PNNs is their speed of learning, because the learning rule (i.e., setting $\mathbf{w}_k = \mathbf{x}_k$) is simple and requires only a single pass through the training data. Another benefit is that new training patterns can be incorporated into a previously trained classifier quite easily; this might be important for a particular on-line application.

Using k_n-Nearest-Neighbor Estimation, we could obtain a family of estimates by taking $k_n = k_1 \sqrt{n}$ and choosing different values for k_1. However, in the absence of any additional information, one choice is as good as another, and we can be confident only that the results will be correct in the infinite data case.

2.1.2 Damage Degree Identification Using Feed-Forward Back-Propagation Neural Network

Neural network learning methods provide a robust approach to approximating real-valued, discrete-valued, and vector-valued target functions for certain types of problems, such as learning to interpret complex real-world sensor data, artificial neural networks are among the most effective learning methods currently known.

The study of artificial neural network (ANNs) has been inspired in part by the observation that biological learning systems are built of very complex webs of interconnected neurons. In rough analogy, artificial neural networks are built out of a densely interconnected set of simple units, where each unit takes a number of real-valued inputs (possibly the outputs of other units) and produces a single real-valued output (which may become the input to many other units).

While ANNs are lossely motivated by biological neural system, there are many complexities to biological neural systems that are not modelled by ANNs, and many features of ANNs we discuss

here are known to be inconsistent with biological systems. For example, we consider here ANNs whose individual units output a single constant value, whereas biological neurons out put a complex time series of spikes.

ANNs learning is well-suited to problems in which the training data correspond to noisy, complex sensor data, such as inputs from cameras and microphones. It is also applicable to problems for which more symbolic representations are often used. The back-propagation algorithm is the most commonly used ANN learning technique. It is appropriate for problems with the following characteristics:

- Instances are represented by many attribute-value pairs. The target function to be learned is defined over instances that can be described by a vector of predefined features. These input attributes may be highly correlated or independent of one another. Input values can be any real values.

- The target function output may be discrete-valued, real-valued, or a vector of several real- or discrete-valued attributes.

- The training examples may contain errors. ANN learning methods are quite robust to noise in the training data.

- Long training times are acceptable. Network training algorithms typically require longer training times than, say, decision tree learning algorithms. Training times can range from a few seconds to many hours, depending on factors such as the number of weights in the network, the number of training examples considered, and the setting of various learning algorithm parameters.

- Fast evaluation of the learning target function may be required. Although ANN learning times are relatively long, evaluating the learning network, in order to apply it to a subsequent instance, is typically very fast.

- The ability of humans to understand the learned target function is not important. The weights learned by neural networks are often difficult for humans to interpret. Learned neural networks are less easily communicated to humans than learned rules.
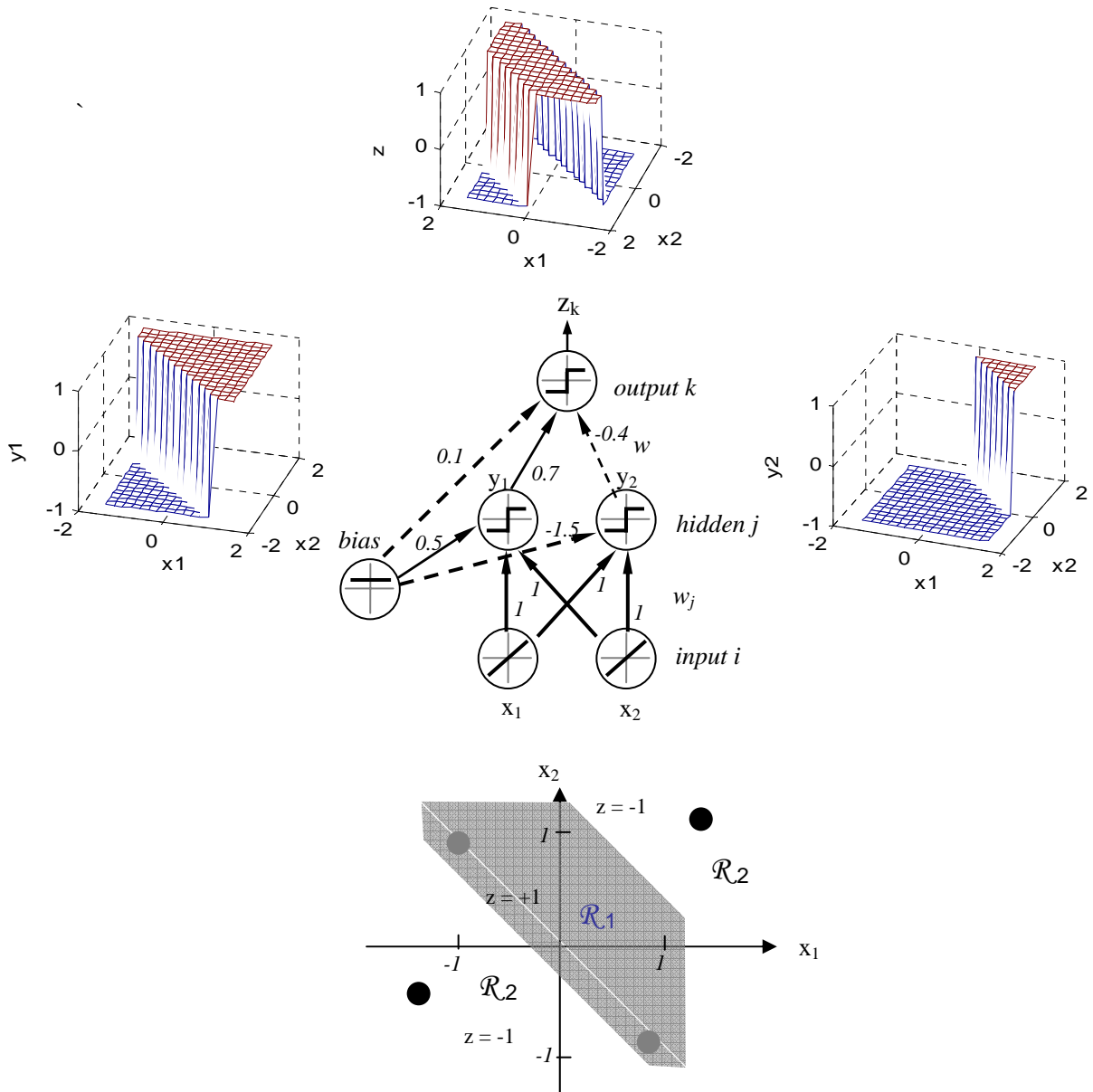
Figure 2.3 Exclusive –OR Problem Solved by a Three-layer Network

Figure 2.3 (Duda et al. 2001) shows a simple three-layer neural network. This one consists of

an input layer, a hidden layer, and an output layer, interconnected by modifiable weights, represented by links between layers. There is, furthermore, a single bias unit that is connected to each unit other than the input units. The function of units is loosely based on properties of biological neurons, and hence they are sometimes called "neurons". We are interested in the use of such networks for pattern recognition, where the input units represent the components of a feature vector and where signals emitted by output units will be the values of the discriminant functions used for classification.

We can clarify our notation and describe the feedforward operation of such a net work on what is perhaps the simplest nonlinear problem: the exclusive-OR (XOR) problem (Figure 2.7); a three-layer network can indeed solve this problem whereas a linear machine operating directly on the features cannot.

Each two-dimensional input vector is presented to the input layer, and the output of each input unit equals the corresponding component in the vector. Each hidden unit computes the weighted sum of its inputs to form its scalar net activation which we denote simple as net. That is, the net activation is the inner product of the inputs with the weights at the hidden unit. For simplicity we augment both the input vector, by appending a feature value $x_0 = 1$, as well as the weight vector, by appending a value w_0, and we can then write

$$net_j = \sum_{i=1}^{d} x_i w_{ji} + w_{j0} = \sum_{i=0}^{d} x_i w_{ji} = \mathbf{w}_j^t \mathbf{x} \tag{2-16}$$

where the subscript i indexes units in the input layer, j in the hidden; w_{ji} denotes the input-to-hidden layer weights at the hidden unit j. In analogy with neurobiology, such weights or connections are sometimes called "synapses" and the values of the connections the "synaptic weights". Each hidden unit emits an output that is a nonlinear function of its activation, $f(net)$, that is,

$$y_j = f\left(net_j\right) \tag{2-17}$$

Figure 2.3 shows a simple threshold or sign function,

$$f\left(net\right) = Sgn\left(net\right) \equiv \begin{cases} 1 & \text{if } net \geq 0 \\ -1 & \text{if } net < 0 \end{cases} \tag{2-18}$$

but as we shall see, other functions have more desirable properties and are hence more commonly used. This $f(\cdot)$ is sometimes called the activation function or merely "nonlinearity" of a unit.

Each output unit similarly computes its net activation based on the hidden unit signals as

$$net_k = \sum_{j=1}^{n_H} y_j w_{kj} + w_{k0} = \sum_{j=0}^{n_H} y_j w_{kj} = \mathbf{w}_k^t \mathbf{y} \tag{2-19}$$

where the subscript k indexes units in the output layer and n_H denotes the number of hidden units. We have mathematically treated the bias unit as equivalent to one of the hidden units whose output is always $y_0 = 1$. In this example, there is only one output unit. However, anticipating a more general case, we shall refer to its output as z_k. An output unit computes the nonlinear function of its net, emitting

$$z_k = f\left(net_k\right) \tag{2-20}$$

where in the figure we assume that this nonlinearity is also a sign function. Clearly, the output z_k can also be thought of as a function of the input feature vector $\mathbf{x}$. When there are c output units,

we can think of the network as computing c discriminant functions $z_k = g_k(\mathbf{x})$, and can classify the input according to which discriminant function is largest. In a two-category case, it is traditional to use a single output unit and label a pattern by the sign of the output z.

It is easy to verify that the three-layer network with the weight values listed indeed solves the XOR problem. The hidden unit computing y_1 and it computes the boundary $x_1 + x_2 + 0.5 = 0$; input vectors for which $x_1 + x_2 + 0.5 \geq 0$ lead to $y_1 = +1$, and all other inputs lead to $y_1 = -1$. Likewise the other hidden unit computes the the boundary $x_1 + x_2 - 1.5 = 0$. The final output unit emits $z_1 = +1$ if and only if and $y_2 = +1$. Using the terminology of computer logic, the units are behaving like gates, where the first hidden unit is an OR gate, the second hidden unit is an AND gate, and the output unit implements

$$
\begin{aligned}
z_k &= y_1 \text{ AND NOT } y_2 = (x_1 \text{ OR } x_2) \text{ AND NOT} (x_1 \text{ AND } x_2) \\
&= y_1 \text{ XOR } y_2
\end{aligned}
\tag{2-21}
$$

giving rise to the appropriate nonlinear decision region shown in the figure—the XOR problem is solved.

From the above example, it should be clear that nonlinear multilayer networks—that is, ones with input units, hidden unit, and output unit—have greater computational or expressive power than similar networks that otherwise lack hidden units. That is, they can implement more functions.

Clearly, we can generalize the above discussion to more inputs, other nonlinearities, and arbitrary number of output units. For classification, we will have c output units, one for each of the categories, and the signal from each output unit is the discriminant function $g_k(\mathbf{x})$. We gather the results from Equations (2-16), (2-17), (2-19) and (2-20), to express such discriminant functions as

$$g_k(\mathbf{x}) \equiv z_k = f\left(\sum_{j=1}^{n_H} w_{kj} f\left(\sum_{i=1}^{d} w_{ji} x_i + w_{j0}\right) + w_{k0}\right)$$

$$k = 1,2,\cdots,c$$

(2-22)

This, then, is the class of functions that can be implemented by a three-layer neural network. In general, the activation function does not have to be a sign function. Indeed, we shall often require the activation functions in the output layer to be continuous and differentiable. We can even allow the activation functions in the output layer to be different from the activation functions in the hidden layer, or indeed have different activation functions for each individual unit.

The Back-Propagation algorithm learns the weights for a multilayer network, given a network with a fixed set of units and interconnections. It employs gradient descent to attempt to minimize the squared error between the network output values and the target values for these outputs.

Because we are considering networks with multiple output units, we need define E to sum the errors over all of the network output units

$$E(\vec{w}) \equiv \frac{1}{2} \sum_{d \in D} \sum_{k \in outputs} (t_{kd} - o_{kd})^2$$

(2-23)

where *outputs* is the set of output units in the network, and t_{kd} and o_{kd} are the target and output values associated with the k th output unit and training example d.

The learning problem faced by Back-Propagation is to search a large hypothesis space defined by all possible weight values for all the units in the network. As in the case of training a single unit, gradient descent can be used to attempt to find a hypothesis to minimize E.

Multilayer network is that the error surface can have multiple local minima. Unfortunately, this means that gradient descent is guaranteed only to converge toward some local minimum, and not necessarily the global minimum error. Despite this obstacle, in practice Back-Propagation has been found to produce excellent results in many real world applications.

The Back-Propagation algorithm is presented in Table 2.1. The algorithm as described here applies to layered feed-forward networks containing two layers of sigmoid units, which units at each layer connected to all units from the preceding layer. This is the incremental, or stochastic, gradient descent version of Back-Propagation. The notation used here is shown below:

An index (e.g., an integer) is assigned to each node in the network, where a "node" is either an input to the network or the output of some unit in the network.

x_{ji} denotes the input from node i to unit j, and w_{ji} denotes the corresponding weight.

δ_n denotes the error term associated with unit n. As we shall see later, $\delta_n = -\dfrac{\partial E}{\partial net_n}$.

Notice the algorithm in Table 2.1. begins by constructing a network with the desired number of hidden and output units and initialized all network weights to small random values. Given this fixed network structure, the main loop of the algorithm then repeatedly iterates over the training examples. For each training example, it applies the network to the example, calculates the error of the network output, computes the gradient with respect to the error on this example, then updates all weights in the network. This gradient descent step is iterated (often thousands of times, using the same training examples multiple times) until the network performs acceptable well.

Table 2.1. The Stochastic Gradient Descent Version of the Back-Propagation Algorithm for

Feed-Forward Networks

Back-Propagation *(training_examples, $\eta, n_{in}, n_{out}, n_{hidden}$)*

Each training example is a pair of the form $\langle \vec{x}, \vec{t} \rangle$, where $\vec{x}$ is the vector of network input

values and $\vec{t}$ is the vector of target network output values.

η is the learning rate (e.g., 0.05). n_{in} is the number of network inputs, n_{hidden} the

number of units in the hidden layer, and n_{out} the number of output units.

The input from unit is denoted x_{ji}, and the weight from unit i to unit j is denoted

---

w_{ji} .

● Create a feed-forward network with n_{in} inputs, n_{hidden} hidden units, and n_{out} output units.

● Initialize all network weights to small random numbers (e.g., between -0.05 and 0.05).

● Until the termination condition is met, Do

    ● For each $\langle \vec{x}, \vec{t} \rangle$ in *training_examples*, Do

        Propagate the input forward throught the network:

        1.   Input the instance $\vec{x}$ to the network an d compute the output o_u od every unit

            u in the network.

        Propagate the errors backward throught the network:

        2.   For each network output unit k , calculate its error term δ_k

$$\delta_k \leftarrow o_k (1 - o_k)(t_k - o_k) \tag{2-24}$$

        3.   For each hidden unit h , calculate its error tern δ_h

$$\delta_h \leftarrow o_h (1 - o_h) \sum_{k \in outputs} w_{kh} \delta_k \tag{2-25}$$

        4.   Update each network weight w_{ji}

$$w_{ji} \leftarrow w_{ji} + \Delta w_{ji}$$

      where

$$\Delta w_{ji} = \eta \delta_j x_{ji} \tag{2-26}$$

The gradient descent weight –update rule (Eq. (2-26)in Table 2.1.) updates each weight in proportion to the learning rate η, the input value x_{ji} to which the weight is applied, and the error in the output of the unit. To understand it intuitively, first consider how δ_k is computed for each network output unit k (Eq. (2-24) in the algorithm). δ_k is multiplied by the fact

$o_k(1-o_k)$, which is the derivative of the sigmoid squashing function. The δ_h value for each

hidden unit h has a similar form (Eq. (2-25) in the algorithm). However, since training examples

provide target values t_k only for network outputs, no target values are directly available to

indicate the error of hidden units' values. Instead, the error term for hidden unit h is calculated

by summing the error terms δ_k for each output influenced by h, weighting each of the δ_k's by

w_{kh}, the weight from hidden unit h to output unit k. This weight characterizes the degree to

which hidden unit h is "responsible for" the error in the output unit k.

The algorithm in Table 2.1 updates weights incrementally, following the presentation of each

training example. This corresponds to a stochastic approximation to gradient descent. To obtain

the true gradient of E one would sum the $\delta_j x_{ji}$ values over all training examples before

altering weight values.

The weight-update loop in Back-Propagation may be iterated thousands of times in a typical

application. A variety of termination conditions can be used to halt the procedure. One may choose

to halt after a fixed number of iterations through the loop, or once the error on the training

examples falls below some threshold, or once the error on a separate validation set of examples

meets some criterion. The choice of termination criterion is an important one.

2.1.3   Experimental Verification

The objective here is to be able to implement the theory in practical applications. The

following deals with a laboratory experiment, imitating the configuration of 5-story shear building,

carried out in order to validate the method developed and results derived. However, the

experiment is a free vibration experiment and excludes damping.

2.1.3.1 **Experimental Setup**

The complete experimental setup is shown in Figure 2.4.

Figure 2.4 Experimental Setup

This experimental setup imitates a 5-story shear frame buildings. The story mass is decided by the aluminium floor slab which is 2.975 kg for the first floor and 3.380 kg for the other four floors. The story stiffness is decided by the bronze plate spring which is $0.0025 \times 0.03 \times 0.24$ m^3. The Young's modulus of bronze is 1×10^{11} N/m^2, so the interfloor stiffness is 1.3563×10^4 N/m.

The damage was introduced by replacing columns by weak columns, which are $0.003 \times 0.006 \times 0.24$ m^3, shown in Figure 2.5.

Figure 2.5 Replace Columns by Weak Columns   Figure 2.6. Impulse Hammer

By replacing two columns for each story, the story stiffness was reduced from 1.3563×10^4 N/m to 9.1254×10^3 N/m and the damage rate was 32.72%.

The impulse loading is imitated by impact of a hammer shown in Figure 2.6. Make sure that the impact of the hammer is quick and sharp.

2.1.3.2 **Procedure**

Acceleration sensors were installed at all stories to obtain six acceleration components. Using PCA, these 6-dimensional data were condensed to 5-dimensional and at the same time we can check whether there was some damage occurred during the measurement period. The modal frequencies were calculated from 5-dimentional time histories of the vibration experiment by applying Eigensystem Realization Algorithm (ERA) (Juang et al. 1985). The health structure

frequency is

$$
\begin{bmatrix}
2.2309 \\
6.9061 \\
10.9297 \\
14.5857 \\
16.4294
\end{bmatrix} \text{Hz.}
$$

This five-order natural frequency of the structure.

Because the training processes would be carried out based on the health structure, it is required high precision of health structure's stiffness matrix. Therefore, the stiffness matrix need to be model updated. Equation arrangement (Zhang er al. 1985) which need to measure frequency and mode shape is applied. However, it is challenging for the mode shape to be measured precisely. So the improved equation arrangement which need frequency only is presented.

$$
\Delta K \Phi_{\mathbf{A}} = M \Phi_A \Lambda_t - K_A \Phi_A = G \tag{2-27}
$$

where, $\Phi_{\mathbf{A}}$ is mass-normalized eigenvector, Λ_t is diagonal matrix of square measured frequencies, and subscripts A, t represent calculated value and measured value respectively. M and K_A are mass and stiffness matrixes. G represents the expression of $M \Phi_A \Lambda_t - K_A \Phi_A$. ΔK is stiffness error.

Equate the both sides of the expression Eq.(2-27), and the equation of ΔK's upper triangular elements ($\Delta k_{ji} = \Delta k_{ij}$ is required) which are indeterminate are created:

$$
\Psi_{\mathbf{k}} \Delta K = G \tag{2-28}
$$

where, Ψ_k is shown as below:

$$(i,p) \rightarrow (1,1)\,(1,2)\ \ldots(1,r)\ \ (2,1)\ \ (2,2)\ \ \ldots\ \ (2,r)\,(3,1)\ldots(3,r)\ldots$$

$$\Psi_k = \begin{bmatrix} \varphi_{11} & \varphi_{12} & \cdots & \varphi_{1r} & 0 & 0 & \cdots & 0 & 0 & \cdots & 0 & \cdots \\ \varphi_{12} & \varphi_{22} & \cdots & \varphi_{2r} & \varphi_{11} & \varphi_{12} & \cdots & \varphi_{1r} & 0 & \cdots & 0 & \cdots \\ \vdots & \vdots & & \vdots & \vdots & \vdots & & \vdots & \vdots & \vdots & \vdots & \\ 0 & 0 & \cdots & 0 & \varphi_{21} & \varphi_{22} & \cdots & \varphi_{2r} & 0 & \cdots & 0 & \cdots \\ \vdots & \vdots & & \vdots & \vdots & \vdots & & \vdots & \vdots & \vdots & \vdots & \\ 0 & 0 & \cdots & 0 & 0 & 0 & \cdots & 0 & 0 & \cdots & 0 & \cdots \\ \vdots & \vdots & & \vdots & \vdots & \vdots & & \vdots & \vdots & \vdots & \vdots & \end{bmatrix} \begin{matrix} (1,1) \\ (1,2) \\ \vdots \\ (2,2) \\ \vdots \\ (s,t) \\ \vdots \end{matrix}$$

$$\uparrow$$
$$(i,j)$$
(2-29)

where, φ_{ip} is Φ_A's element of row i and column p.

then,

$$\Delta K = \left(\Psi_{\mathbf{k}} \cdot \Psi_k^{\ T}\right)^{-1} \cdot \Psi_k \cdot G, \quad \det\left(\Psi_{\mathbf{k}} \cdot \Psi_k^{\ T}\right) \neq 0, \forall k \tag{2-30}$$

$$K = K_A + \Delta K \tag{2-31}$$

K need to be substituted for K_A into Eq.(2-27) to update several times so as to get higher precision.

The updated stiffness is

$$\begin{bmatrix} 0.7006 \\ 0.9649 \\ 0.7535 \\ 1.1105 \\ 1.0763 \end{bmatrix} \times 10^4 \quad \text{Hz.}$$

According to this stiffness, the frequency is

$$\begin{bmatrix} 2.2357 \\ 6.9055 \\ 10.9301 \\ 14.5855 \\ 16.4300 \end{bmatrix} \quad \text{Hz.}$$

The value is very close to measured value, so the update stiffness matrix of health structure is appropriated to be used in the following research.

By replacing two columns for each story, the story stiffness damage rate was 32.72%. The frequency of the different damage structure is shown in Table 2.2

Table 2.2 Frequency of Damage Structure

	damage@1F	damage@2F	damage@3F	damage@4F	damage@5F
Frequency (Hz)	2.059	2.118	2.094	2.192	2.229
	6.393	6.955	6.648	6.326	6.653
	10.610	10.533	10.344	10.626	10.203
	14.163	13.099	14.279	14.105	13.961
	16.170	16.276	15.993	15.582	16.019

2.1.3.3 **Damage identification results**

Using Parzen Window method and establishing Probabilistic Neural Networks (PNNs), the experimental data in Table 2.2 were inputted into the network trained by the data based on the model data, and the damage location can be decided as in Figure 2.7.
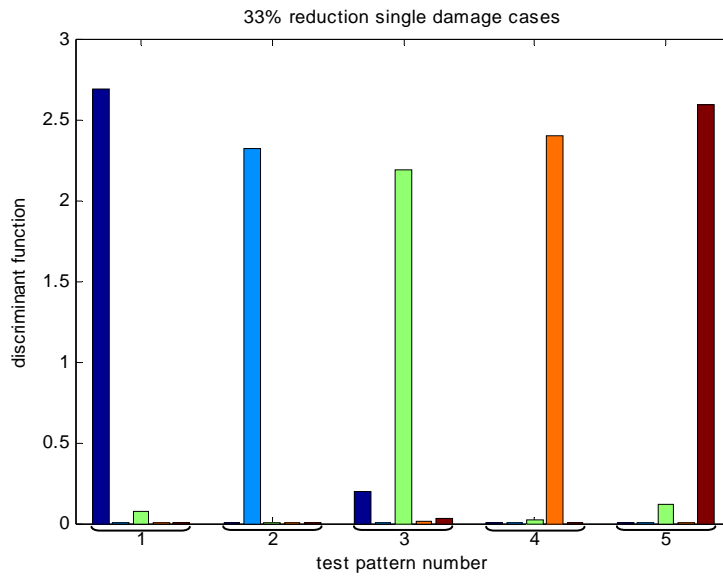
Figure 2.7. Damage Location Identification

(For the first test pattern, the first bar is maximal, which means the damage is at the first floor.

The similar to the other cases)

Figure 2.7 shows that the damage locations of the different damage structures can be decided accurately.
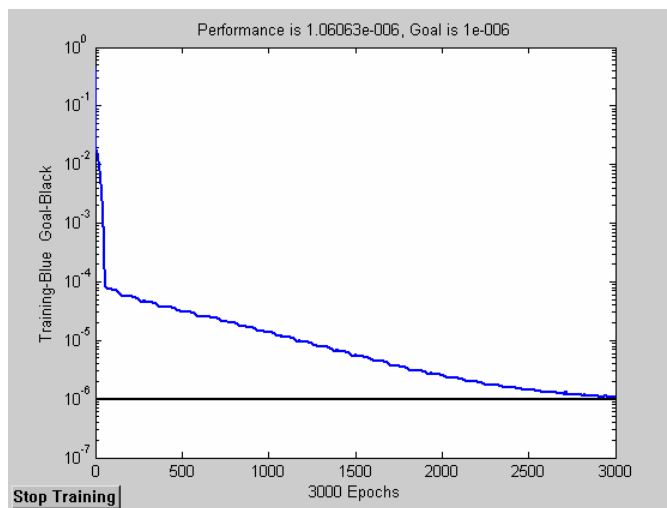
Figure 2.8. Mean Squared Error

After damage location has been determined, damage on this floor would be quantified by neural network with error-back-propagation algorithms. For instance, if the damage location is identified to be 3rd-floor, the value of 3rd-floor's stiffness which equals to 1.0, 0.95, 0.9, 0.8, 0.7, 0.6, 0.5 and 0.4 times of the health value would be used to train neural network with Gradient descent with momentum and adaptive learning rate back-propagation. In this study, for the five-story frame structure, the number of neurons of input, hidden and output layer is 5, 5 and 1 respectively. The mean squared error curve during training is as in Figure 2.8.

The input is the frequency variety rate and output is stiffness reduction rate of the damage floor identified by Parzen-window method. And then based on the trained evaluation neural network, the stiffness reduction rate can be identified when experimental frequency variety rate shown in Table 2.3 is inputted to the neural network.

Table 2.3 Damage Extent Identification by BP Network

damage rate	1F	2F	3F	4F	5F
calculated	0.3560	0.2734	0.3470	0.2507	0.3373
actual	0.3300	0.3300	0.3300	0.3300	0.3300

In order to observe them easily and intuitively, these values were drawn as a bar graph in Figure 2.9.
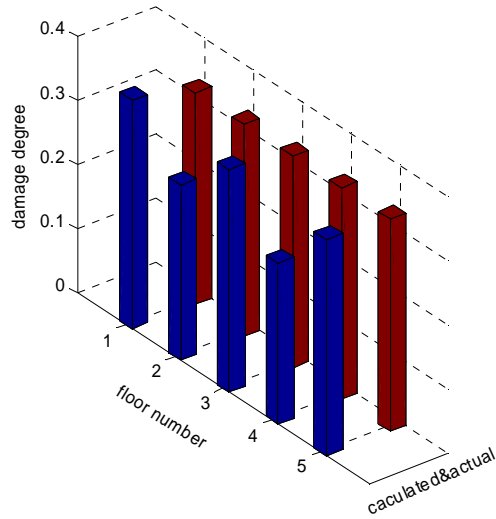
Figure 2.9. Damage Extent Identification by Neural Network

The result above shows that there is some error in the identified damage extent that arose from various reasons such as environmental disturbance, inaccuracy of measuring device and so on. In order to reduce the error and improve the accuracy, we consider injecting randomness into training data so that the trained network will be of noise-tolerance within a certain range: $\mathbf{V} = \mathbf{V}(1 + \alpha \cdot \mathbf{R})$. $\mathbf{V}$ is training data vector. α is the random ratio. $\mathbf{R}$ is a vector with random entries, chosen from a normal distribution with mean zero, variance one and standard deviation one. Here the random ratio is 0.02. The improved damage extent identification is shown in Table 2.4.

Table 2.4 Improved Damage Extent Identification by Network

damage rate	1F	2F	3F	4F	5F
calculated	0.3368	0.3595	0.3298	0.3497	0.3637
actual	0.3300	0.3300	0.3300	0.3300	0.3300

In order to observe them easily and intuitively, these values were drawn as a bar graph in Figure 2.10.
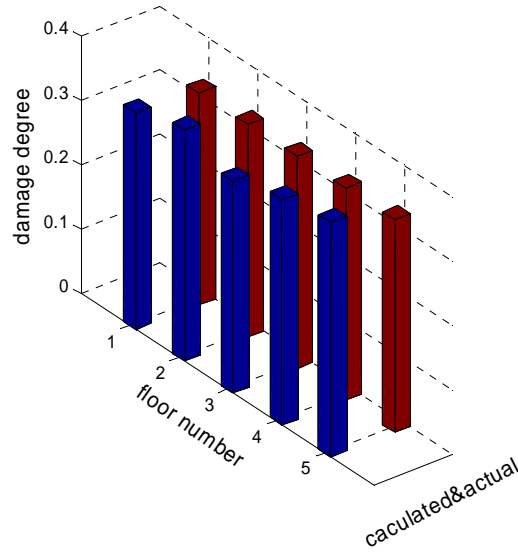
Figure 2.10. Improved Damage Extent Identification by Neural Network

The result above shows when the random number is injected into the training data, the identification accuracy can be improved and the damage extent of different damage structure can de decided ideally.

With the purpose of implementing the theory in practical applications, the laboratory experiments were carried out in order to validate the method. A 5-story shear frame building made of aluminium and bronze was used. The modal frequencies were calculated by the Eigensystem Realization Algorithm. Using the frequency change rate, the structure damage location was identified by the Parzen method. Similarly the structure damage extent was identified by the Neural network. The identification accuracy can be improved by considering variations in signals. The damage extent of different damage structure was indeed identified correctly.

2.2 Time series-based damage identification techniques

Most currently available damage detection methods are global in nature, i.e., the dynamic properties (natural frequencies and mode shapes) are obtained for the entire structure from the input–output data using global structural analyses e.g., (Doebling, et al. 1996). However, natural frequencies and mode shapes are not sensitive to minor damage and local damage. Salawu (1995) pointed out that a 5% frequency shift might be required to detect structural damage with confidence when using frequencies only. In addition, frequency shifts alone might not necessarily indicate that damage has occurred in the structure. As Aktan (1994) reported, significant frequency shifts (exceeding 5%) caused by changes in ambient conditions have been measured for bridges in a single day.

The techniques using time series dynamic responses are appealing and promising.

Ghobarah et al. (1999) presented a new approach for damage assessment providing a measure of the physical response characteristics of the structure and is better suited for non-linear structural analysis based on the static pushover analysis. An adaptive on-line parametric identification algorithm based on the variable trace approach is proposed by Lin et al. (2001) for the identification of non-linear hysteretic structures. At each time step, this recursive least-square-based algorithm upgrades the diagonal elements of the adaptation gain matrix by comparing the values of estimated parameters between two consecutive time steps. Fasel et al. (2005) applied an auto-regressive model with exoganous inputs (ARX) in the frequency domain to structural health monitoring. Damage sensitive features that explicitly consider non-linear system input/output relationships were extracted from the ARX model. Furthermore, because of the non-Gaussian nature of the extracted features, Extreme Value Statistics (EVS) is employed to develop a robust damage classifier.

In all these algorithms, technical challenges related to the system's uniqueness and observability are encountered; these are inherent in many structural systems, due to the presence

of redundant structural members and to a limited number of sensors (Agbabian et al. 1991). The development of procedures to handle these problems has drawn wide attention in the past two decades because of the rapid developments in digital instrumentation and computer technologies.

In the time domain identification arena, various algorithms have been developed. Among those, the Eigensystem Realization Algorithm with Data Correlation (ERA/DC) (Juang et al. 1985) provides a systematic and formal way for obtaining modal parameter identification of linear structural systems. Complementary to ERA/DC, an observer/Kalman filter identification algorithm was developed (Juang et al. 1994) by introducing an asymptotically convergent observer. Such an approach was extended to the seismic analysis of structures in the work by Lus et al. (1999).

Some information about structural parameters and dynamic properties can be identified by the direct use of these time-domain response. Nair et al. (2006) proposed a damage detection and localization algorithm based on time series modeling. The vibration signals obtained from sensors are modelled as autoregressive moving average (ARMA) time series. A new damage-sensitive feature, DSF, is defined as a function of the first three auto regressive (AR) components. Moreover, there is an approach by directly using dynamic responses in time series without extraction of dynamic properties proposed by Xu et al. (2003), where acceleration, velocity and displacement time histories were used as the input of the emulator neural network. This approach was improved by Xu & Chen (2005), where only acceleration time histories were used as the input of the emulator neural network. They called it acceleration-based emulator neural network (AENN) for free vibration. The AENN will be extended to forced vibration beyond the limitation of free vibration in the following chapters.

2.3 Summary

This chapter reviewed a typical damage localization and quantification approach using pattern classification methods, as well as some of the existing direct identification of structural parameters from dynamic responses. Vibration-based damage detection methods are important because there is no requirement of a prior knowledge of damage location. Direct identification of structural

parameters from dynamic responses is highly desired. In the following chapter, we will discuss direct damage detection using acceleration response.

CHAPTER 3

Acceleration-Based Damage Occurrence Alarm

for Building Structures

3.1 Introduction

This chapter is the first phase of the approach proposed. Acceleration-based damage occurrence alarm for building structures under earthquakes using artificial neural network emulators is proposed. The ground acceleration is included into the input layer of neural network as forced vibration in addition to the acceleration data at several floors. The method is improved by using the acceleration at later time steps as the output of the neural network. The time delay is optimized as a tunable band to provide the most sensitive signals. The method uses limited number of acceleration time histories only and could be applied to multi-input as well as single input systems. The necessary number of acceleration histories at different floors can be effectively reduced by increasing the previous time steps of the acceleration. The minimal one sensor needed provides the high practicability and flexibility. The applied structures can be under diverse excitations even very small impacts.

Based on the numerical simulation for a five-story shear structure, the appropriate parameters, generality and efficacy of the neural network are studied. The damage index, the relative root mean square (RRMS) error, is calculated for the single structural damage, followed by double damages at different damage locations. Several ground motions are used to certify the generality

of this approach. The appropriate parameters for the neural network emulator are proposed according to the damage patterns.

An approach directly using dynamic responses in time series without extraction of dynamic properties, which used acceleration, velocity and displacement time histories as the input to an emulator neural network was proposed by Xu et al. (2003), and was improved by Xu & Chen (2005), through the use of acceleration time histories only as the input to the emulator neural network. The method was called an acceleration-based emulator neural network (AENN) for free vibration.

In this research, the AENN is extended to forced vibration beyond the limitation of free vibration to be applicable to arbitrary excitation. Minimally, only a single sensor is needed for response measurement for the damage alarm. Acceleration time histories, which are readily available in real structures, being the only necessity. Thus, this method is feasible for practical application. Furthermore, the accuracy of AENN is improved significantly by increasing time histories of the response into the input layer.

3.2 Identification of Structural Changes with Neural Network Based on Acceleration Measurement

3.2.1 ANN Emulator Using Displacement, Velocity and Acceleration as Inputs

The basic idea of identification of structural changes using a neural network based on response time histories is to establish an emulator neural network that represents the characteristics of the structure. Input of the neural network is the response at time step k, and output is the response at time step *k+1* as in Figure 3.1 (Xu et al. 2003).

The neural network is to be trained using an existing response time history from a past earthquake excitation. Provided the structure has incurred no damage, the trained emulator neural network should be applicable to the same structure under subsequent earthquakes. Given this, the error between the output of the neural network and the real measurement provides information

regarding structural damage.
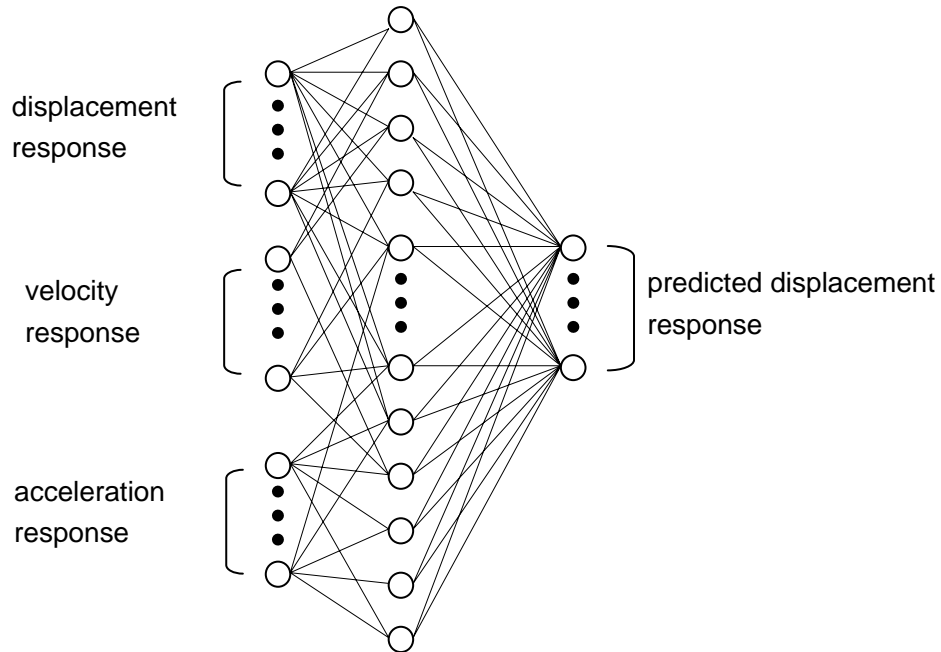
Figure 3.1 Neural Network to Represent the Characteristics of Structure

Xu & Chen (2005) improved this approach by using acceleration time histories only as the input of the emulator neural network for free vibration. We have extended the study beyond the limitation of free vibration by including ground motion in the NN input layer so that the applied structure can be under arbitrary excitation, and the number of required response measurements can possibly be mineralized.

3.2.2 Proposed ANN Emulator Using Acceleration Only as Inputs

Neural networks may work as good black-box models even for nonlinear systems. Although ARX (Auto-Regressive eXtra input) models represent linear system dynamics, it could offer some revelation to application of neural networks. An ARX model (Mita 2003) is given by

$$A(q)y(t) = B(q)u(t) + e(t) \tag{3-1}$$

where q is the shift operator, $qy(t) = y(t+1)$. Auto-Regression model $A(q)$ in terms of q is defined by

$$A(q) = 1 + a_1 q^{-1} + \cdots + a_{n_a} q^{-n_a} \qquad (3\text{-}2)$$

Moving average part is defined by

$$B(q) = b_1 q^{-1} + \cdots + b_{n_b} q^{-n_b} \qquad (3\text{-}3)$$

A pragmatic and useful way to see Eq. (3-1) is to view it as a way of determining the next output value given previous observations:

$$y(t) = -a_1 y(t-1) - \cdots - a_{n_a} y(t-n_a) + b_1 u(t-1) + \cdots + b_{n_b} u(t-n_b) + e(t) \qquad (3\text{-}4)$$

This representation indicates that the prediction of the response requires several previous time steps for response as well as inputs. Neural networks can be used as an alternative to the ARX model, to represent the relationship determining the next output value given previous observations and extra input. The advantage of neural networks is applicability to nonlinear systems, as well as linear systems.

An acceleration-based emulator neural network (AENN) trained to represent the mapping between acceleration at different time steps can be established as in Figure 3.2. Here we use acceleration time histories as observations. Since they are readily available in real structures, using accelerations provides much convenience. The acceleration of ground is beyond the consideration of the neural network's target, so it is included as T_k, into the NN input layer. T_k is the kth time step. And $T_{k-1}, \ldots T_{k-n}$ are previous time steps.
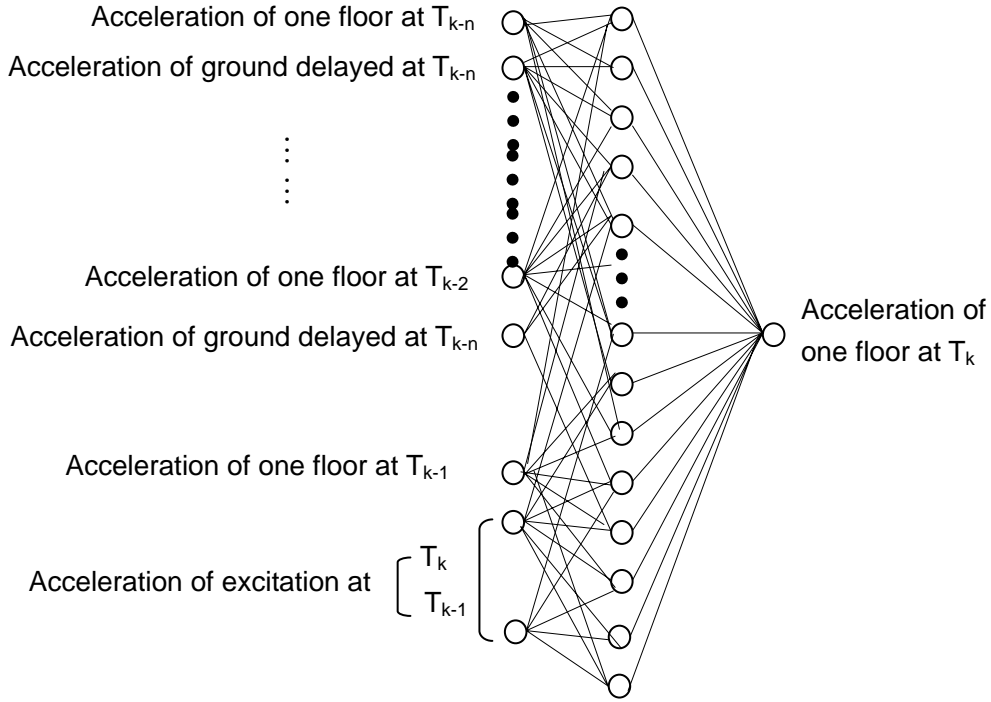
Figure 3.2 Acceleration-based emulator neural network

Here, one floor means a certain floor.

The trained AENN is a non-parametric model for the structure and can be used to forecast the acceleration response under later earthquake.

Relative root mean square (RRMS) error e is defined by

$$e = \frac{\sqrt{\sum_{m=1}^{M}\left(\ddot{x}_m^{f} - \ddot{x}_m\right)^2}}{\sqrt{\sum_{m=1}^{M}\left(\ddot{x}_m\right)^2}} \tag{3-5}$$

where, M is the number of sampling data; $\ddot{x}_m^{f}$ the output of trained neural networks at

sampling step m; $\ddot{x}_m$ the acceleration corresponding which is the real dynamic response under earthquake excitations at sampling step m.

RRMS shows the change between the output of the neural network and the real dynamic response and provides the information regarding structural damage. If this value is quite large, it would be thought that the structure is not healthy.

3.2.3 Modified ANN Emulator

Using acceleration at time steps k-2 and k-1 to forecast the acceleration at time step k, RRMS error is frequently too small to be regarded as an index of damage occurrence alarm. Considering this, the approach was improved by using the acceleration at later time steps, including k-2 and k-1 as the output of the neural network
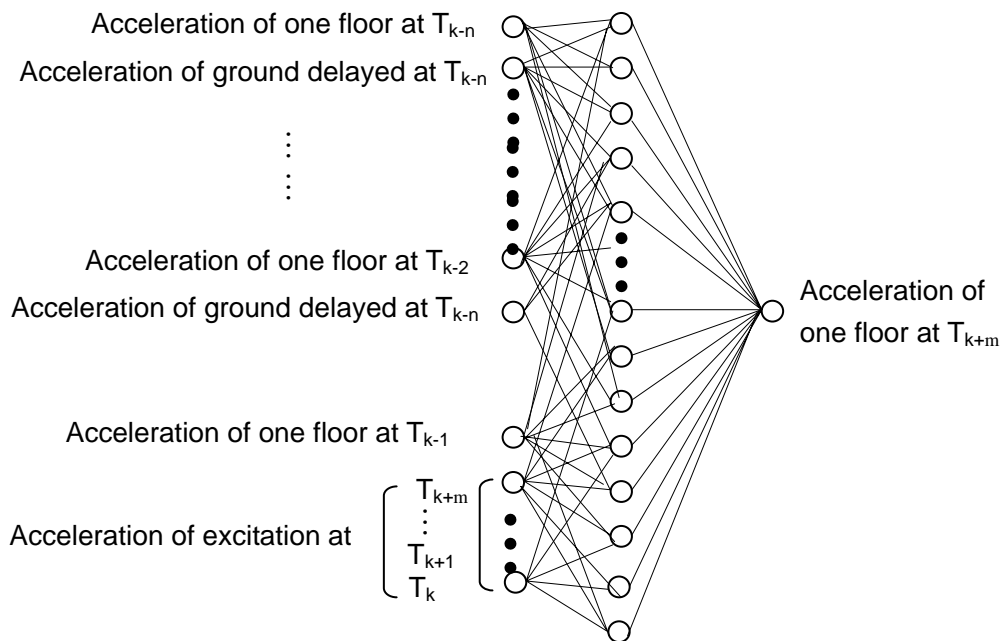
Figure 3.3 Improved AENN

The accelerations of the ground floor is not synchronous with the accelerations of the above-ground floors in the input layer, as shown in Figure 3.3. The acceleration of ground has a time delay of $m \times \Delta t$ such that the emulator neural network can forecast the acceleration of each floor at later time steps. The delay $m \times \Delta t$ is considered as a tunable band corresponding to different structures.

3.3 Parameters Determination Based on Simulation

Acceleration stream number, n and time delay of ground acceleration, $m \times \Delta t$ in Figure 3.3, are chosen parameters. Δt is sampling time. The number of acceleration streams, n, should be large enough to make the RRMS error for healthy structures a stably small value, while the appropriate time delay of ground acceleration $m \times \Delta t$ should make RRMS error difference between healthy structures and damaged structures a comparatively large value. The search for appropriate values for these two parameters was based on numerical simulation and will be discussed in this section.
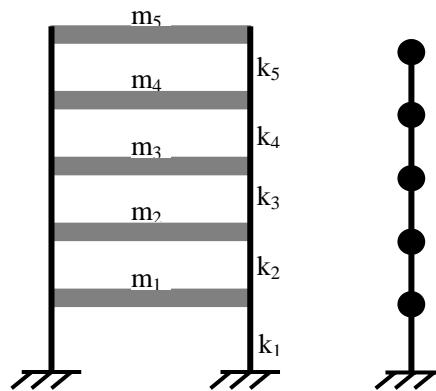
Figure 3.4. Five stories frame structure and its limped mass model

Table 3.1. Structural parameters of the object structure

DOF	1	2	3	4	5
Mass (kg)	4000	3000	2000	1000	800
Stiffness (kN/m)	2000	2000	2000	2000	2000

Table 3.2. Modal parameters of the object structure

DOF	1	2	3	4	5
Frequency (Hz)	1.65	4.11	6.16	8.11	12.3
Damping Ratio	0.005	0.013	0.019	0.026	0.039

Because the goal of this section is to search for appropriate parameters for an AENN that is generally applicable, a basic structure is used to for simplicity and generality. We used a 5-story shear frame structure as the object structure, and modelled it as a 5 degree-of-freedom lumped mass system, depicted in Figure 3.4, with structural parameter values as shown in Table 3.1. The modal frequencies of the frame structure are 1.65 Hz, 4.11 Hz, 6.16 Hz, 8.11 Hz, and 12.29 Hz, as shown in Table 3.2. The damping matrix is assumed to be Rayleigh damping which can be expressed in the following form,

$$\mathbf{C} = a\mathbf{M} + b\mathbf{K} \tag{3-6}$$

Where, $\mathbf{C}, \mathbf{M}, \mathbf{K}$ are damping, mass and stiffness matrixes respectively. a and b are selected to have damping ratios 0.005 for the first mode and 0.013 for the second mode.

The AENN is trained using a network training function that updates weight and bias values according to Levenberg-Marquardt optimization. The output layer includes 1 neuron. In this structure, the acceleration at the fifth floor is measured. The neuron number of input layer is decided by n and $m \times \Delta t$ in Figure 3.3, and the neuron number of hidden layer is twice of that of

input layer. The neuron number was decided according to experience of previous research.
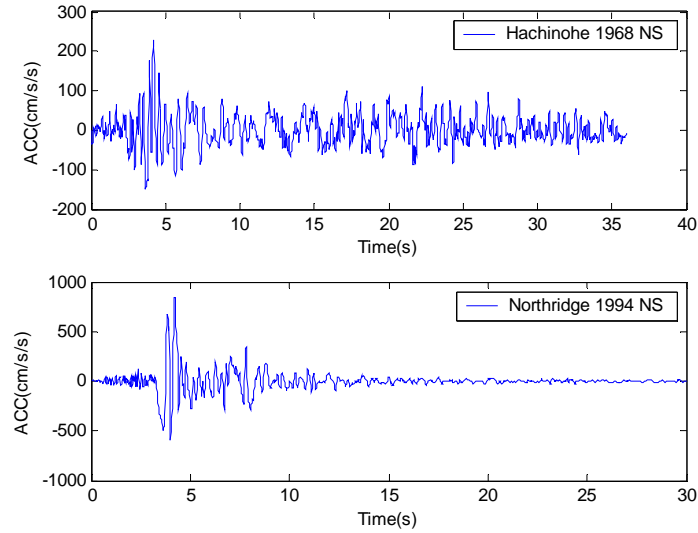
Figure 3.5. Earthquake records, Hachinohe and Northridge

Acceleration time histories obtained from the top floor of the 5-story shear structure under the Hachinohe earthquake (16th May, 1968, Hachinohe City) ground motion were used as training data sets. Test data sets were under the Northridge earthquake (17th January, 1994, Northridge, California) ground motion. These two earthquake records are shown in Figure 3.5. The sampling time is 0.02 second, and all time histories were normalized.

During the numerical simulation, acceleration stream number, n, was incrementally changed from 1 to 15. The delay, $m \times \Delta t$ was changed from 0.02 to 0.2 second, say, 1~10 times the sampling time. The two values, RRMS error for healthy structure and difference of RRMS errors between healthy structure and damaged structure, are shown in Figure 3.6 and Figure 3.7, to reach a stably small value for the former RRMS and comparatively large value for the latter RRMS. The difference of RRMS errors was defined by

$$\Delta e = e_{damage} - e_{health} \tag{3-7}$$
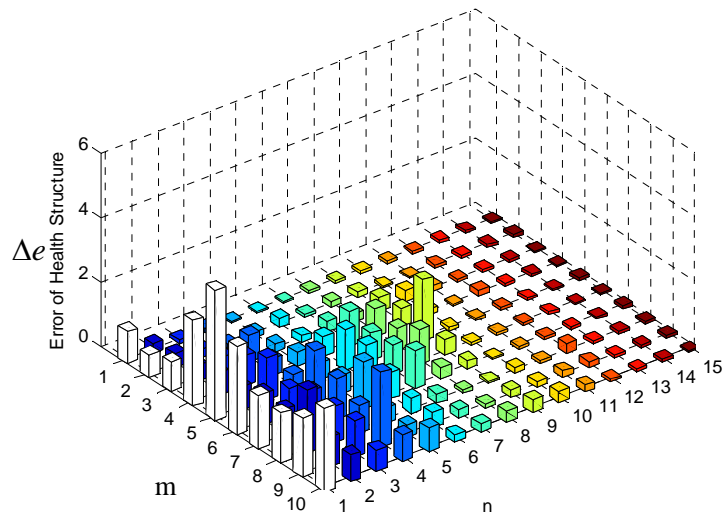
Figure 3.6. Error for health structure changed

by acceleration stream number and delay
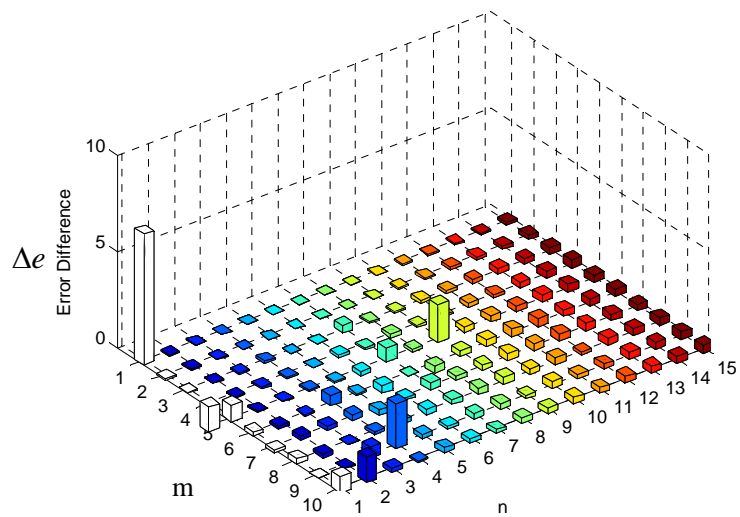
Figure 3.7. Error difference between health and damage structures

With the goal of more easily deciding the proper AENN parameters, severe damage, stiffness reduction of 20% at each floor, was utilized.

Prediction accuracy is raised by incrementing the number of acceleration streams at different time steps to an appropriate value. The value of RRMS error decreases to a stable value when the number of acceleration streams achieves the appropriate value. The information in Figure 3.6 showing error for healthy structure *vs* acceleration stream number and delay was used to decide an appropriate acceleration stream number. In Figure 3.6, it could be seen that error for healthy structure is stably small for acceleration stream numbers 10 or above. Therefore, the necessary acceleration stream number for the 5-story shear structure should be 10, which is understandable and reasonable considering this method analogy with ARX Models. As for the other structures, the necessary acceleration stream number should be twice of the number of freedom. For example, a 10-story shear structure, the necessary acceleration stream number would turn out to be 20.

The error difference between healthy and damaged structures in Figure 3.7 was used to decide an appropriate time delay of ground acceleration. In Figure 3.7, it can be seen that the error difference corresponding to $n=10$ is comparatively large with time delay of ground acceleration seven times of sampling time, say, 0.14 second. So the appropriate time delay of ground acceleration is 0.14 second for this structure. The first order natural frequency of this structure is 1.65 Hz. We suggest that time delay of ground acceleration of approximately 1/4 of structural periodic time is appropriate.

3.4 Consideration of Noise Effect

Damage is introduced to the structure as shown in Figure 3.4 with the intent of demonstrating whether the RRMS errors can provide an effective damage alarm. To evaluate the effect of measurement noise on the accuracy of damage detection, the accelerations are corrupted with 2% and 5% RMS Gaussian white noise. The structural parameters and the earthquake excitations are the same as in the previous section. Only minimal output, the acceleration at floor 5, is used.

Damage detection results for clean, 2% RMS corrupted, and 5% RMS corrupted signals are shown in Figure 3.8, Figure 3.9, and Figure 3.10 respectively. Figure 3.8 shows that in the no noise case the value of RRMS error is 0.0540, 0.0995, and 0.2133 for the healthy structure, for the structure with 10% damage at the second floor, and for the structure with 20% damage at the second floor. In the 2% noise case, i.e. in Figure 3.9, the of RRMS errors were 0.0724, 0.1187, and 0.2288, again for the healthy structure, for the structure with 10% damage at the second floor, and for the structure with 20% damage at the second floor. And finally, in the 5% noise case, i.e. in Figure 3.10, the analogous values of RRMS error were 0.0947, 0.1504, and 0.2405. For these three cases, the differences between no damage and 10% damage were 0.0455, 0.0463 and 0.0557. The differences between no damage and 20% damage were 0.1593, 0.1564 and 0.1458. There are consistent and detectable differences between the healthy and damaged structure.

For SHM, the objective is not to identify exact index values but to detect variations in a relative sense, and/or changes in magnitude in the absolute sense. The results of the damage detection simulation with clean signals and corrupted signals showed the relative values of RRMS errors for damage scenarios to be detectable. Thus, a damage alarm is provided by the observation of RRMS error, regardless, within reason, of signal corruption level.
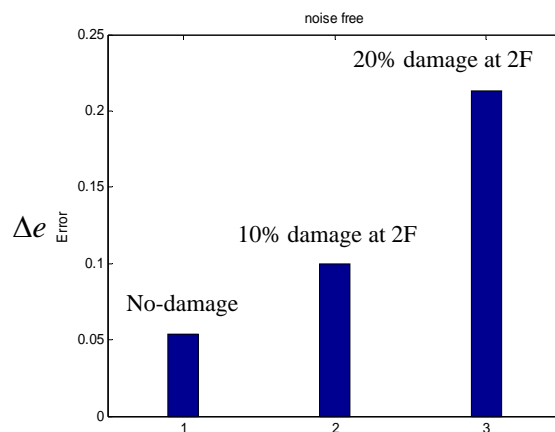
Figure 3.8 Damage detection with clean signals
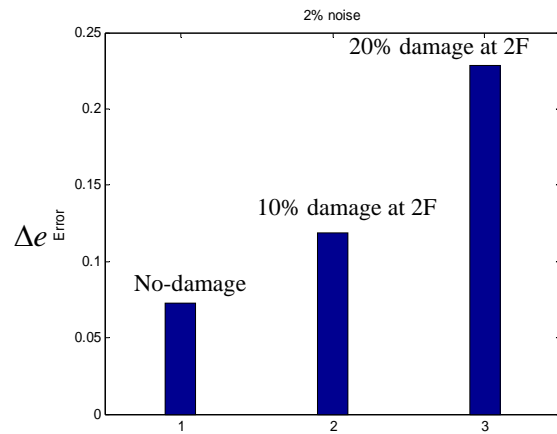
Figure 3.9 Damage detection with 2% noise signals
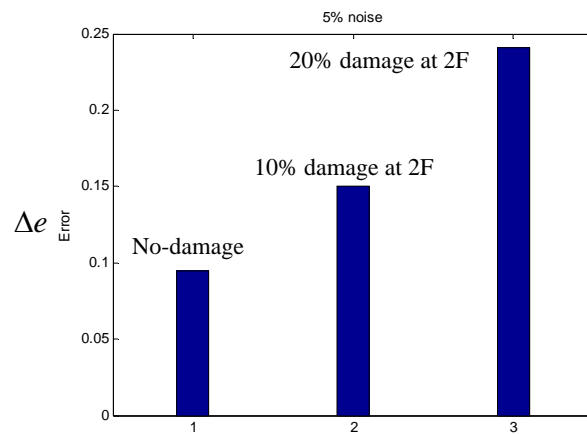
Figure 3.10 Damage detection with 5% noise signals

3.5 Discussion on Multi-Output

The AENN described Figure 3.3 has only acceleration at a single floor as output. Here, we

consider using more accelerations at different floors in a multi-output NN as shown in Figure 3.11.
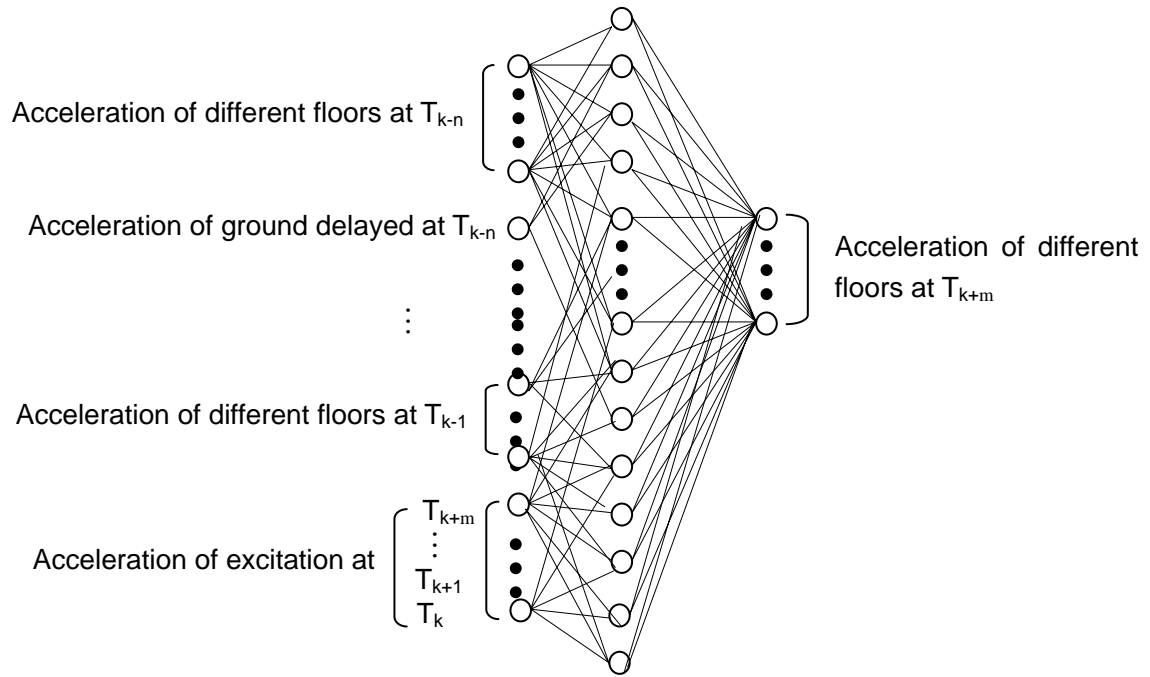
Figure 3.11 AENN with multi-output

Utilizing acceleration at more multiple floors in this manner decreases the necessary number of acceleration streams at different time steps, denoted by *n* in Figure 3.11.

Still using the 5-story shear structure depicted in Figure 3.4, the acceleration time histories for excitation under Hachinohe earthquake (16th May, 1968, Hachinohe City) (Figure 3.5) ground motion were used as training data sets, and those under the ground motion of the Northridge earthquake (17th January, 1994, Northridge, California) (Figure 3.5) were used as test data sets. Consideration was given to the acceleration of the 3rd and 5th floors, followed by consideration of the 2nd, 4th and 1st floor.
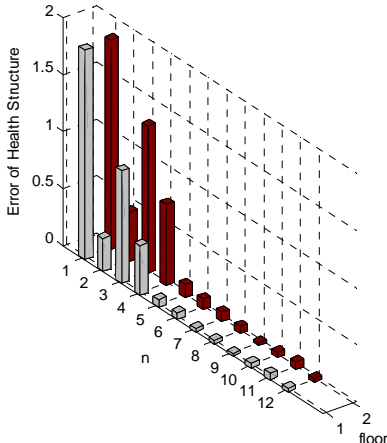
Figure 3.12 Error changed by n with accelerations of the 3&5th floors
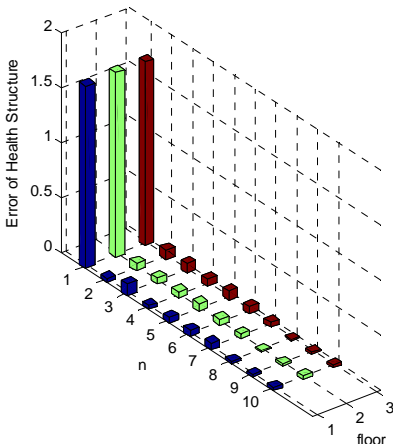
Figure 3.13 Error changed by n with accelerations of the 2,3&5th floors
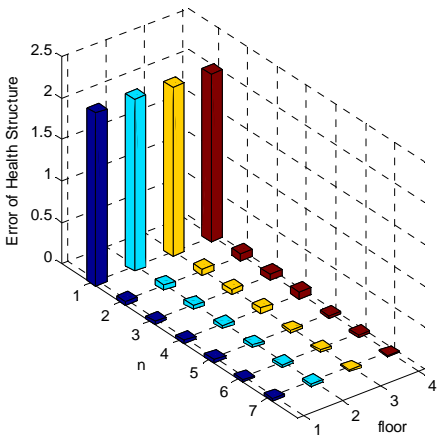
Figure 3.14 Error changed by n with accelerations of the 2,3,4&5th floors
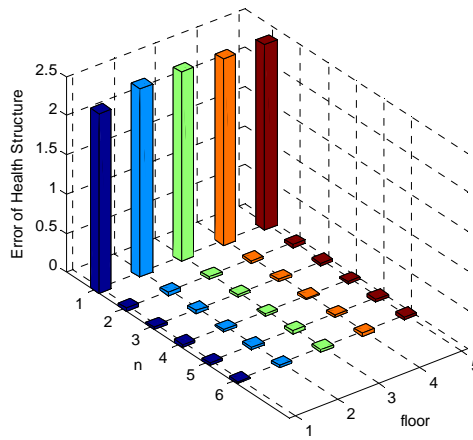
Figure 3.15 Error changed by n with accelerations of the 1,2,3,4&5th floors

From Figures 3.12-3.15 it is seen that increased utilization of acceleration at multiple floors decreases the necessary number of acceleration streams at different time steps, *n*, needed for ensuring stably small values of error.

According to the simulation results, when the accelerations of two floors (Figures 3.12) are included in the neural networks n should be 5. When the accelerations of more than two floors are included (Figures 3.13-3.15), this number is reduced to only 2 only.

Using multiple outputs provides higher reliability, and increasingly low cost microelectromechanical (MEMS) sensors and wireless solutions for structural measurement which allow for a dense network of sensors to be deployed in structures make this option not unrealistic. However, the proposed method does not require the use of accelerations from multiple floors. The minimum is only one, and using just one floor acceleration provides high convenience and practicability, though longer time series periods are needed. Our approach is flexible, and on either end, using a single output or multi-outputs, shows practicality.

3.6 AENN Efficacy and Generality

To verify the efficacy of the AENN presented in Figure 3.11, simulation using the structure

described in Figure 3.4 was performed with acceleration of each floor. The input, hidden, and output layers of the AENN include 17, 34 and 5 neurons, respectively.

For the healthy structure, the comparison between the output of the neural network and the real value decided through dynamic analysis is shown in Figure 3.16. Since the value is normalized, there is no unit for acceleration here. It is seen that identification using the neural network can be carried out with high accuracy. The improved AENN can be trained to achieve a desired accuracy for modelling the dynamic behaviour of the healthy structure
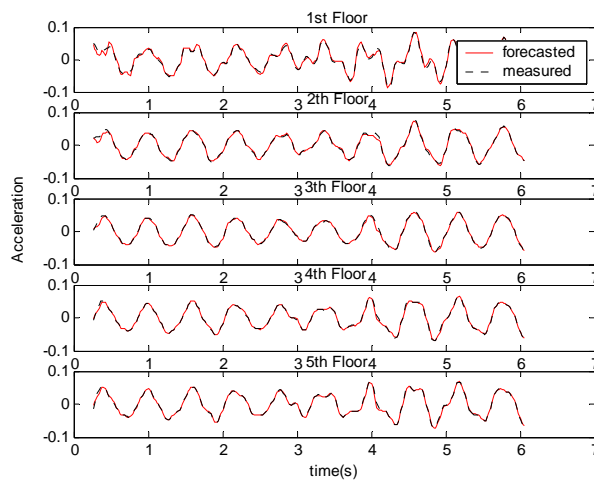
Figure 3.16. Comparison between the output of neural network and the real value

Further study was carried out considering the existence of structural damage, firstly instituting single damage of 20% stiffness reduction on the third floor. As before, the acceleration of the damaged structure under the Northridge earthquake was used as the test data. Using the output of the neural network, RRMS error was calculated according to Eq. (3-5). Consideration was then extended to double-damage: 20% stiffness reduction on the third and fifth floors. Similarly, RRMS error was calculated as before. Figure 3.17 shows the different values of RRMS errors of healthy, single-damage, and double-damage structures. RRMS error shows the change between the output of the neural network and the real dynamic response, providing information regarding structural damage. If this value is quite large, it is thought that the structure is not healthy. Therefore, the RRMS error can be used as a damage occurrence alarm index.
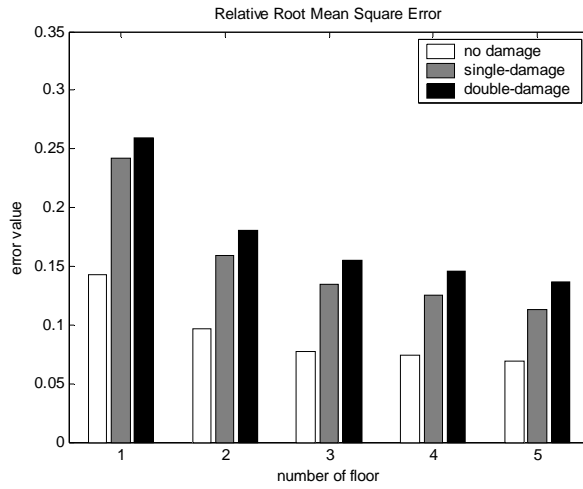
Figure 3.17. RRMS errors of healthy and damaged structures

To verify the generality of the proposed AENN, the results under different ground motions were observed for a healthy structure, to show that the trained AENN can achieve desired accuracy not just for a specific ground motion.   Ground motions of the previously used Northridge earthquake, the Kobe earthquake (Jan. 17, 1995, Kobe Japanese), and white-noise were used as the test data sets for this purpose. These three RRMS error values are shown in Figure 3.18.
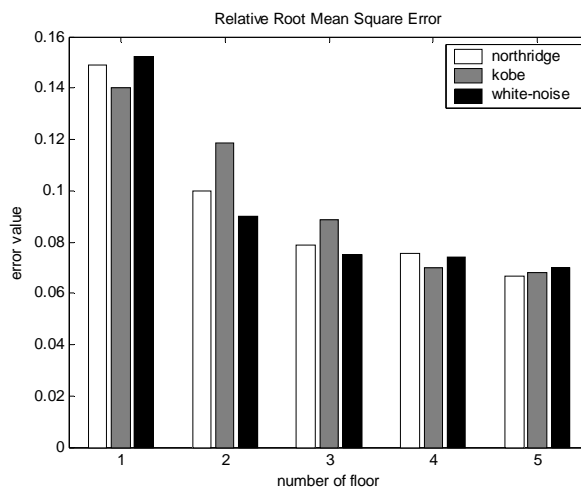
Figure 3.18. RRMS errors under different ground motions

From Figure 3.18, it is seen that under the different ground motions, the trained neural network achieves similar accuracy, certifying the generality of the proposed AENN. Similarity of damage errors under the different earthquake excitations also shows the stability and reliability of the proposed method.

3.7 Acceleration-Based Damage Evaluation Synthesis

The key features of our Acceleration-Based Damage Evaluation of Building Structures with Neural Networks are summarized as follows:

- The damage evaluation approach uses only acceleration time histories, and only with consideration of similarity to ARX models.

- A time delay was introduced to the ground acceleration in order that the emulator neural network could forecast the acceleration of the each floor at later time steps.

- For a 5-story structure, the necessary number of acceleration streams at different time steps for the single-input network is 10. We suggest the time delay of ground acceleration, which is 1/4 of structural periodic time.

- It is proposed that more acceleration histories at different floors are used for the multi-output emulator neural network in order to decrease multi-output. The necessary number of acceleration streams at different time steps could be decreased.

CHAPTER 4

Acceleration-Based Damage Localization

and Quantification of Structures

4.1 Introduction

This chapter is the second phase of the proposed approach. After knowing the damage occurrence, the next phase is necessary to be performed for the goal of determining the damage location and quantity. Most currently available damage localization approaches are mostly based on pattern recognition methods to classify the different damage location. However, such approaches need analytical data for all damage case situations, which can be computationally expensive and even impossible. Therefore, the system identification is utilized for damage determination. In this research the system identification problem is formulated as an optimization problem using the Particle Swarm Optimization (PSO).

Based on the numerical simulations for a five-story shear structure, the performance of this method is studied for both full output information and partial output information. Moreover the advantage of this method is verified by comparison with the other global search methods, e.g. Simulated Annealing (SA) and Genetic Algorithm (GA).

4.2 System Identification as an Optimization Problem

The identification problem can be understood as an optimization problem in which the error between the actual physical measured response of a structure and the simulated response of a numerical model is minimized (Franco et al. 2004). In order to show this in more detail, let us consider a physical system as shown in Figure 3.4 with q outputs of acceleration responses y_j^M for $j = 1,2,\cdots,q$. Let y_j^M for $j = 1,2,\cdots,q$ denotes the value of the acceleration responses of the actual system.

Suppose that a model that is able to capture the behaviour of the physical system is developed and that this model depends upon a set of n parameters, contained in a vector $\mathbf{x} = \{x_i\}$ for $i = 1,2,\cdots,n$. Call the newly formed model of the system and its parameters the identified system or candidate system, and let y_j for $j = 1,2,\cdots,q$ denotes the value of the acceleration responses of the identified system. T is time step. At this point, let us now build the vectors y_j^M and y_j as

$$\mathbf{y}_j^M = [y_j^M(0) \quad y_j^M(1) \quad \cdots \quad y_j^M(T)] \qquad j = 1,2,\cdots,q \tag{4-1}$$

$$\mathbf{y}_j = [y_j(0) \quad y_j(1) \quad \cdots \quad y_j(T)] \tag{4-2}$$

containing all sampled values of the *j*th output of the actual and identified systems, respectively. Now consider the vectors y_j^M and y_j, as the stacked vectors of all available output records for each system, which can be written as

$$\mathbf{y}^M = [y_1^M(0) \quad y_1^M(1) \quad \cdots \quad y_1^M(T) \big| y_1^M(0) \quad \cdots \big| \cdots \big| y_q^M(0) \quad \cdots y_q^M(T)] \tag{4-3}$$

$$\mathbf{y} = [y_1(0) \quad y_1(1) \quad \cdots \quad y_1(T)|y_1(0) \quad \cdots |\cdots |y_q(0) \quad \cdots y_q(T)] \tag{4-4}$$

and compute the error norm of all the simulated outputs of the identified system with respect to those measured from the actual system, defined as:

$$\mathrm{F}(\mathbf{x}) = \sqrt{\left(\mathbf{y}^M - \mathbf{y}\right)\left(\mathbf{y}^M - \mathbf{y}\right)^T} \tag{4-5}$$

In order to obtain a successful identification, the candidate system must be able to accurately reproduce the output of the physical system for any given input. Therefore, our interest lies in minimizing the error norm of the outputs. Formally, the optimization problem requires finding a vector $\mathbf{x} \in S$, where S is the search space, so that a certain quality criterion is satisfied, namely that the error norm $\mathrm{F}: S \rightarrow R$ is minimized. The function F is commonly called a cost function or objective function. In evolutionary computation, typically a fitness function is used which reflects the goodness of the solution. The better the solution, the fitter it is for survival. As our problem is a minimization problem, a fitter solution will be characterized with a lower value of the cost function. Therefore, the fitness function can be defined as the negative of the cost function, i.e., $-\mathrm{F}$. Minimization of F is then equivalent to maximize the fitness $-\mathrm{F}$. Vector $\mathbf{x}^*$ will be called a solution to the minimization problem if $\mathrm{F}(\mathbf{x}^*)$ is the global minimum of F in S, or

$$\mathbf{x}^* \in S | \mathrm{F}(\mathbf{x}^*) \leq \mathrm{F}(\mathbf{x}) \qquad \forall \mathbf{x} \in S \tag{4-6}$$

The search space S is defined by a set of maximum and minimum values for each parameter. It is conceived as an n-dimensional domain delimited by vectors $\mathbf{x}_{max}$ and $\mathbf{x}_{min}$ containing the

upper bounds of the n parameters and the lower bounds respectively or

$$S = \left\{ \text{ space } \quad x \in R^n \middle| x_{min,i} \leq x_i \leq x_{max,i} \quad \forall i = 1,2,\cdots,n \right\}$$ (4-7)

The problem of identification is thus treated as a linearly constrained (due to the delimited n-dimensional search space) nonlinear (due to the nonlinear cost function) optimization problem.

4.3 Particle Swarm Optimization (PSO)

Particle swarm adaptation has been shown to successfully optimize a wide range of continuous functions (Angeline 1998).   The algorithm, which is based on a metaphor of social interaction, searches a space by adjusting the trajectories of individual vectors, called "particles" as they are conceptualized as moving points in multidimensional space. The individual particles are drawn stochastically toward the positions of their own previous best performance and the best previous performance of their neighbours.

A population of particles is initialized with random positions $\vec{x}_i$ and velocities $\vec{v}_i$, and a function, *f*, is evaluated, using the particle's positional coordinates as input values. Positions and velocities are adjusted, and the function evaluated with the new coordinates at each time-step. When a particle discovers a pattern that is better than any it has found previously, it stores the coordinates in a vector $\vec{p}_i$. The difference between $\vec{p}_i$ (the best point found by *i* so far) and the individual's current position is stochastically added to the current velocity, causing the trajectory to oscillate around that point. Further, each particle is defined within the context of a topological neighborhood comprising itself and some other particles in the population.   The stochastically weighted difference between the neighborhood's best position $\vec{p}_g$ and the individual's current position is also added to its velocity, adjusting it for the next time-step.   These adjustments to the particle's movement through the space cause it to search around the two best positions.

The algorithm in pseudocode follows:

Initialize population

Do

   For i= 1 to Population Size

  if $f(\vec{x}_i) < f(\vec{p}_i)$ then $\vec{p}_i = \vec{x}_i$

  $\vec{p}_g = \min(\vec{p}_{neighbors})$

      For d = 1 to Dimension

$$v_{id} = v_{id} + \varphi_1\left(p_{id} - x_{id}\right) + \varphi_2\left(p_{gd} - x_{id}\right)$$

$$v_{id} = \text{sign}(v_{id}) \cdot \min(\text{abs}(v_{id}), V_{\max}))$$

$$x_{id} = x_{id} + v_{id}$$

      Next d

   Next i

Until termination criterion is met

The variables φ_1 and φ_2 are random positive numbers, drawn from a uniform distribution and defined by an upper limit $\varphi_{\max}$ which is a parameter of the system. In this version, the term variable v_{id} is limited to the range $\pm V_{\max}$, for reasons which will be explained below. The values of the elements in $\vec{p}_g$ are determined by comparing the best performances of all the members of i's topological neighborhood, defined by indexes of some other population members, and assigning the best performer's index to the variable g. Thus $\vec{p}_g$ represents the best position found by any member of the neighborhood.

The random weighting of the control parameters in the algorithm results in a kind of explosion or a "drunkard's walk" as particles' velocities and positional coordinates careen toward infinity. The explosion has traditionally been contained through implementation of a V_{max} parameter, which

limits step-size, or velocity.   The current paper however demonstrates that the implementation of properly defined constriction coefficients can prevent explosion; further, these coefficients can induce particles to converge on optima.

An important source of the swarm's search capability is the interactions among particles as they react to one another's findings.   Analysis of interparticle effects is beyond the scope of this paper, which focuses on the trajectories of single particles.

The algorithm is stripped down to a most simple form.   The particle swarm formula adjusts the velocity $\vec{v}_i$ by adding two terms to it.   The two terms are of the same form, that is, $\varphi(\vec{p} - \vec{x}_i)$, where $\vec{p}$ is the best position found so far, by the individual particle in the first term, or by any neighbor in the second term.   The formula can be shortened by redefining p_{id} as follows:

$$p_{id} \leftarrow \frac{\varphi_1 p_{id} + \varphi_2 \, p_{gd}}{\varphi_1 + \varphi_2} \tag{4-8}$$

Thus we can simplify our initial investigation by looking at the behavior of a particle whose velocity is adjusted by only one term:

$$v_{id}(t+1) = v_{id}(t) + \varphi(p_{id} - x_{id}(t)) \tag{4-9}$$

where $\varphi = \varphi_1 + \varphi_2$.   This is algebraically identical to the standard two-term form.

When the particle swarm operates on an optimization problem, the value of $\vec{p}_i$ is constantly updated, as the system evolves toward an optimum. In order to further simplify the system and make it understandable, we set $\vec{p}_i$ to a constant value in the following analysis.   The system will also be more understandable if we make φ a constant as well; where normally it is defined as a random number between zero and a constant upper limit, we will remove the stochastic

component initially and reintroduce it in later sections. The effect of φ on the system is very important, and much of the present paper is involved in analyzing its effect on the trajectory of a particle.

The system can be simplified even further by considering a 1-dimensional problem space, and again further by reducing the population to one particle.   Thus we will begin by looking at a stripped-down particle by itself, e.g., a population of one, one-dimensional, deterministic particle, with a constant p.

Thus we begin by considering the reduced system:

$$\begin{cases} v(t+1) = v(t) + \varphi(p - x(t)) \\ x(t+1) = x(t) + v(t+1) \end{cases} \tag{4-10}$$

where p and φ are constants.   No vector notation is necessary, and there is no randomness.

4.4 Acceleration-Based System Identification with PSO for Full Output Information

Suppose that a structure that is able to capture the behavior of the physical system is developed and that this structure depends upon a set of n parameters, contained in a vector $\mathbf{x} = \{x_i\}$ for $i = 1, 2, \cdots, n$. This vector may include mass, stiffness, damping ratio et al. Call the newly formed structure of the system and its parameters the identified system or candidate system, and let a_j for $j = 1, 2, \cdots, q$ denotes the value of the acceleration responses of the identified system. At this point, let us now build the vectors $\mathbf{a}_j^M$ and $\mathbf{a}_j$ as

$$\mathbf{a}_j^M = [a_j^M(0) \quad a_j^M(1) \quad \cdots \quad a_j^M(T)] \tag{4-11}$$

$$\mathbf{a}_j = [a_j(0) \quad a_j(1) \quad \cdots \quad a_j(T)] \tag{4-12}$$

containing all sampled values of the *j*th output of the actual and identified systems, respectively. Now consider the vectors $\mathbf{a}_j^M$ and $\mathbf{a}_j$, as the stacked vectors of full output records for each system, which can be written as

$$\mathbf{a}^M = [a_1^M(0) \quad a_1^M(1) \quad \cdots \quad a_1^M(T) | a_1^M(0) \quad \cdots | \cdots | a_q^M(0) \quad \cdots] \tag{4-13}$$

$$\mathbf{a} = [a_1(0) \quad a_1(1) \quad \cdots \quad a_1(T) | a_1(0) \quad \cdots | \cdots | a_q(0) \quad \cdots] \tag{4-14}$$

and compute the error norm of all the simulated outputs of the identified system with respect to those measured from the actual system, defined as:

$$F(\mathbf{x}) = \sqrt{(\mathbf{a}^M - \mathbf{a})(\mathbf{a}^M - \mathbf{a})^T} \tag{4-15}$$

In order to obtain a successful identification, the candidate system must be able to accurately reproduce the output of the physical system for any given input. Therefore, our interest lies in minimizing the error norm of the outputs. Formally, the optimization problem requires finding a vector $\mathbf{x} \in S$, where S is the search space, so that a certain quality criterion is satisfied, namely that the error norm $F: S \to R$ is minimized. If we suppose that the structural damage only causes the change to the story stiffness, $\mathbf{x} = \{x_i\} = \{k_i\}$. Vector $\mathbf{x}^* = \{k_i^*\} = \mathbf{k}^*$ will be called a solution to the minimization problem if $F(\mathbf{k}^*)$ is the global minimum of F in S, or

$$\mathbf{k}^* \in S \big| F(\mathbf{k}^*) \le F(\mathbf{k}) \qquad \forall \mathbf{x} \in S \tag{4-16}$$

The search space S is defined by a set of maximum and minimum values for each story stiffness. It is conceived as an n-dimensional domain delimited by vectors $\mathbf{x}_{\max}$ and $\mathbf{x}_{\min}$ containing the upper bounds of the n parameters and the lower bounds respectively or

$$S = \left\{ k \in R^n \middle| k_{\min,i} \leq k_i \leq k_{\max,i} \qquad \forall i = 1,2,\cdots,n \right\} \tag{4-17}$$

The problem of structural identification is thus treated as an optimization problem.

The PSO is used to optimize $F(\mathbf{k})$ by the algorithm in pseudocode follows:

> Initialize population
>
> Do
>
>> For *i*= 1 to Population Size
>>
>> if $F(\vec{k}_i) < F(\vec{p}_i)$ then $\vec{p}_i = \vec{k}_i$
>>
>> $\vec{p}_g = \min(\vec{p}_{neighbors})$
>>
>>> For *d* = 1 to Dimension
>>>
>>> $$v_{id} = v_{id} + \varphi_1\left(p_{id} - k_{id}\right) + \varphi_2\left(p_{gd} - k_{id}\right)$$
>>>
>>> $$v_{id} = \text{sign}(v_{id}) \cdot \min(\text{abs}(v_{id}), V_{\max}))$$
>>>
>>> $$k_{id} = k_{id} + v_{id}$$
>>>
>>> Next *d*
>>
>> Next *i*
>
> Until termination criterion is met

4.5 Numerical Simulations for full output information

4.5.1 Numerical Verification

In order to verify the performance of the proposed methods, let us analyze the structure described in former sections represented in Figure 4.1, Table 4.1 and 4.2.
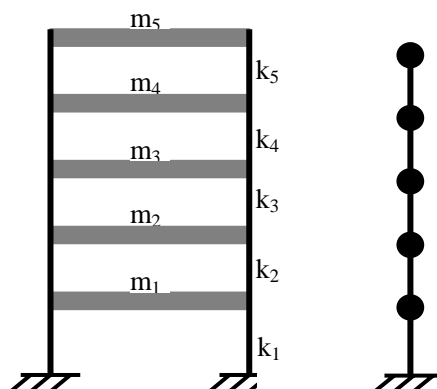
Figure 4.1. Five stories frame structure

Table 4.1. Structural parameters of the object structure

DOF	1	2	3	4	5
Mass (kg)	4000	3000	2000	1000	800
Stiffness (kN/m)	2000	2000	2000	2000	2000

Table 4.2. Modal parameters of the object structure

DOF	1	2	3	4	5
Frequency (Hz)	1.65	4.11	6.16	8.11	12.3
Damping Ratio	0.005	0.013	0.019	0.026	0.039

The full output information is used. The simulated output data of noise-free, and with 5%

noise, 10% noise, 20% noise are considered. The results are show in Table 4.3.

Table 4.3 Results of numerical simulation for full output information

	True Value	Calculated Value			
		no noise	5% noise	10% noise	20% noise
k_1	20	20	20.020	20.002	19.516
k_2	20	20	19.853	20.071	20.567
k_3	20	20	20.448	20.017	20.636
k_4	20	20	18.722	20.973	21.138
k_5	20	20	22.207	17.024	15.003
Error		0.00%	4.10%	4.04%	7.82%

Here, the error is RMS error.

Table 4.3 shows that using PSO the structure can be identified both for the noise-free output data and noise-polluted output data.

4.5.2 Comparison with Genetic Analysis (GA) and Simulated Annealing (SA) Results

To verify the performance and compare it with other global search methods, the results obtained with the usage of the Simulated Annealing (SA) and Genetic Algorithm (GA) are presented in Tables 4.4, along with the results obtained with the PSO for the sake of comparison. The unit of the stiffness value is 100 kN/m.

Table 4.4. Comparison Results of numerical simulation for full output information

	Value	no noise			5% noise			10% noise			20% noise		
		PSO	SA	GA	PSO	SA	GA	PSO	SA	GA	PSO	SA	GA
k_1	20	20	20.000	20.007	20.020	20.020	20.017	20.002	20.002	20.009	19.516	19.516	19.511
k_2	20	20	20.000	19.997	19.853	19.853	19.852	20.071	20.071	20.052	20.567	20.567	20.570
k_3	20	20	20.000	19.958	20.448	20.448	20.479	20.017	20.017	20.076	20.636	20.636	20.660
k_4	20	20	20.000	20.132	18.722	18.722	18.598	20.973	20.972	20.638	21.138	21.138	21.078
k_5	20	20	20.000	19.735	22.207	22.207	22.692	17.024	17.024	17.550	15.003	15.003	15.047
Err		0.00%	0.00%	0.45%	4.10%	4.10%	4.74%	4.04%	4.04%	3.22%	7.82%	7.82%	7.75%

For square competition, these three methods are with the same termination criterion, 1,000 maximum generations; the same upper bound of the search space, twice the actual value of the parameters, lower bound, one tenth of their actual values; and the same random values added as noise.

The analysis of the results contained in Tables 4.4 leads to the following observations:

In general, in the full output information scenario, the PSO performed similarly to the SA and GA in the noise-free case. Also, the PSO performed similarly to the SA and GA at all levels of noise tested. This time full output information was utilized, and the situation with larger meaning using partial output information is studied and described below.

4.6 **Acceleration-Based System Identification with PSO for Partial Output Information**

Suppose that a structure that is able to capture the behavior of the physical system is developed and that this structure depends upon a set of n parameters, contained in a vector $\mathbf{x} = \{x_i\}$ for $i = 1, 2, \cdots, n$. This vector may conclude mass, stiffness, damping ratio et al. Partial output information only can be measured, extremely only one floor acceleration available.

$$\mathbf{a}^M = [a^M(0) \quad a^M(1) \quad \cdots \quad a^M(T)] \tag{4-18}$$

$$\mathbf{a} = [a(0) \quad a(1) \quad \cdots \quad a(T)] \tag{4-19}$$

Compute the error norm of all the simulated outputs of the identified system with respect to those measured from the actual system, defined as:

$$F(\mathbf{x}) = \sqrt{(\mathbf{a}^M - \mathbf{a})(\mathbf{a}^M - \mathbf{a})^T} \tag{4-20}$$

In order to obtain a successful identification, the candidate system must be able to accurately reproduce the output of the physical system for any given input. Therefore, our interest lies in minimizing the error norm of the outputs. Formally, the optimization problem requires finding a vector $\mathbf{x} \in S$, where S is the search space, so that a certain quality criterion is satisfied, namely that the error norm $F: S \to R$ is minimized. If we suppose that the structural damage only causes the change to the story stiffness, $\mathbf{x} = \{x_i\} = \{k_i\}$. Vector $\mathbf{x}^* = \{k_i^*\} = \mathbf{k}^*$ will be called a solution to the minimization problem if $F(\mathbf{k}^*)$ is the global minimum of F in S, or

$$\mathbf{k}^* \in S \big| F(\mathbf{k}^*) \le F(\mathbf{k}) \qquad \forall \mathbf{x} \in S \tag{4-21}$$

The search space S is defined by a set of maximum and minimum values for each story stiffness. It is conceived as an n-dimensional domain delimited by vectors $\mathbf{x}_{max}$ and $\mathbf{x}_{min}$ containing the upper bounds of the n parameters and the lower bounds respectively or

$$S = \left\{ k \in R^n \big| k_{min,i} \le k_i \le k_{max,i} \qquad \forall i = 1, 2, \cdots, n \right\} \tag{4-22}$$

The problem of structural identification is thus treated as an optimization problem.

The PSO is used to optimize $F(\mathbf{k})$ by the algorithm in pseudocode follows:

Initialize population

Do

For $i = 1$ to Population Size

if $F(\vec{k}_i) < F(\vec{p}_i)$ then $\vec{p}_i = \vec{k}_i$

$\vec{p}_g = \min(\vec{p}_{neighbors})$

For $d = 1$ to Dimension

$$v_{id} = v_{id} + \varphi_1(p_{id} - k_{id}) + \varphi_2(p_{gd} - k_{id})$$

$$v_{id} = \text{sign}(v_{id}) \cdot \min(\text{abs}(v_{id}), V_{\max})$$

$$k_{id} = k_{id} + v_{id}$$

Next d

Next i

Until termination criterion is met

4.7 Numerical Simulations for Partial output information

4.7.1 Numerical Verification

In order to verify the performance of the proposed methods, let us analyze the structure described in former sections represented in Figure 4.1, Table 4.1 and 4.2. During this simulation, the partial output information is used. The acceleration at the fifth floor is only used. The simulated output data of noise-free, and with 5% noise, 10% noise, 20% noise are considered. The results are show in Table 4.5.

Table 4.5. Results of numerical simulation for partial output information

	True Value	Calculated Value			
		no noise	5% noise	10% noise	20% noise
k_1	20	20.555	19.153	17.950	22.008
k_2	20	19.457	21.223	22.740	18.576
k_3	20	19.090	20.833	25.899	16.034
k_4	20	20.513	20.853	16.138	30.413
k_5	20	21.018	17.325	22.518	17.936
Error		3.54%	6.43%	17.07%	19.88%

The results contained in Tables 4.4 leads to the following observations:

Even though only the acceleration at one floor is measure, the structure can still be identified both for the noise-free output data and noise-polluted output data. This point is of great advantage because for a building structure it is expensive and almost impossible to measure full output information. Therefore, it helps that the structure can be identified with partial output information.

4.7.2 Comparison with Genetic Analysis (GA) and Simulated Annealing (SA) Results

To verify the performance and compare it with other global search methods, the results obtained with the usage of the Simulated Annealing (SA) and Genetic Algorithm (GA) are presented in Tables 4.6 for partial output information, along with the results obtained with the PSO for the sake of comparison. The unit of the stiffness value is 100kN/m.

Table 4.6 Comparison Results of numerical simulation

for partial output information

	Value	no noise			5% noise			10% noise			20% noise		
		PSO	SA	GA	PSO	SA	GA	PSO	SA	GA	PSO	SA	GA
k_1	20	20.555	19.513	20.522	19.153	17.051	21.576	17.950	17.086	17.201	22.008	16.955	16.845
k_2	20	19.457	20.555	19.485	21.223	25.541	18.807	22.740	24.463	24.298	18.576	29.465	27.960
k_3	20	19.090	20.880	19.183	20.833	26.421	17.058	25.899	30.824	29.245	16.034	18.110	20.581
k_4	20	20.513	19.622	20.292	20.853	19.595	24.663	16.138	15.499	16.082	30.413	37.935	37.319
k_5	20	21.018	18.909	21.403	17.325	12.506	19.867	22.518	17.610	17.079	17.936	15.418	10.028
Error		3.54%	3.39%	3.55%	6.43%	22.81%	10.51%	17.07%	25.09%	23.18%	19.88%	36.92%	38.99%

For square competition, these three methods are with the same termination criterion, 1,000 maximum generations; the same upper bound of the search space, twice the actual value of the parameters, lower bound, one tenth of their actual values; and the same random values added as noise.

The analysis of the results contained in Tables 4.6 leads to the following observations:

In general, in the minimal output information scenario, the PSO performed similarly to the SA and GA in the noise-free case. However, the PSO performed better than the SA and GA at all levels of noise tested. It can be seen that the system identification based on PSO is feasible and advantageous for damage localization and quantification with possibly few response output.

4.7.3 Damage localization and quantification using PSO

The structure described in former sections represented in Figure 4.1, Table 4.1 and 4.2 is used to study the performance of PSO used for damage localization and quantification with partial output information. Both single damage cases and multi damage cases are considered. The various damage severities are also considered. For damage identification, the stiffness of the structure will only decrease from the healthy structure to the damaged structure. Therefore, the upper bound of

the stiffness of the candidate damaged structure can be set as the stiffness of the healthy structure.

The down bound will be set as 10% of the stiffness of the healthy structure.

Table 4.7 Damage Identification for Single-Damage at the 2nd floor

	True Value	Calculated Value		
		no noise	5% noise	10% noise
k_1	20	20.000	20.000	19.995
k_2	18	18.000	18.057	18.100
k_3	20	20.000	20.000	19.996
k_4	20	20.000	20.000	20.000
k_5	20	20.000	20.0000	20.000
Error		0	0.058%	0.11%

Table 4.8 Damage Identification for Single-Damage at the 4nd floor

	True Value	Calculated Value		
		no noise	5% noise	10% noise
k_1	20	20.000	20.000	20.000
k_2	20	20.000	20.000	19.831
k_3	20	20.000	19.713	20.000
k_4	16	16.000	16.139	16.676
k_5	20	20.000	20.000	18.902
Error		0	0.44%	2.02%
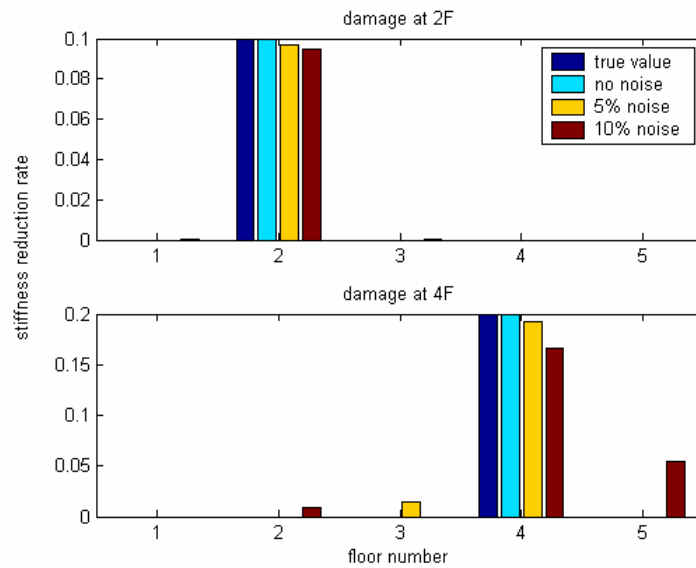
Figure 4.2 Damage identification for single-damage cases

Firstly, the single-damage cases are studied. Both noise-free and noise-polluted output information are used. The results of single damage cases with 10% stiffness reduction at the second floor and 20% at the fourth floor are in Table 4.7 and 4.8 illustrated in Figure 4.2. It is observed that there is influence in a whole on the estimates by noise presence even though there is no influence for some certain values

Table 4.9 Damage Identification for Double-Damage at the 3rd and 5th floors

	True Value	Calculated Value		
		no noise	5% noise	10% noise
k$_1$	20	20.000	20.000	20.000
k$_2$	20	20.000	20.000	20.000
k$_3$	18	17.972	17.992	18.373
k$_4$	20	20.000	19.904	20.000
k$_5$	19	19.370	19.131	17.512
Error		0.41%	0.24%	1.92%

Table 4.10 Damage Identification for Double-Damage at the $2nd$ and 4th floors

	True Value	Calculated Value		
		no noise	5% noise	10% noise
k_1	20	20.000	20.000	20.000
k_2	19	19.000	18.975	19.002
k_3	20	20.000	19.691	20.000
k_4	17	17.000	17.440	16.545
k_5	20	20.000	20.000	20.000
Error		0.00%	0.81%	0.48%
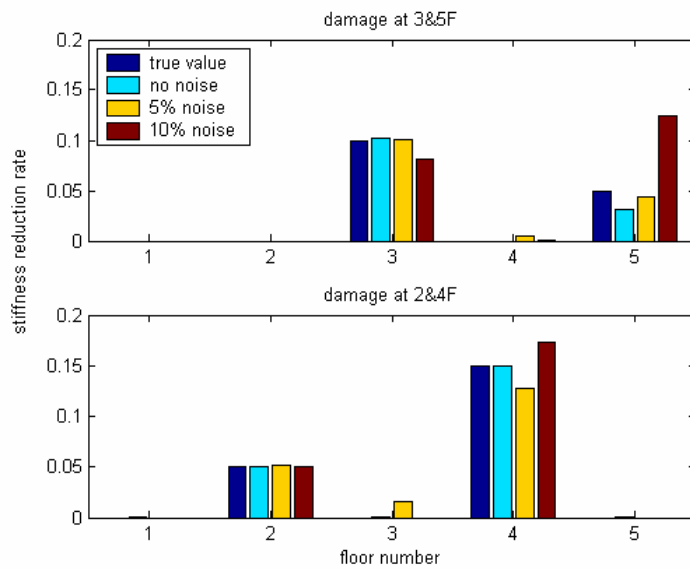
Figure 4.3 Damage identification for double-damage cases

Secondly, the double-damage cases are studied. The result of double-damage case with both 10% stiffness reduction at the third floor and 5% at the fifth floor is in Table 4.9. The result of double-damage case with both 5% stiffness reduction at the second floor and 15% at the fourth floor is in Table 4.10. These two tables are illustrated in Figure 4.3.

Table 4.11 Damage Identification for Multi-Damage at 2, 3&5F

	True Value	Calculated Value		
		no noise	5% noise	10% noise
k_1	20	20.000	20.000	20.000
k_2	17	17.038	16.895	16.943
k_3	18	17.958	18.315	18.142
k_4	20	20.000	20.000	20.000
k_5	19	19.074	17.121	19.575
Error		0.16%	2.45%	0.82%

Table 4.12 Damage Identification for Multi-Damage at 1, 3&4F

	True Value	Calculated Value		
		no noise	5% noise	10% noise
k_1	18	18.000	18.032	17.887
k_2	20	20.000	20.000	20.000
k_3	17	17.000	16.873	17.763
k_4	19	19.000	19.177	17.868
k_5	20	20.000	20.000	20.000
Error		0.00%	0.36%	2.14%
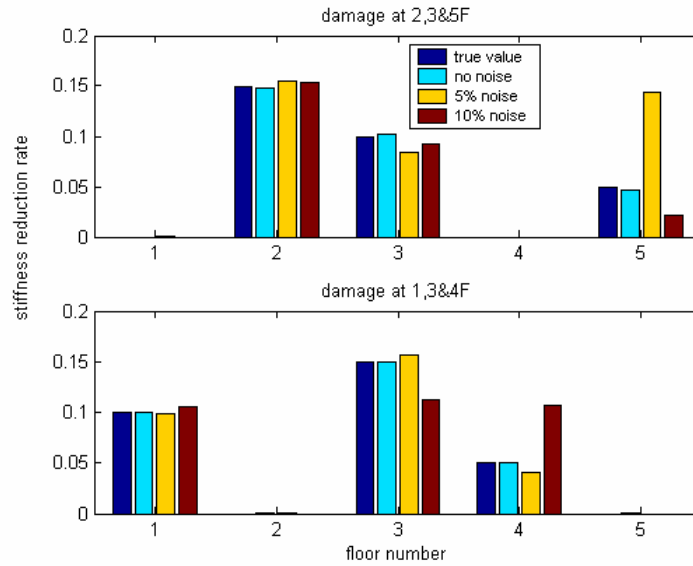
Figure 4.4 Damage identification for triple-damage cases

Table 4.13 Damage Identification for Multi-Damage at 1, 3, 4&5F

	True Value	Calculated Value		
		no noise	5% noise	10% noise
k_1	18	18.000	18.174	17.967
k_2	20	20.000	20.000	20.000
k_3	17	17.000	16.635	17.057
k_4	19	19.000	19.556	19.279
k_5	16	16.000	15.571	16.000
Error		0.00%	1.69%	0.41%

Table 4.14 Damage Identification for Multi-Damage at 1, 2, 3&5F

|	True Value	Calculated Value		
		no noise	5% noise	10% noise
k_1	18	18.298	18.385	17.526
k_2	19	18.651	18.693	19.469
k_3	17	16.630	16.444	18.412
k_4	20	20.000	19.362	20.000
k_5	16	16.000	18.329	13.185
Error		2.06%	4.68％	5.74%
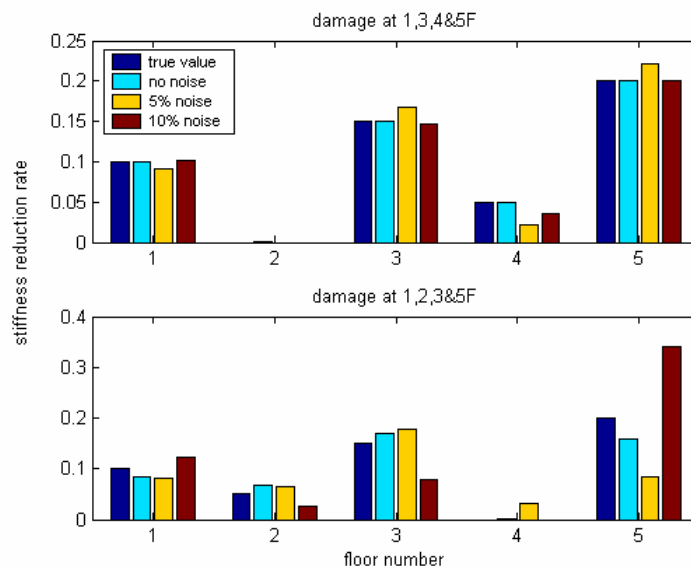
Figure 4.5 Damage identification for multi-damage cases

Finally, the multi-damage cases are studied. The result of multi-damage case with 15% stiffness reduction at the second floor, 10% at the third floor and 5% at the fifth floor is in Table 4.11. The result of multi-damage case with 10% stiffness reduction at the first floor, 15% at the

third floor and 5% at the fourth floor is in Table 4.12. These two tables are illustrated in Figure 4.4. The result of multi-damage case with 10% stiffness reduction at the first floor, 15% at the third floor, 5% at the fourth floor and 20% at the fifth floor is in Table 4.13. The result of multi-damage case with 10% stiffness reduction at the first floor, 5% at the second floor, 15% at the third floor and 20% at the fifth floor is in Table 4.12. These two tables are illustrated in Figure 4.5.

The analysis of the results contained in Tables 4.7-4.14 and Figures 4.2-4.5 leads to the following observations:

Even though only the acceleration at one floor is measure, the structural damage can be localized and quantified both for the noise-free output data and noise-polluted output data. This point is of great advantage because for a building structure it is expensive and almost impossible to measure full output information. Therefore, it helps that the structural damage can be identified with minimal output information.

4.8 Summary

The method named as Acceleration-Based Damage localization and quantification of Building Structures with Partial Swarm Optimization is summarized as follows:

- The damage localization and quantification for building structures is through the identification of structural stiffness.
- The system identification is realized by transferring to optimization problem..
- The Partial Swarm Optimization (PSO) is utilized to obtain the minimize the error between the actual physical measured response of a structure and the simulated response of a numerical model.
- The minimal output information, extremely only acceleration at one floor, is needed for damage identification.
- The healthy structure is firstly identified by PSO given the full output information or partial output information.
- With very limited response measurement, the structural damage can be identified for

both single-damage cases and multi-damage cases by setting the stiffness upper bound of search as the stiffness of the healthy structure. The damage can be localized and quantified for different damage severities.

CHAPTER 5

Experimental Verification and Application

5.1 Introduction

To better assess the performance of the distributed computing SHM strategy proposed above, experimental validation of the proposed approach has been conducted. Following the detailed description of the experimental setups, experimental results employing the distributed computing SHM strategy are provided which show the proposed approach to be very promising. Two different structural models, small model and large steel model, are utilized to verify the proposed approach. A five-story structure was initially healthy with all original columns intact. Two columns of one floor were then replaced by weak columns (of the same material and integrity as healthy columns, but with smaller cross-sectional area) to simulate single-damage case. The double-damage case was simulated by replacing the columns of two different floors. Under the basement of the structure, there were some bearings so that the structure could have a ground motion. Another steel structure on shake-table was used to verify the proposed method. It was also a five-story frame structure, with height 5 m and floor plate 3 m x 2 m. The damages were introduced by re-moving the splices at different location, loosing the bolts and damaging the beams.

5.2 Small model

5.2.1   Experimental Setup

A series of experiments were performed to verify the performance of our proposed approach.

The small model structure is depicted in Figure 5.1.

Figure 5.1 Experimental Setup of Small Model

This experimental setup imitates a five-story shear frame buildings. The story mass is decided by the aluminium floor slab which is 2.43 kg for each floor. The story stiffness is decided by the bronze plate spring which is $0.0025 \times 0.03 \times 0.24$ m^3. The Young's modulus of bronze is 1×10^{11} N/m^2, so the interfloor stiffness is 1.3563×10^4 N/m. The structure was initially healthy with all original columns intact.

Figure 5.2 Healthy and Damage Columns

The damage was introduced by replacing columns by weak columns, which are $0.003 \times 0.006 \times 0.24$ m^3, shown in Figure 5.2. By replacing two columns in the story, the story stiffness was reduced by 33%.
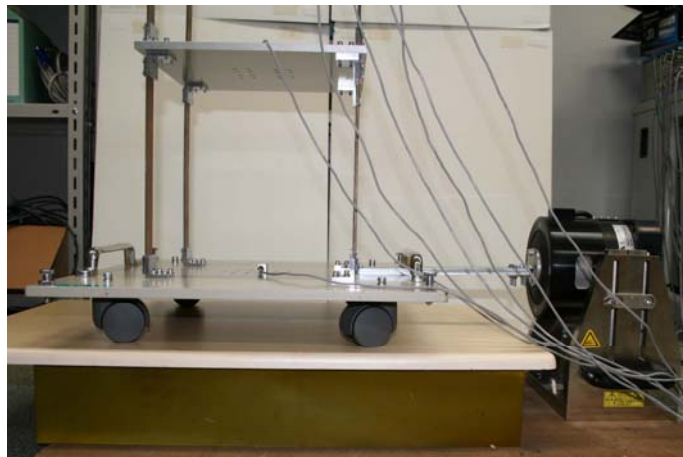
Figure 5.3 Bearings & Shaker

Under the basement of the structure, there were some bearings so that the structure could have a ground motion. The force input to the structure is provided with an electrodynamic shaker as

shown in Figure 5.3. One acceleration sensor was installed on the basement to measure the ground motion. The sensor installed on each floor plate was used to measure the acceleration response of each floor.

5.2.2   Procedure

The five-story structure was firstly healthy with all original columns. The force input to the structure was provided by the shaker to obtain the acceleration data of the healthy structure. Two acceleration sets were recorded, one of which was used as training data to establish the AENN. The other set was healthy test data used for comparison with damage data.

Then, two columns of one floor were replaced by weak columns to simulate single-damage case. The shaker provided excitation again so that the accelerometers could measure the acceleration data of the single-damage structure.

Finally, double-damage case was simulated by replacing the columns of two different floors. The structure was excited by the shaker again to acquire the acceleration data of the double-damage structure. One typical acceleration signal measured is as in Fig 5.4
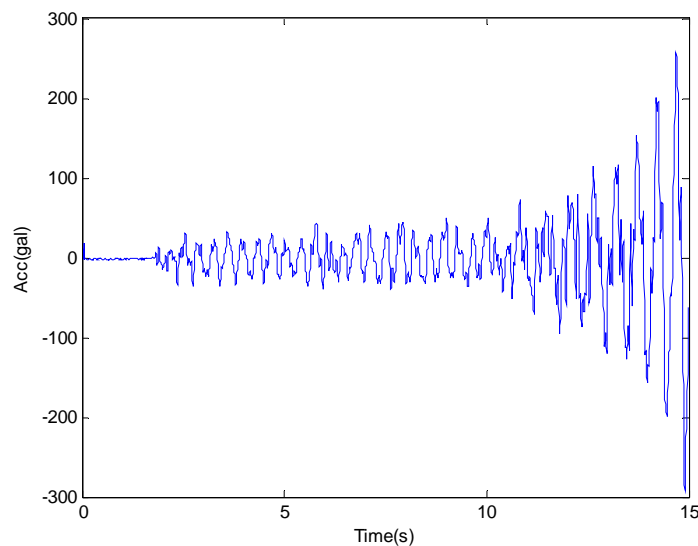
Figure 5.4 One typical acceleration signal

5.2.3 Damage Identification Results

The first phase, damage occurrence alarm by AENN (Figure5.5), was performed using full-floor-acceleration, followed by using the fifth floor acceleration alone (Figure 5.6).

Measured Accelerations of floors at T_{k-n}

Measured Acc of ground delayed at T_{k-n+1}

Measured Acc of different floors at T_{k-1}

Measured Acc of excitation at $\begin{matrix} T_{k+m} \\ \vdots \\ T_{k+1} \\ T_k \end{matrix}$

Measured Accelerations of different floors at T_{k+m}
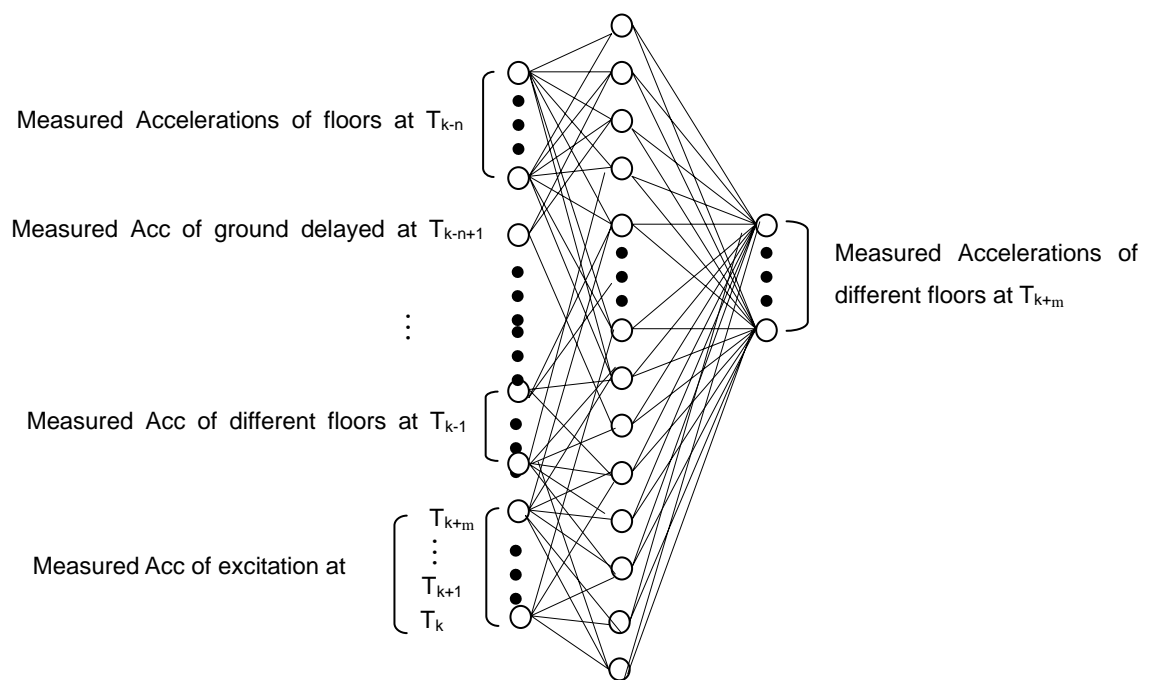
Figure 5.5 Multi-output AENN for experimental data
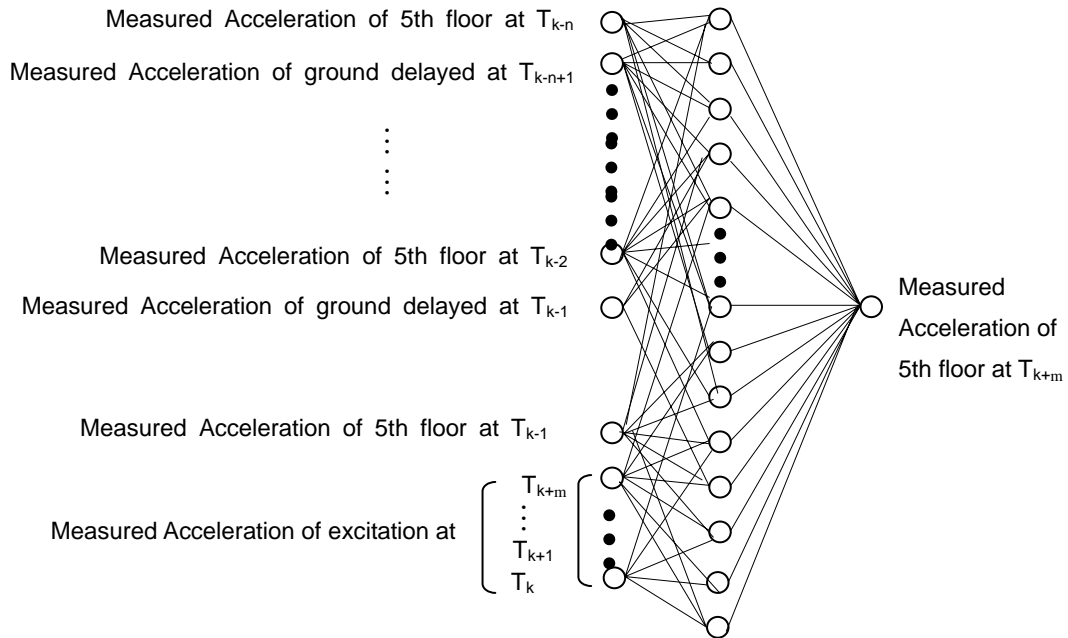
Figure 5.6 Single-output AENN for experimental data

Figure 5.7 is the prediction of the test data for the healthy structure using the trained multi-output AENN emulator. Since the value is normalized, there is no unit for acceleration here.
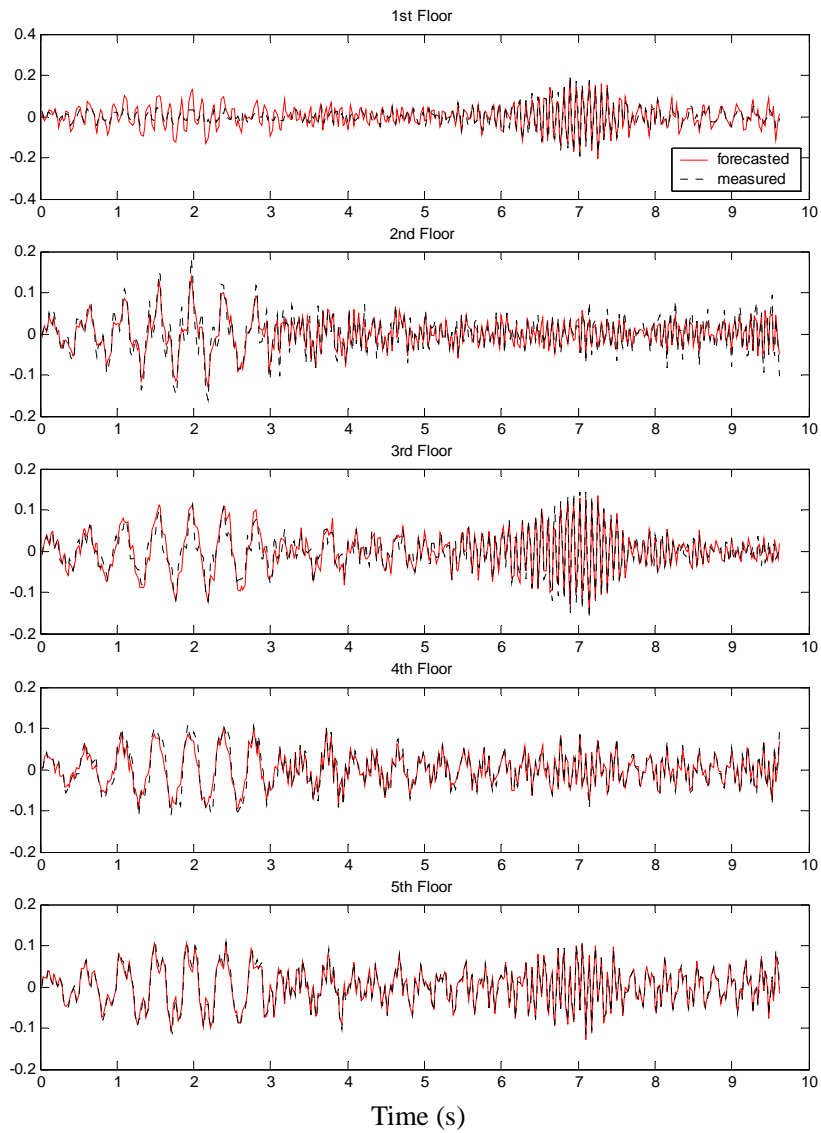
Figure 5.7 Prediction of test data for healthy structure using full accelerations

Figure 5.8 is the prediction of the test data for the healthy structure using the trained single-output AENN emulator. Since the value is normalized, there is no unit for acceleration here.
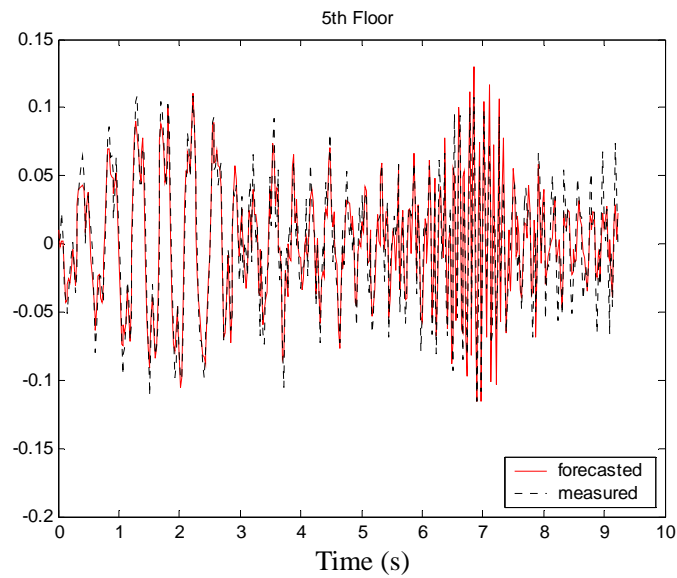
Figure 5.8 Prediction of test data for healthy structure using acceleration at 5F

Figure 5.9 shows RRMS errors of healthy, single-damage, double-damage and triple-damage structures.

The result of RRMS errors of healthy, single-damage, double-damage structures using multi-output AENN is shown in Figure 5.9 (a), and the result using single-output AENN is shown in Figure 5.9 (b). These RRMS errors represent the difference between the output of the neural network and the real dynamic response, thus providing an indication of structural damage. The magnitude of the RRMS error corresponds to the severity of damage, and therefore can be looked at as a damage occurrence alarm index. Using one floor acceleration is effective, as well as multi-floor acceleration. This shows high flexibility with this method.
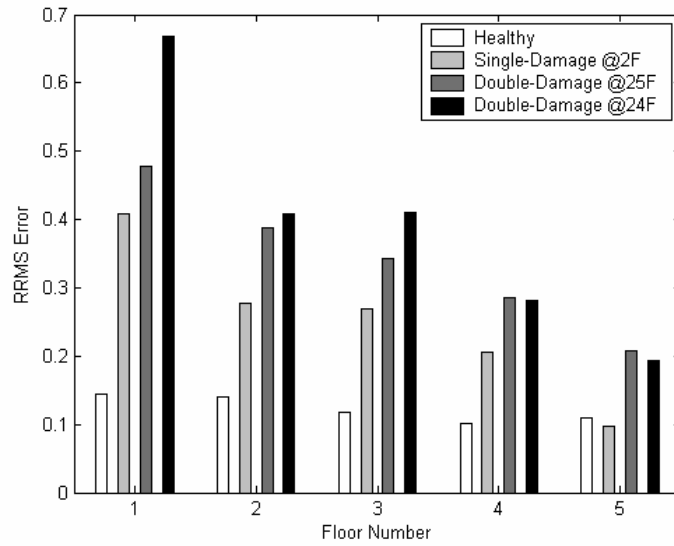
(a) Multi-input AENN
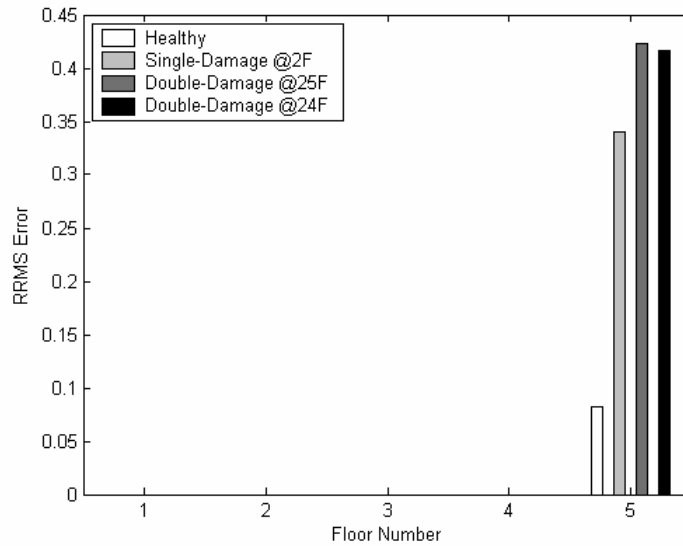
(b) Single-input AENN

Figure 5.9. Damage alarm: results of first phase
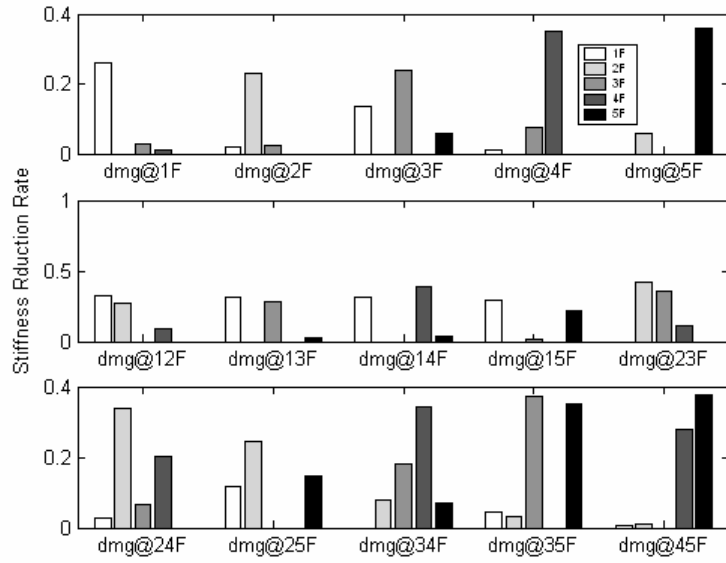
(a) Full acceleration information
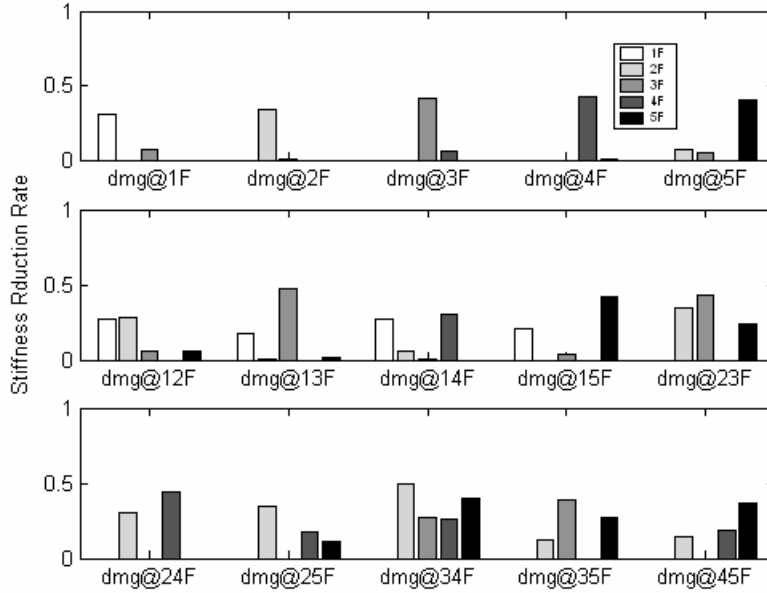
(b) Partial acceleration information

Figure 5.10. System ID by PSO: results of second phase

The second phase was performed after knowing there was some damage in the structure. All cases of single-damage cases and double-damage cases were considered and depicted in Figure 5.8. This phase was also studied using full-floor-acceleration, followed by using the fifth floor acceleration only. Figure 5.10 (a) is the result with full acceleration information, and Figure 5.10 (b) is the result with partial acceleration information. Figure 5.8 shows, in general, the damage localization and quantification can be determined by the phase. Naturally the result using full information is slightly better than using partial information.

5.3 Experiment Using Large Steel Model

5.3.1 Experimental Setup
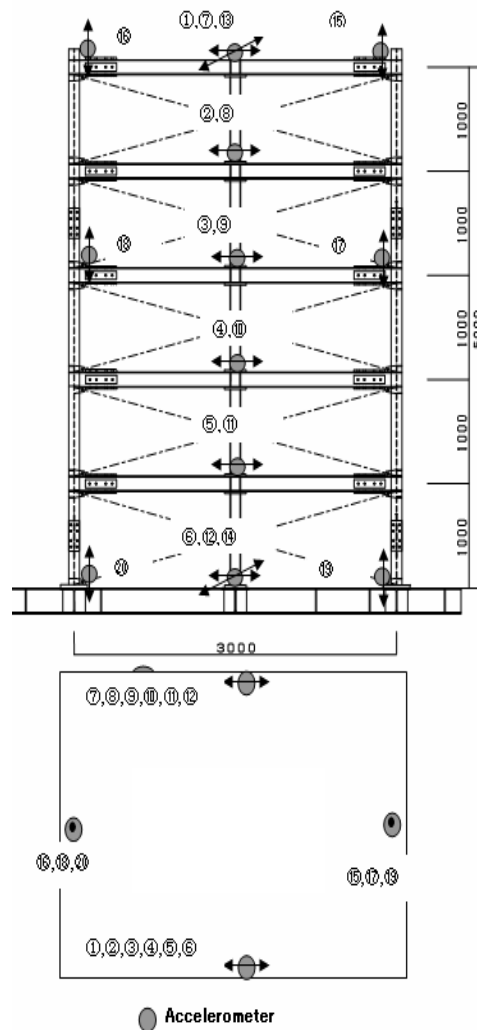
Figure 5.11. Shake-table Experimental setup

A series of experiments were performed for a different 5-story steel structure using a shake table (Figure 5.11) to further verify the proposed method.

This 5-story steel frame structure had a height of 5 m and a floor plate 3 m×2 m. The section of column is H148×100×6/9(SS400), beam H148×100×6/9(SS400), middle column H100×50×5/7(SS400). The weight of each floor is 2.57 ton.

The sensors are 1G accelerometer made by Kyowa Electronic Instruments Co., Ltd. Japan. The model is AS-1GB. The frequency response (at 23 ℃) is DC to 40 Hz, ±5%. The resonance frequency (App.) is 70 Hz.

The shake table is in the Building Research Institute (BRI), Ministry of Construction, Japan. The maximal bearing capacity is 20 ton. The maximal amplitude of shake is ±150 mm. The maximal acceleration is ±1 G. The maximal input force is 30 ton. The range of frequency is 0-50 Hz.

5.3.2   Procedure

First of all, the white noise force input to the structure was provided by the shake table to obtain the acceleration data of the healthy structure.

Damage was introduced by removing splice, loosening bolts and damaging beams at different locations. In every damage case, the white noise force input to the structure was provided by the shake table to obtain the acceleration data of the damaged structure.

Considering the damage would cause the stiffness reduction at the horizontal direction in Figure 5.11, the input provided by shake table was at the same direction so the acceleration at the direction of sensor number 6 in Figure 5.11 was utilized. Moreover the acceleration at the direction of sensor number 14 in Figure 5.11 was checked to be small enough to be ignored. The PGA of the white noise force input is 0.1 G.

One typical acceleration signal measured is as in Figure 5.12
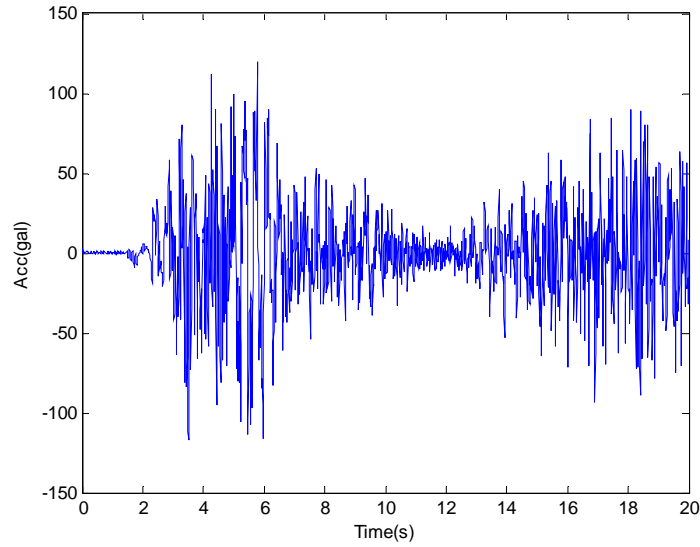
Figure 5.12 One typical acceleration signal

5.3.3 Damage Identification Results

The first phase, damage occurrence alarm by AENN, was performed. The detection results for this redundant experiment are shown in Figure 5.13.
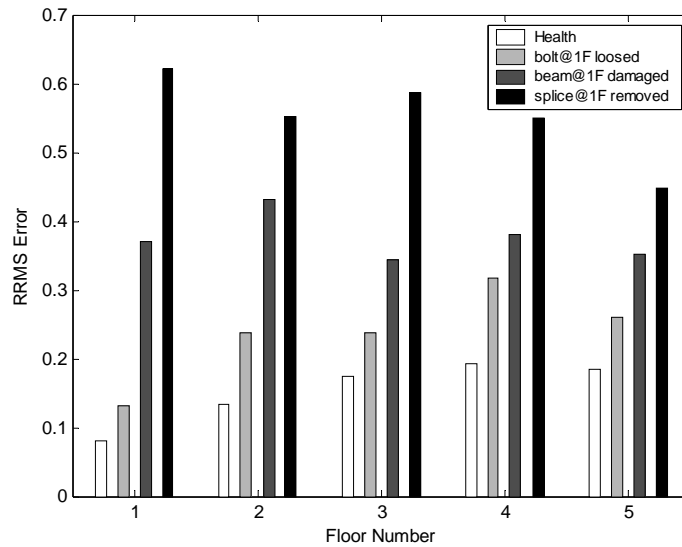
Figure 5.13 RRMS errors of healthy and damaged structure cases

The analysis of the results contained in Figure 5.13 leads to observations in concordance with the first experiment: The value of RRMS error can be considered as a damage occurrence alarm index. The value of the RRMS error is up along with the damage severity increases. We can obtain the structural damage alarm by observing this index. As the acceleration information of the structure is needed only here with the necessity of structural modal information, we may conclude that the AENN-based damage alarm method can indeed provide damage alarm to realistic problems.
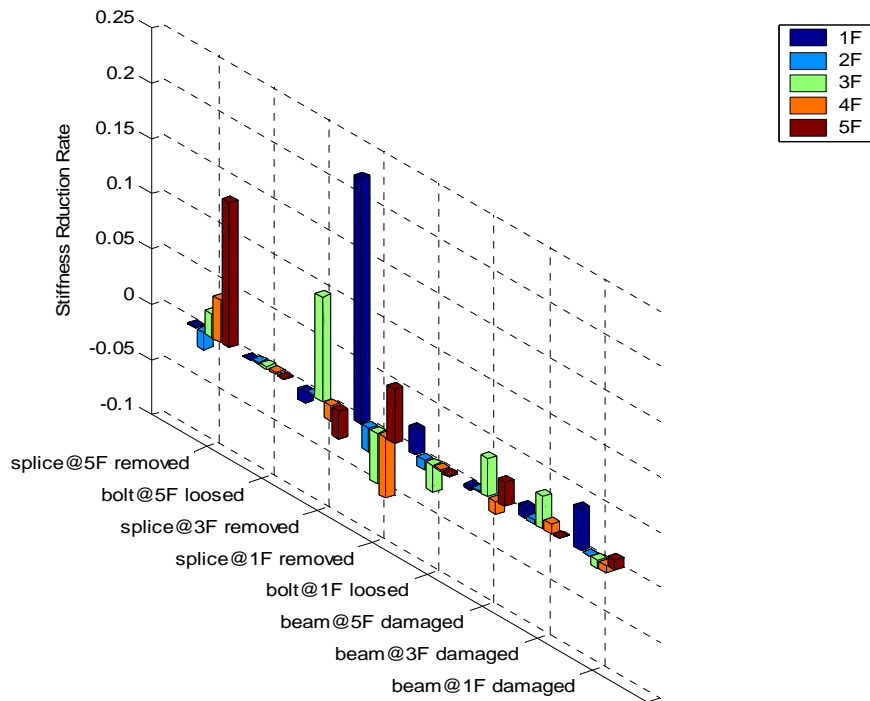
Figure 5.14. Damage Localization Results of Shake-table experiment

The second phase was performed after knowing there was some damage in the structure. The identification results are shown in Figure5.14. The analysis of the results leads to the following observations: the damage location was identified for the different damage cases by the obtained stiffness reduction rate. From the figure, we may conclude that the method is indeed applicable to realistic problems.

5.4 Application to real building

5.4.1 Description of the real building

This study proposed the first application of AENN to real buildings.

Table 5.1. Data used for structural evaluation

	Date	Maximal value of acceleration in Y direction (cm/s^2)			
		1F	5F	10F	14F
Training data	Oct. 15, 2003	22.1	26.4	22.3	18.4
Test data 1	Nov. 12, 2003	11.9	20.4	19.7	12.4
Test data2	Jul. 23, 2005	35.1	34.3	39.7	41.0

The applied building, Nikken Sekkei Tokyo Building located in Iidabashi of Tokyo, was constructed in March, 2003. It is 60 meters high, with one-story underground and 14-story overground. The accelerators were installed on the B1F, 1F, 5F, 10F and 14F to measure the acceleration time histories of horizontal two directions and vertical direction. Three sets of acceleration time histories shown in Table 5.1 would be used for evaluation. The first two identified natural frequencies of this building in horizontal Y direction are about 0.7 Hz and 2.3 Hz.

5.4.2 Evaluation of Structure by AENN with the Performance of Filter

The proposed AENN was established for structural evaluation of this real building.

Here, the acceleration time histories of the first floor was considered as the acceleration of

ground which would be inputted into the AENN delayed by time T, and the acceleration of the 5, 10, 14th floor was considered as the normal floor, as in Figure 5.15.

Accelerations of 5, 10 and 14th floors at time step T_{k-2}

Acceleration of 1st floor at $T_{k-1}+T$

Accelerations of each 5, 10 and 14th floors at time step T_{k-1}

Acceleration of 1st floor at T_k+T

Accelerations of 5, 10 and 14th floors at time step T_k+T
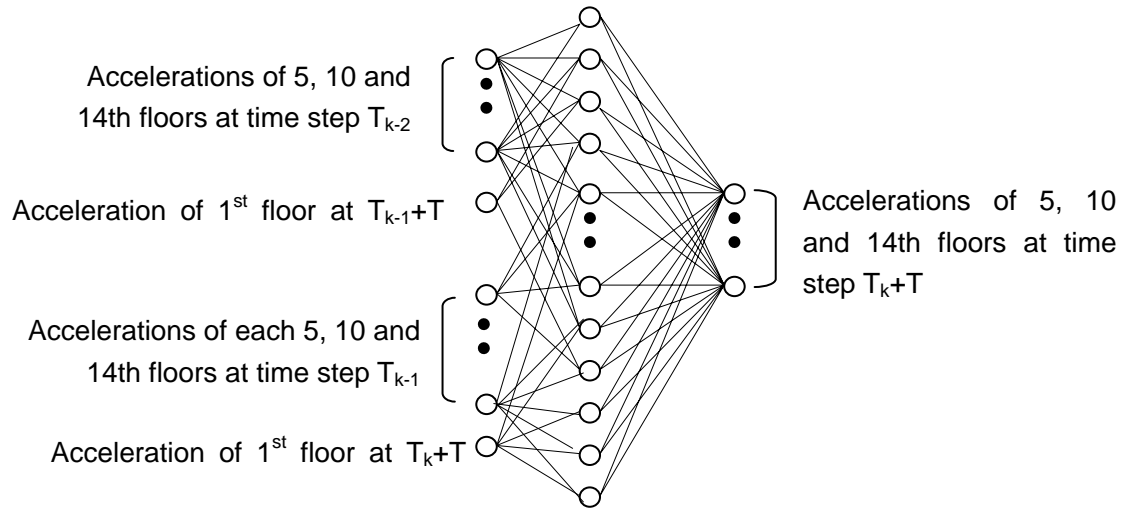
Figure 5.15. AENN Applied to the Real Building

For a real building, the measured response is unavoidably polluted by noise, which would decrease the accuracy of the structural evaluation. In order to handle this problem, filtering was performed to the measured accelerations. Firstly, lowpass Butterworth filter whose cutoff frequency was 0.8 Hz was applied to obtain the signal near the first-order natural frequency of structure. Then, bandpass Butterworth filter whose passband frequency was [1.8, 3] Hz was applied to obtain the signal near the second-order natural frequency of structure. At last, the results of evaluation through these two filters were combined linearly to obtain the final structural evaluation, as in Figure5.16. Since the value is normalized, there is no unit for acceleration here.
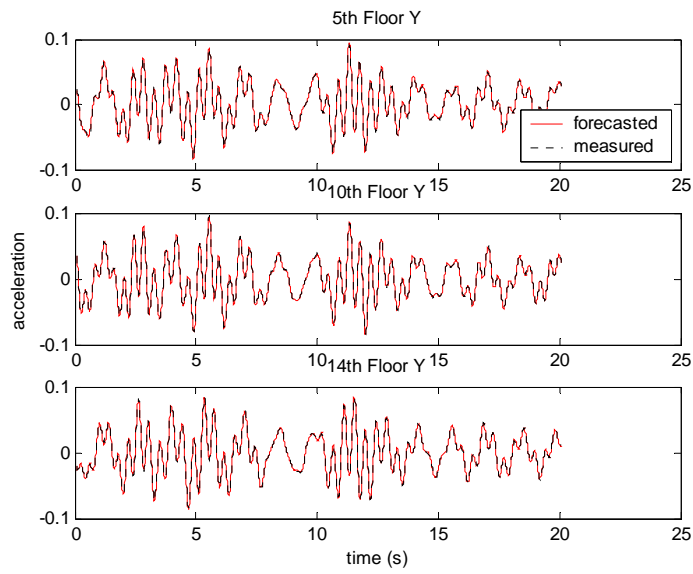
(a) test data1 on Nov. 12, 2003
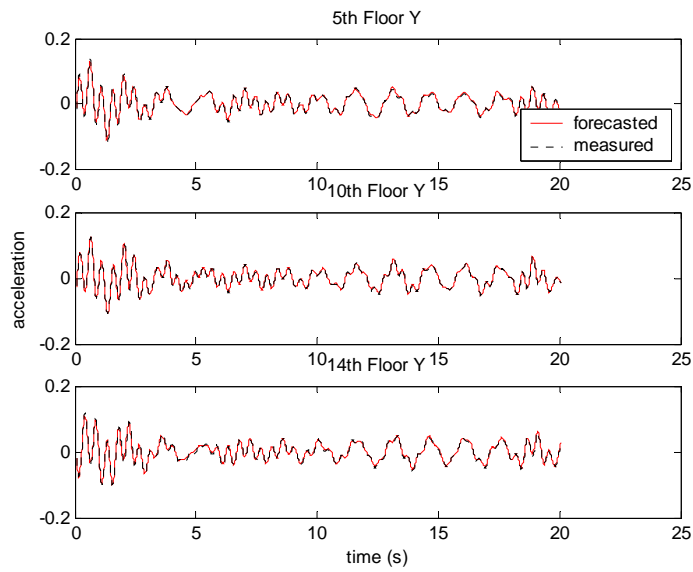
(b) test data2 on Jul. 23, 2005

Figure 5.16. Comparison between the output of neural network and the measured value
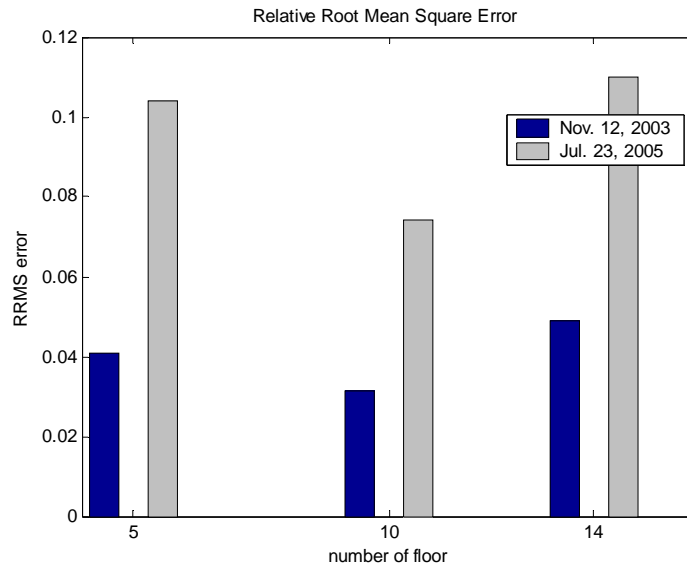
Figure 5.17. RRMS errors for test data1 and test data2

The RRMS error values were calculated for test data1 and test data2, respectively (Figure 5.17). Due to only one-month interval between the dates of the training data and test data1, it is reasonable to suppose there would not be much deterioration of this building structure, which means the RRMS error for test data1 would be a small value. However, after almost two years passed, when the test data2 was measured, the thought of some deterioration and change occurring to the building structure could be acceptable and of high possibility, which means the RRMS error for test data2 would be a larger value than before. Therefore, the error value of test data2 should be quite larger than that of test data2. These are consistent with the result shown in Figure 5.17.

It is verified that the proposed acceleration-based approach could implement structural evaluation effectively and economically. This characteristic makes the approach very useful for practical application. Such far this building has not apparent localized damage, so only the first phase of the proposed approach was implemented here.

5.5 Summary

In this chapter, the computing strategy for SHM was experimentally verified using two structural models, small model and large steel model. A five-story structure was initially healthy with all original columns intact. Two columns of one floor were then replaced by weak columns (of the same material and integrity ad healthy columns, but with smaller cross-sectional area) to simulate single-damage case. The double-damage case was simulated by replacing the columns of two different floors. Under the basement of the structure, there were some bearings so that the structure could have a ground motion. Another steel structure on shake-table was used to verify the proposed method. It was also a five-story frame structure, with height 5m and floor plate 3m x 2m. The damages were introduced by re-moving the splices at different location, loosing the bolts and damaging the beams. Both single and multiple damage scenarios were studied.

The experimental results have shown that the proposed approach can successfully monitor structural health only utilizing measured acceleration information for various damage scenarios under different excitation conditions. The proposed approach was shown promising for application of SHM on buildings.

This study proposed the first application of AENN to real buildings. The applied building, Nikken Sekkei Tokyo Building located in Iidabashi of Tokyo, 60 meters high, with one-story underground and 14-story overground. It is verified that the AENN could implement structural evaluation effectively and economically. This characteristic makes the approach very useful for practical application.

At the first phase, the index RRMS error can provide the damage alarm even for small damage based on the verification results. During the steel structure experiment, loosing bolt only caused less than 5% stiffness reduction. In that case by observing RRMS error damage alarm can be obtained. However, the localization and quantification of the damage are meant to be decided at the second phase, which was verified by the two experiments described in this chapter.

CHAPTER 6

Conclusions and Future Studies

6.1 Conclusions

Damage identification of structures using pattern classification and direct identification of structural parameters from dynamic responses were addressed in this dissertation. The emphasis was placed on direct identification of structural parameters from dynamic responses.

This research presented a possible solution for damage identification of structures using pattern classification methods with the goal of using possibly least data. Two steps were included in the damage identification process. The damage location was identified in the first step using Parzen-window approach, while the corresponding damage degree was estimated in the second step using feed-forward back-propagation neural network. A series of numerical simulations were conducted to verify the performance of our proposed approach. The measured structural vibration responses data always contain noise. The output inevitably has some errors when the data with noise was input into the classifiers network. The approach was thus enhanced to have stability against such noise by considering variations in signals. The results of numerical simulations showed that by the approach the structural damage could be identified and identification accuracy could be improved by randomness injected. An appropriate range of random ratio was proposed corresponding to modal parameters with various noise ratios. In order to implement the theory in practical applications, a series of vibration experiments for five-story shear frame structure were conducted to verify the performance of the approach. The results show that for shear buildings,

damage degree and extent can be determined through measuring the frequency change.

The backbone of this dissertation is the direct identification of structural parameters from dynamic responses. An evaluation approach for building structures under earthquakes was proposed to provide damage alarm and detailed damage information. It is a time-domain evaluation procedure capable of alarming, localizing and quantifying damage using limited acceleration measurements. The technique is a combination of the damage detection based on acceleration-based emulator neural network (AENN) and the system identification using the particle swarm optimization (PSO).

To implement the concept, a two-phase approach is used.

In the first phase, the AENN used for emulating the structural response was tuned to properly model the hysteretic nature of building response. This approach takes into account ground acceleration by including it in the input layer up to the most recent time step. It requires only a limited number of acceleration time histories and can be applied to single or multi-output systems. Furthermore, we found that increasing the previous time steps of the acceleration can effectively reduce the necessary number of acceleration histories at different floors. This, and the minimal requirement of only a single sensor, gives the method high practicability and flexibility. Input excitations are not limited, i.e., the structures can be under diverse excitations, even very small impacts. Based on numerical simulation of a five-story shear structure, appropriate parameters of the neural network emulators were suggested. The efficacy of the approach was studied by comparing healthy and damaged structures. Its generality was verified by considering different earthquake accelerations. Experiments using two five-story shear structure models were performed, and the effectiveness of the proposed approach was well verified. In our proposed evaluation approach, alarms of damage occurrence can be obtained practically and economically using readily available acceleration time histories only.

After knowing the damage occurrence, the next phase was necessary to be performed to determine the damage location and quantity. Most currently available damage localization approaches were mostly based on pattern recognition methods to classify the different damage

location. However, such approaches need analytical data for all damage case situations, which can be computationally expensive and even impossible. Therefore, the system identification is utilized for damage determination. In this paper the system identification problem was formulated as an optimization problem using the PSO.

A series of numerical simulations were carried out to evaluate the performance of this two-phase approach. The damage alarm can be accurately obtained only using the acceleration information of the healthy and damaged structures without the necessary of structural model information. Also the damage localization and quantification can be obtained in the following phase.

In order to prove that the method is indeed applicable to realistic problems, the computing strategy for SHM was experimentally verified. Two different structural models, small model and large steel model, are utilized to verify the proposed approach. A five-story structure was initially healthy with all original columns intact. Two columns of one floor were then replaced by weak columns (of the same material and integrity ad healthy columns, but with smaller cross-sectional area) to simulate single-damage case. The double-damage case was simulated by replacing the columns of two different floors. Under the basement of the structure, there were some bearings so that the structure could have a ground motion. Another steel structure on shake-table was used to verify the proposed method. It was also a five-story frame structure, with height 5m and floor plate 3m x 2m. The damages were introduced by re-moving the splices at different location, loosing the bolts and damaging the beams. Both single and multiple damage scenarios were studied. The experimental results have shown that the proposed approach can successfully monitor structural health only utilizing measured acceleration information for various damage scenarios under different excitation conditions. The proposed approach was shown promising for application of SHM on buildings.

This study proposed the first application of AENN to real buildings. The applied building, Nikken Sekkei Tokyo Building located in Iidabashi of Tokyo, 60 meters high, with one-story underground and 14-story overground. It is verified that the AENN could implement structural

evaluation effectively and economically. This characteristic makes the approach very useful for practical application.

6.2 Future Studies

Although this research has successfully addressed some of the challenges for application of damage identification algorithms to buildings, several questions remain. A few directions for further research in the future are presented in this section.

6.2.1 Extension of the two-phase approach to more complicated structures

It is important to extend the proposed two-phase approach to more complicated structures. The proposed approach has been shown to work well for shear structures. However, real world consists of different types of structures. It is desirable to extend the proposed approach to handle more complicated structures. It would be of special meaning if the proposed approach can apply on such structures as bridges, TV towers and so on.

The essence of the extension is how to apply the second phase to more complicated structures. As the first phase do not need any structural model information, it will be convenient to implement this phase to various structures. However, for the second phase, the problem on that calculation cost will arise since the measured responses need to find the matching responses provided by calculated model. Therefore, how to simplify the procedure and save calculation cost will be the key point to implement the extension of the proposed two-phase approach to more complicated structures.

6.2.2 Reliability Analysis

Reliability analysis should be performed to better assess the efficacy of the proposed approach in practice. Many uncertainties exist when detecting damage under real conditions. Excitations of real structures can be quite different from the simulated ones in numerical examples and

experiments. Environmental conditions (e.g. temperature, humidity contents, etc.) can change from time to time. Development of analytical model for real structures is certainly more difficult than modelling relatively simpler structures in laboratory. Therefore, modelling errors are inevitable. All these factors create uncertainties which affect the performance the proposed approach. Modeling these uncertainties and evaluating their effects on the performance of the proposed approach using numerical methods, e.g. Monte Carlo simulation, is certainly desired and very useful for better understanding this approach.

6.2.3 Implementation of the two-phase approach on smart sensor networks

In the field of structural health monitoring, sensors and sensor networks research and designing are attracting a keen attention. Embedding the damage identification algorithm into sensors or sensor networks is of great meaning.

For the proposed time domain damage identification technique, it would be of advantage and convenience that the approach utilizes the acceleration directly. However, it would have some challenges for application of the second phase because at in this stage the structural model is needed. The simplification work will be needed to ensure the computational cost and time remain at a reasonable level.

6.2.4 Performance-based SHM strategy using long-term monitoring data

There are still many challenges in the field of SHM, especially in civil engineering. We can get the good results from simulation, and maybe we can also obtain good results from experiments. However how about the real structure, in which there are so many uncertainties? Just in one day, the signal measured from real structures can change much. And for many large structures, even through we can know there is damage in one of members, who cares if there is damage in only one of trusses? We already did much on modal analysis or system identification which is from the angle of structures. Are there any other angles we can get on SHM, like performance-based monitoring, just form the data themselves, considering there are already a lot of system installed

and huge long-term performance data are readily available?

And what is the appropriate definition of damage? Of course crack is damage. Structural deterioration is damage. Can we also call the structure reliability change damage? Can we assure the structural reliability from the analysis of performance data to see the reliability reduction even through no apparent damage occurs so that it will be much easier to let people see the real meaning and real role of the SHM system? Therefore, there will be more apparent economic significance of the SHM field research and development.

REFERENCES

- Abdelghani, M., Verhaegen, M., Van Overschee, P., and De Moor, B., "Comparison study of subspace identification methods applied to flexible structures", *Mechanical System and Signal Processing*, 12, 679-692, 1998.

- Adams, D. E. and Farrar, C. R., "Application of Frequency Domain ARX Features for Linear and Nonlinear Structural Damage Identification", *NDE for Health Monitoring and Diagnostics*, San Diego, CA, USA, 4702-19, 2002.

- Aktan A. E., "Modal testing for structural identification and condition assessment of constructed facilities", Proceesings of 12th IMAC: 462-468, 1994.

- Allen, D. W., Sohn, H., Worden, K. and Farrar, C. R., "Utilizing the Sequential Probability Ratio Test for Building Joint Monitoring," *SPIE's 7th Annual International Symposium on NDE for Health Monitoring and Diagnostics*, San Diego, CA, USA, March 17-21, 2002.

- Amaravadi, V., Rao, V.S., Mitchell, K., et al., "Structural Integrity Monitoring of Composite Patch Repairs Using Wavelet Analysis and Neural Network", *NDE for Health Monitoring and Diagnostics*, San Diego, CA, USA,4701-17, 2002.

- Amizic, B., Rao, B., Amarvadi, V. and Derriso, M., "Two-dimensional wavelet mapping techniques. for damage detection", *Smart Structures and Materials*, San Diego, CA, USA,4693-32, 2002.

- Angeline, P., "Evolutionary optimization versus particle swarm optimization: Philosophy and performance differences", *In V. W. Porto, Saravanan, N., Waagen, D., and Eiben, A. E. (Eds.), Evolutionary Programming VII*, Berlin: Springer, 601-610, 1998.

- Balis Crema, L., and Mastroddi, F., "Frequency-domain based approaches for damage

detection and localization in aeronautical structures", *Proceedings of the 13th International Modal Analysis Conference*, Florida, U.S.A., 1322-1330, 1995.

● Banks, H. T., Inman, D. J., Leo, D. J., and Wang, Y., "An experimentally validated damage detection theory in smart structures", *Journal of Sound and vibration*, 191, 859-880, 1996

● Banon, H., and Veneziano, D., "Seismic safety of reinforced members and structures", *Earthquake Engineering and Structural Dynamics*, 10, 179-193, 1982.

● Barai, S. V., and Pandey, P. C., "Vibration signature analysis using artificial neural networks", *Journal of Computing in Civil Engineering*, 9, 259-265, 1995.

● Baruch, M., "Damage detection based on reduced measurements", *Mechanical Systems and Signal Processing*, 12, 23-46, 1998.

● Basseville, M., Benveniste, A., Gach, B., Goursat, M., Bonnecase, D., Dorey, P., Prevosto, M., and Olagnon, M., "In-situ damage monitoring in vibration mechanics: diagnostics and predictive maintenance", *Mechanical Systems and Signal Processing*, 7, 401-423, 1993.

● Birren, J. E., and Morrison, D. F., "Analysis of WAIS subtests in relation to age and education", *Journal of Gerontology*, 16, 363-369, 1961.

● Bishop, C. M., "Neural Networks and their Applications", *Review of Scientific Instrumentation* 65(6): 1803-1832, 1994.

● Bishop, C. M., Neural Networks for Pattern Recognition, *Oxford University Press*, Oxford, 1995.

● Bosse, A., Tasker, F., and Fisher, S., "Real-time modal parameter estimation using subspace methods: applications", *Mechanical System and Signal Processing*, 12, 809-823, 1998.

● Brincker, R., Zhang, L. M., and Andersen, P., "Modal identification from ambient responses using frequency domain decomposition", *Proceedings of the 18th International Modal Analysis Conference*, Texas, U.S.A., 625-630, 2000.

● Brincker, R., Zhang, L. M., and Andersen, P., "Modal identification of output-only systems using frequency domain decomposition", *Smart Material and Structures*, 10, 441-445, 2001.

● Cabanas, L., Benito, B., and Herraiz, M., "An approach to the measurement of the potential

structural damage of earthquake ground motions", *Earthquake Engineering and Structural Dynamics*, 26, 79-92, 1997.

- Carlin, R. A., and Garcia, E., "Parameter optimization of a genetic algorithm for structural damage detection", *Proceedings of the 14th International Modal Analysis Conference*, Michigan, U.S.A., 1292-1298, 1996.

- Casas, J. R., "An experimental stud on the use of dynamic tests for surveillance of concrete structures", *Materials and Structures*, 27, 588-595, 1994.

- Casas, J. R., and Aparicio, A. C., "Structural damage identification from dynamic test data", *Journal of Structural Engineering, ASCE*, 120, 2437-2450, 1994.

- Cattarius, J., and Inman, D. J., "Time domain analysis for damage detection in smart structures", *Mechanical Systems and Signal Processing*, 11, 409-423, 1997.

- Cawley, P. and Adams, R.D., "The Location of Defects in Structures from Measurements of Natural Frequencies", *Journal of Vibration and Acoustics*, 14(2): 49-57, 1979.

- Chaghajerdi, A. H. and Shoureshi, R., "Optimal Sensor Location Using Observability Analysis of Distributed Structures", *Proceedings of the ASME. Dynamic System and Control Division,* Vol. 67, 1999.

- Chang, C.C., Sze, V. and Sun, Z. "Structural damage assessment using principal component analysis", *SPIE's 11th Annual International Symposium on NDE for Health Monitoring and Diagnostics*, San Diego, CA, USA, 2004.

- Chan, T. H. T., Ko, J. M., Ni, Y. Q., Lau, C. K., and Wong, K. Y., "A feasibility study on damage detection of three cable-supported bridges in Hong Kong using vibration measurements", *Proceedings of the International Workshop on Research and Monitoring of Long Span Bridges, Hong Kong*, China, 204-211, 2000.

- Chan, T. H. T., Ni, Y. Q., and Ko, J. M., "Neural network novelty filtering for anomaly detection of Tsing Ma Bridge cables", *Structural Health Monitoring 2000*, F. K. Chang (ed.), Lancaster, Pennsylvania, 430-439, 1999.

- Chan, T. H. T., Wang, J. Y., Ni, Y. Q., and Ko, J. M., "Importance of longitudinal stabilizing

cables in dynamic characteristics of Ting Kau Bridge", *Advances in Structural Dynamics*, J. M. Ko and Y. L. Xu (eds.), Elsevier Science Ltd., Oxford, UK, Vol. Ⅰ, 467-474, 2000.

● Chance, J., Tomlinson, G. R., and Worden, K., "A simplified approach to the numerical and experimental modeling of the dynamics of a cracked beam", *Proceedings of the 12th International Modal Analysis Conference*, Hawaii, U.S.A., 778-785, 1994.

● Chaudhry, Z., and Ganino, A. J., "Damage detection using neural networks-an initial experimental study on debonded beams", *Journal of Intelligent Material Systems and Structures*, 5, 585-589, 1994.

● Chen, H. L., Spyrakos, C. C., and Venkatesh, G., "Evaluating structural deterioration by dynamic response", *Journal of Structural Engineering, ASCE*, 121, 1197-1204, 1995.

● Chen, J. C., and Garba, J. A., "On-orbit damage assessment for large space structures", *American Institute of Aeronautics and Astronautics Journal*, 26, 1119-1126, 1998.

● Chiostrini, S., Foraboschi, P., and Vignoli, A., "Structural analysis and damage evaluation of existing masonry buildings by dynamic experimentation and numerical modeling", *Proceedings of the 10th World Conference on Earthquake Engineering*, Madrid, Spain, 3481-3486, 1992.

● Cobb, R., and Liebst, B., "Structural damage identification using assigned partial eigenstructure", *American Institute of Aeronautics and Astronautics Journal*, 35, 152-158, 1997.

● Crema, B. L., Castellani, A., and Coppotelli, G., "Generalization of non-destructive damage evaluation using modal parameters", *Proceedings of the 13th International Modal Analysis Conference*, Florida, U.S.A., 428-431, 1995.

● Crema, B. L., and Mastroddi, F., "Frequency-domain based approaches for damage detection and localization in aeronautical structures", *Proceedings of the 13th International Modal Analysis Conference*, Florida, U.S.A., 1322-1330, 1995.

● Dang, H. S., Structural Damage Identification and Signal Processing, *A dissertation Submitted to the Tongji University for the Degree of Doctor of Philosophy*, 2002.

- Dang, N. H. and Rao, V.S., "Embedded Systems for the Assessment of Structural Damages", *NDE for Health Monitoring and Diagnostics*, San Diego, CA, USA, 4701-18, 2002.

- Danilo, C., and Fabrizio, V., "Monitoring of structural systems by using frequency data", *Earthquake Engineering and Structural Dynamics*, 28, 447-461, 1999.

- Diamantaras, K. I., and Kung, S. Y., Principal Component Neural Networks: Theory and Application, *A Wiley-Interscience Publication*, 1996.

- Dipasquale, E., and Cakmak, A. S., "Detection of seismic structural damage using parameter-based global damage indices", *Journal of Probabilistic Engineering Mechanics*, 5, 60-65, 1990.

- Doebling, S. W., Farrar, C. R., Prime, M. B., and Shevitz, D. W., "Damage identification and health monitoring of structural and mechanical systems from changes in their vibration characteristics: a literature review", Report No. LA-13070-MS, *Los Alamos National Laboratory*, 1996.

- Doebling, S. W., and Peterson, L. D., "Computing statically complete flexibility from dynamically measured flexibility", *Journal of Sound and Vibration*, 205, 631-645, 1997.

- Dong, C., Zhang, P. Q., Feng, W. Q., and Huang, T. C., "The sensitivity study of the modal parameters of a cracked beam", *Proceedings of the 12th International Modal Analysis Conference*, Hawaii, U.S.A., 98-104, 1994.

- Dos Santos, J. M. C, and Zimmerman, D. C., "Damage detection in complex structures using component mode synthesis and residual modal force vector", *Proceedings of the 14th International Modal Analysis Conference*, Michigan, U.S.A., 1299-1305, 1996.

- Duda, R. O., Hart, P. E. and Stork, D. G., Pattern Classification, 2nd Edition, *John Wiley & Sons,* New York, USA, 2001.

- Dunteman, G. H., Principal Components Analysis, *New Delhi*, London, 1989.

- EI-Borgi, S., Choura, S., Ventura, C.E., Baccouch, M. and Cherif, F., "Modal Identification and Model Updating of a Reinforced Concrete Bridge", *Journal of Smart Structures and Systems*, 1(1), 83-101,   2005.

● Elenas, A., "Correlation between seismic acceleration parameters and overall structural damage indices of buildings", *Journal of Soil Dynamics and Earthquake Engineering*, 20, 93-100, 2000.

● Elenas, A., and Meskouris, K., "Correlation study between seismic acceleration parameters and damage indices of structures", *Engineering Structures*, 23, 698-704, 2001.

● Escobar, J. A., Sosa, J. J., and Gomez, R., "Damage detection in framed buildings", *The Canadian Journal of Civil Engineering*, 28, 35-47, 2001.

● Ewins, D. J., Modal Testing: Theory and Practise, *John Wiley and Sons*, New York, 1995.

● Ewins, D. J., Modal Testing: Theory, Practice and Application, *Research Studies Press*, Baldock, Hertfordshire, UK, 2000.

● Faravelli, L. and Pisano, A.A., "Damage Assessment Toward Performance Control. Structural Damage Assessment Using Advanced Signal Processing Procedures", *Proceedings of DAMAS '97, University of Sheffield*, UK: 185-198, 1997.

● Farrar, C. R., and Cone, K. M., "Vibration testing of the I-40 bridge before and after the introduction of damage", *Proceedings of the 13th International Modal Analysis Conference*, Florida, U.S.A., 203-209, 1995.

● Fasel, T. R., Sohn, H., Park ,G. and Farrar, C. R., "Active sensing using impedance-based ARX models and extreme value statistics for damage detection", *Earthquake Engineering & Structural Dynamics*, 34- 7:763-785, 2005.

● Fuhr, P. L., Huston, D. R., and Ambrose, T. P., "An internet observatory: remote monitoring of instrumented civil structures using the information superhighway", *Journal of Smart Material and Structure*, 4, 1-6, 1995.

● Furuta, H., Shiraishi, N., Umano, M., and Kawakami, K., "Knowledge-based expert system for damage assessment based on fuzzy reasoning", *Computers and Structures*, 40, 137-142, 1991.

● Gambarotta, G., and Lagomarsino, S., "Damage models for the seismic response of brick masonry shear walls. Part Ⅰ: The mortar joint model and its applications", *Earthquake*

Engineering and Structural Dynamics, 26, 423-439, 1997.

- Gambarotta, G., and Lagomarsino, S., "Damage models for the seismic response of brick masonry shear walls. Part Ⅱ: The continuum model and its applications", *Earthquake Engineering and Structural Dynamics*, 26, 441-462, 1997.

- Georgiades, A., Saha, G., Kalamkarov, A., Rokkam, S. and Newhook J., "Embedded Smart GFRP Reinforcements for Monitoring Reinforced Concrete Flexural Components", *Journal of Smart Structures and Systems*, 1(4), 369 – 384, 2005.

- Ghobarah, A., Abouelfath, H., and Ashraf, B., "Response-based damage assessment of structures", *Earthquake Engineering and Structural Dynamics*, 28, 79-104, 1999.

- Gianni, B., Andrea, C., and Vittorio, G., "Monitoring systems on historic buildings: the Brunelleschi dome", *Journal of Structural Engineering, ASCE*, 122, 663-673, 1996.

- Gomez, S. R., Cakmak, A. S., and Shinozuka, M., "Damage analysis of simulated I-880 structures under the Loma Prieta earthquake", *Soil Dynamics and Earthquake Engineering*, 14, 313-319, 1995.

- Gudmundson, P., "Eigenfrequency changes of structures due to cracks, notches, or other geometrical changes", *Journal of the Mechanics and Physics of Solids*, 30, 339-353, 1982.

- Gudmundson, P., "The dynamic behavior of slender structures with cross-sectional cracks", *Journal of the Mechanics and Physics of Solids*, 31, 329-345. 1983.

- Gupta, V. K., Nielsen, S. R. K., and Kirkegaard, P. H., "A preliminary prediction of seismic damage-based degradation in RC structures", *Earthquake Engineering and Structural Dynamics*, 30, 981-993, 2001.

- Hamamoto, T., and Kondo, I., "Damage detection of existing building structures using two-stage system identification", *Journal of Theoretical and Applied Mechanics*, 41, 147-158, 1999.

- Hasselman, T. K., and Anderson, M. C., "Principal components analysis for non-linear model correlation, updating and uncertainty evaluation", *Proceedings of the 16th International Modal Analysis Conference*, Santa Barbara, U.S.A., 644-651, 1998.

- Hasselman, T. K., and Anderson, M. C., "Linking FEA and SEA by principal components analysis", *Proceedings of the 16th International Modal Analysis Conference*, Santa Barbara, U.S.A., 1285-1291, 1998.

- Hassiotis, S., ASCE, M., and Grigoriadis, K. M., "Identification of structural damage", *Journal of Structural Engineering, ASCE*, 122, 1107-1114, 1996.

- Hearn, G., and Testa, R. B., "Modal analysis for damage detection in structures", *Journal of Structural Engineering, ASCE*, 117, 3042-3063, 1991.

- Heylen, W., Lammens, S., and Sas, P., Modal Analysis Theory and Testing, *Department of Mechanical Engineering, Katholieke Universiteit Leuven,* Leuven, Belgium, 1995.

- Hjelmstad, K. D., and Shin, S., "Crack identification in a cantilever beam from modal response", *Journal of Sound and Vibration*, 198, 527-545, 1996.

- Housner, G. W., Bergman, L. A., Caugher T. K., et al., "Structural Control: Past, Present, and Future", *ASCE, Journal of Engineering Mechanics*, 123(9):897-971, 1997.

- Hua, Y., and Sarkar, T. K., "Matrix pencil method for estimating parameters of exponentially damped/undamped sinusoids in noise", *IEEE Transaction on Acoustic, Speech, and Signal Processing*, 38, 814-824, 1990.

- Huang, C. S., and Lin, H. L., "Modal identification of structures from ambient vibration, free vibration, and seismic response data via a subspace approach", *Earthquake Engineering and Structural Dynamics*, 30, 1857-1878, 2001.

- Huang, M., Aaron, R., and Shiffman, C. A., "Maximum entropy method for magnetoencephalography", *IEEE Transaction on Biomedical Engineering*, 44, 97-103, 1997.

- Ismail, F., Ibrahim, A., and Martin, H. R., "Identification of fatigue cracks from vibration testing", *Journal of Sound and Vibration*, 140, 305-317, 1990.

- Jauregui, D. V., and Farrar, C. R., "Comparison of damage identification algorithms on experimental modal data from a bridge", *Proceedings of the 14th International Modal Analysis Conference*, Michigan, U.S.A., 1423-1429, 1996.

- Jolliffe, I. T., Principal Component Analysis, *Springer-Verlag*, New York, 1986.

- Ju, F., "Structural dynamic theory in health monitoring", *Vibration, Shock, damage, and Identification of Mechanical Systems*, ASME, 64, 39-46, 1993.

- Juan, C., Dyke, J. S., and Erik, A. J., "Health monitoring based on component transfer functions", *Advances in Structural Dynamics*, Elsevier Science Ltd., Oxford, UK, Vol.Ⅱ, 997-1004, 2000.

- Juang J. N. et al., "An Eigenystem Realization Algorithm for Modal Parameter Identification and Modal Reduction", *J. of Guidance, Control and Dtnamic*, 8(5): 620-627,1985.

- Juang, J. N, Applied System Identification, *Prentice Hall Press*, New Jersey, 1994.

- Katayama, T., and Picci, G., "Realization of stochastic systems with exogenous inputs and subspace identification methods", *Automatica*, 35, 1635-1652, 1999.

- Kato, M., and Shimada, S., "Vibration of PC bridge during failure process", *Journal of Structural Engineering, ASCE*, 112, 1692-1703, 1986.

- Kay, S. M., Modern Spectral Estimation, *Prentice-Hall Press*, New Jersey, 1987.

- Kay, S. M., and Marple, S. L., "Spectrum analysis-a modern perspective", *IEEE Proceedings*, Vol. 69, 1380-1419, 1981.

- Keven, K. F., and Wang, Y. M., "Energy-based damage assessment on structures during earthquakes", *The Structural Design of Tall Buildings*, 10, 135-153, 2001.

- Khaldoon, B., Jamshid, G., and Stephen, P. S., "Experimental study of identification and control of structures using neural network part 1: identification", *Earthquake Engineering and Structural Dynamics*, 28, 995-1018, 1999.

- Kim, H. M., and Bartkowicz, T. J., "Damage detection and health monitoring of large space structures", *Journal of Sound and Vibration*, 27, 12-17, 1993.

- Kim, J. T., and Norris, S., "Damage detection in offshore jacket structures from limited modal information", *International Journal of Offshore and Polar Engineering*, 5, 58-66, 1995.

- Klaus, G. T., and Norris, S., "Non-destructive damage evaluation of a structure from limited modal parameters", *Earthquake Engineering and Structural Dynamics*, 24, 1427-1436, 1995.

- Klenke, S. E., and Paez, T. L., "Damage identification with probabilistic neural networks", *Proceedings of the 14th International Modal Analysis Conference*, Michigan, U.S.A., 99-104, 1996.

- Ko, J. M., and Ni, Y. Q., "Development of vibration-based damage detection methodology for civil engineering structures", *Proceedings of the First International Conference on Structural Engineering*, Kunming, China, 37-56, 1999.

- Ko, J. M., Ni, Y. Q., and Chan, T. H. T., "Dynamic monitoring of structural health in cable-supported bridges", *Smart Structures and Materials: Smart Systems for Bridges, Structures, and Highways*, SPIE Vol. 3671, 161-172, 1999.

- Ko, J. M., Ni, Y. Q., and Chan, T. H. T.，"Feasibility of damage detection of Tsing Ma Bridge using vibration measurements"，*Nondestructive Evaluation of Highways, Utilities, and Pipelines Ⅳ*, , SPIE Vol. 3995, 370-381, 2000.

- Ko, J. M., Ni, Y. Q., and Wang, J. Y., "Tsing Ma Suspension Bridge: ambient vibration survey campaigns", *Proceedings of the International Conference on Advanced Problems in Vibration Theory and Applications*, Xi'an, China, 285-291, 2000.

- Ko, J. M., Ni, Y. Q., Wang, J. Y., Sun, Z. G., and Zhou, X. T., "Studies of vibration-based damage detection of three cable-supported bridges in Hong Kong", *Proceedings of the International Conference on Engineering and Technological Sciences2000 - Session 5: Civil Engineering in the 21st Century*,   Beijing, China, 105-112, 2000.

- Ko, J. M., Ni, Y. Q., Zhou, X. T., and Wang, J. Y., "Structural damage alarming in Ting Kau Bridge using auto-associative neural networks"，*Advances in Structural Dynamics*, Vol. Ⅱ, 1021-1028, 2000.

- Ko, J. M., Sun, Z. G., and Ni, Y. Q., "Modal analysis of cable-stayed Kap Shui Mun Bridge taking cable local vibration into consideration"，*Advances in Structural Dynamics*, Vol. Ⅰ, 529-536, 2000.

- Ko, J. M., Sun, Z. G., and Ni, Y. Q., "A three-stage scheme for damage detection of Kap

Shui Mun cable-stayed bridge", *Proceedings of the International Conference on Structural Engineering, Mechanics and Computation*, Cape Town, South Africa, 2001.

- Ko, J. M., Wong, C. W., and Lam, H. F., "Damage detection in steel framed structures by vibration measurement approach", *Proceedings of the 12th International Modal Analysis Conference*, Hawaii, U.S.A., 280-286, 1994.

- Koh, C. G., See, L. M., and Balendra, T., "Damage detection of buildings: numerical and experimental studies", *Journal of Structural Engineering, ASCE*, 121, 1155-1160, 1995.

- Kondo, I., and Hamamoto, T., "Local damage detection of flexible offshore platforms using ambient vibration measurement", *Proceedings of the Fourth International Offshore and Polar Engineering Conference*, Osaka, Japan, 400-407, 1994.

- Kong, F, Liang, Z., and Lee, G. C., "Bridge damage identification through ambient vibration signature", *Proceedings of the 14th International Modal Analysis Conference*, Michigan, U.S.A., 717-724, 1996.

- Koy, H. U., Nielsen, S. R. K., and Kirkegaard, P. H., "Prediction of global and localized damage and future reliability for RC structures subject to earthquakes", *Earthquake Engineering and Structural Dynamics*, 26, 463-475, 1997.

- Krawczuk, M., and Ostachowicz, W. M., "Parametric vibrations of a beam with crack", *Archive of Applied Mechanics*, 62, 463-473, 1992.

- Krawczuk, M., Qin, X. and Barrish, R. A., "Detection of Delaminations in Cantilevered Beams Using Soft Computing Methods", *European COST F3 Conference on System Identification and Structural Health Monitoring*, Madrid, Spain: 243-252, 2000.

- Krishnan Nair K., Kiremidjian A. S., Law K. H.. Time series-based damage detection and localization algorithm with application to the ASCE benchmark structure. Journal of Sound and Vibration 291 (2006) 349–368.

- Lin, J. W., Betti, R., Smyth, A. W. and Longman, R. W., "On-line identification of non-linear hysteretic structural systems using a variable trace approach", *Earthquake Engineering and Structural Dynamics* 30: 1279-1303, 2001.

● Lee I.W., Kim D.O. and Jung, G.H., "Natural Frequency and Mode Shape Sensitivities of Damped Systems: Part I, Distince Natural Frequencies", *Journal of Sound and Vibration*, 223(3): 399-412, 1999.

● Lee I.W., Kim D.O. and Jung, G.H., "Natural Frequency and Mode Shape Sensitivities of Damped Systems: Part II, Multiple Natural Frequencies, *Journal of Sound and Vibration*, 223(3): 413-424, 1999.

● Liu, S.C., Tomizuka, M. and Ulsoy, A.G., "Challenges and Opportunities in the Engineering of Intelligent Systems," *Journal of Smart Structures and Systems*, 1(1), 1-12. 2005.

● Lus, H., Betti, R., and Longman, R.W., "Identification of Linear Structural Systems Using Earthquake Induced Vibration Data", *Earthquake Engineering and Structural Dynamics*, 28, 1449-1467, 1999.

● Ma, J. and Pines, D. J., "Damage detection in a framed building structure", *Proceedings of SPIE-the International Society for Optical Engineering*, 305-315, 1999.

● Maeck, J., Peeters, B., and De Roeck, G., "Damage identification on the Z24 Bridge using vibration monitoring", *Smart Materials and Structures*, 10, 512-517,,2001.

● Maia, N. M. M., Silva, J. M. M., He, J., Lieven, N. A. J., Lin, R. M., Skingle, G. W., To, W. M., and Urgueira, A. P. V., Theoretical and Experimental Modal Analysis, *Research Studies Press*, Taunton, Somerset, UK, 1997.

● Marple, S. L., "Spectral line analysis via a fast Prony algorithm", *Proceedings of the IEEE International Conference on Acoustics, Speech, and Signal Processing*, Paris, France, 1375-1378, 1982.

● Marple, S. L., Digital Spectral Analysis with Applications, *Prentice-Hall Press*, New Jersey, 1987.

● Marwala, T., and Hunt, H. E. M., "Fault identification using finite element models and neural networks", *Mechanical Systems and Signal Processing*, 13, 475-490, 1999.

● Masri, S. F., Bekey, G. A., and Sassi, H., "Non-parametric identification of a class of non-linear multi-degree dynamic systems", *Earthquake Engineering and Structural*

Dynamics, 10, 1-30, 1982.

● Masri, S.F., Chassiakos, A.G. and Caughey, T.K., "Identification of Nonlinear Dynamic System Using Neural Networks", *Journal of Applied Mechanics, Trans., ASME*, 60:123-133, 1993

● Mayes, R. L., "An experimental algorithm for detecting damage applied to the I-40 Bridge over the Rio Gande", *Proceedings of the 13th International Modal Analysis Conference*, Florida, U.S.A., 219-225, 1995.

● Mioduchowski, A., "Shear waves in buildings with discontinuous distribution of micro-cracks", *Proceedings of the 11th International Modal Analysis Conference*, Florida, U.S.A., 108-114, 1993.

● Miranda, E., and Bertero, V. V., "Seismic performance of an instrumented ten-storey reinforced concrete building", *Earthquake Engineering and Structural Dynamics*, 25, 1041-1059, 1996.

● Mita, A., Structural Dynamics for Health Monitoring, *SANKEISHA Co.,Ltd.,* Nagoya, Japan, 2003.

● Mita, A. and Hagiwara, H., "Damage Diagnosis of a Building Structure Using Support Vector Machine and Modal Frequency Patterns", *Smart Structures and Materials 2003: Smart Systems and NDE for Civil Infrastructures*, Vol.5057:118-125, 2003.

● Mitsuru, N., Sami, F. M., and Chassiakos, A. G., "A neural network approach to damage detection in a building from ambient vibration measurements", *Proceedings of SPIE-the International Society for Optical Engineering*, 3321, 1025-1032, 1998.

● Mitsuru, N., Sami, F. M., Chassiakos, A. G., and Caughey, T. K., "A neural network approach to damage detection in a building from ambient vibration measurements", *Proceedings of SPIE Far East and Pacific Rim Symposium on Smart Material, Structure and MEMS*, Bangalore, India, 126-137, 1996.

● Morassi, A., and Rovere, N., "Localizing a notch in a steel frame from frequency measurements", *Journal of Engineering Mechanics*, ASCE, 123, 422-432, 1997.

- Naidu, P. S., Modern Spectrum Analysis of Time Series, *CRC Press*, Florida, 1995.

- Narayana, K. L., and Jebaraj, C., "Sensitivity analysis of local/global modal parameters for identification of a crack in a beam", *Journal of Sound and Vibration*, 228, 977-994, 1999.

- Narkis, Y., "Identification of crack location in vibrating simply supported beams", *Journal of Sound and Vibration,* 172, 49-558, 1994.

- Ni, Y.Q., Ko, J.M., Hua, X.G. andZhou, H.F., "Variability of measured modak frequencies of a cable-stayed bridge under different wind conditions", *Journal of Smart Structures and Systems*, 3(3), 341-356, 2007.

- Ni, Y. Q., Ko, J. M., and Wong, C. W., "Identification of dynamic properties of large structures by ambient vibration measurements", *Proceedings of the International Symposium on Structures and Foundations in Civil Engineering*, Hangzhou, China, 193-198, 1994.

- Ni, Y. Q., Wang, B. S., and Ko, J. M., "Selection of input vectors to neural networks for structural damage identification", *Smart Structures and Materials: Smart Systems for Bridges, Structures, and Highways*, SPIE Vol. 3671, 270-280, 1999.

- Ni, Y. Q., Wang, B. S., and Ko, J. M., "Simulation studies of damage location in Tsing Ma Bridge deck", *Nondestructive Evaluation of Highways, Utilities, and Pipelines Ⅳ*, SPIE Vol. 3995, 312-323, 2000.

- Ni, Y. Q., Wang, J. Y., and Ko, J. M., "Modal interaction in cable-stayed Ting Kau Bridge", *Advances in Structural Dynamics*, Vol. Ⅰ, 537-544, 2000.

- Nokes, J. P., and Cloud, G. L., "The application of interferometric techniques to the nondestructive inspection of fiber-reinforced materials", *Experimental Mechanics*, 33, 314-319, 1993.

- Norris, M. A., and Meirovitch, L., "On the problem of modeling for parameter identification in distributed structures", *International Journal for Numerical Methods in Engineering*, 28, 2451-2463, 1989.

- Nuno, M. M., and Julio M. M. S., Theoretical and Experimental Modal Analysis, *John Wiley and Sons*, New York, 1997.

- Nwosu, D. I., Swamidas, A. S. J., Guigne, J. Y., and Olowokere, D. O., "Studies on influence of cracks on the dynamic response of tubular T-Joints for nondestructive evaluation", *Proceedings of the 13th International Modal Analysis Conference*, Florida, U.S.A., 1122-1128, 1995.

- Pajunen, P. and Karhunen, J., "A maximum likelihood approach to nonlinear blind source separation", *In Proceedings of the 1997 Int. Conf. on Artificial Neural Networks (ICANN'97)*: 541–546, Lausanne, Switzerland, 1997.

- Pandey, A. K., and Biswas, M., "Damage detection in structures using changes in flexibility", *Journal of Sound and Vibration*, 169, 3-17, 1994.

- Pandey, A. K., Biswas, M., and Samman, M. M., "Damage detection from changes in curvature mode shapes", *Journal of Sound and Vibration,* 145, 321-332, 1991.

- Paolozzi, A., and Peroni, I., "Detection of debonding damage in a composite plate through natural frequency variations", *Journal of Reinforced Plastics and Composites,* 9, 369-389, 1990.

- Peeters, B., and Roeck, G. D., "Reference-based stochastic subspace identification for output-only modal analysis", *Mechanical Systems and Signal Processing,* 13, 855-878, 1999.

- Peeters, B., and Roeck, G. D., "Stochastic system identification for operational modal analysis: a review", *Journal of Dynamic Systems, Measurement, and Control*, 123, 659-667, 2001.

- Pines, D. J., and Lovell, P. A., "Conceptual framework of a remote wireless health monitoring system for large civil structures", *Journal of Smart Materials and Structures*, 7, 627-636, 1998.

- Powell, G. H., and Allahabadi, R., "Seismic damage prediction by deterministic methods: concepts and procedures", *Earthquake Engineering and Structural Dynamics*, 16, 719-734, 1998.

- Prabhu, K. M. M., and Bagan, K. B., "Resolution capability of nonlinear spectral estimation methods for short data lengths", *IEEE Proceedings,* Part F, Vol. 136, 135-142, 1989.

- Prion, H. G. L., Ventura, C. E., and Rezai, M., "Damage detection of steel frame by modal testing", *Proceedings of the 14th International Modal Analysis Conference*, Michigan, U.S.A., 1430-1436, 1996.

- Qian, Y. and Mita, A., "Structural damage identification using Parzen-window approach and neural networks", *Structural Control and Health Monitoring,* 14: 576-590, 2007

- Qian, Y. and Mita, A., "Time Series-Based Damage Evaluation Algorithm with Application to Building Structures", *Proceedings of the 1st Asia-Pacific Workshop on Structural Health Monitoring,* Keio Univ., Yokohama, Japan, 2006.

- Qian, S., and Chen, D., Joint Time-frequency Analysis: Methods and Applications, *Prentice-Hall Press*, New Jersey, 1996.

- Qin, Q., Li, H. B., and Qian, L. Z., "Modal identification of Tsing Ma Bridge by using improved eigensystem realization algorithm", *Journal of Sound and Vibration*, 247, 325-341, 2001.

- Rahman, M. A., and Yu, K. B., "Improved frequency estimation using total least squares approach", *Proceedings of the IEEE International Conference on Acoustics, Speech, and Signal Processing*, Tokyo, Japan, 1397-1400, 1986.

- Richardson, M. H., and Mannan, M. A., "Remote detection and location of structural faults using modal parameters", *Proceedings of the 10th International Modal Analysis Conference*, Florida, U.S.A., 502-507, 1992.

- Ricles, J. M., and Kosmatka, J. B., "Damage detection in elastic structures using vibratory residual forces and weighted sensitivity", *American Institute of Aeronautics and Astronautics Journal*, 30, 2310-2316, 1992.

- Rizos, P. F., Aspragathos, N., and Dimarogonas, A. D., "Identification of crack location and magnitude in a cantilever beam from the vibration modes", *Journal of Sound and Vibration*, 138, 381-388, 1990.

- Ruotolo, R., and Surace, C., "Damage assessment of multiple cracked beams: numerical results and experimental validation", *Journal of Sound and Vibration*, 206, 567-588, 1997.

- Salane, H. J., Baldwin, J. W., and Duffield, R. C., "Dynamic approach for monitoring bridge deterioration", *Transportation Research Record,* 832, 21-28, 1981.

- Salawu, O. S., "Bridge assessment using forced-vibration testing", *Journal of Structural Engineering, ASCE,* 121, 161-173, 1995.

- Samman, M. M, and Biswas, M., "Vibration testing for nondestructive evaluation of bridges", *Journal of Structural Engineering, ASCE*, 120, 290-306, 1994.

- Sampaio, R. P. C., Maia, N. M. M., and Silva, J. M. M., "Damage detection using the frequency-response-function curvature method", *Journal of Sound and Vibration*, 226, 1029-1042, 1999.

- Shama, A. A., Zarghamee, M. S., Ojdrovic, R. P., and Schafer, B. W., "Seismic damage evaluation of a steel building using stress triaxiality", *Engineering Structures,* 25, 271-279, 2003.

- Shen, M. H. H., and Chu, Y. C., "Vibration of beams with a fatigue crack", *Computers and Structures*, 45, 79-93, 1992.

- Shifrin, E. I., and Ruotolo, R., "Natural frequencies of a beam with an arbitrary number of cracks", *Journal of Sound and Vibration*, 222, 409-423, 1999.

- Shiga, T., Shibata, A., and Takahashi, T., "Earthquake damage and wall index of reinforced concrete buildings", *Proceedings of Tohoku District Symposium*, Architectural Institute of Japan, 29-32, 1968.

- Shih, C. Y., Tsuei, Y. G., Allemang, R. J., and Brown, D. L., "Complex mode indication function and its applications to spatial domain parameter estimation", *Proceedings of the 7th International Modal Analysis Conference,* Nevada, U.S.A., 1078-1086, 1989.

- Silva, J. M. M., and Gomes, A. J. M. A., "Experimental dynamic analysis of cracked free-free beams", *Experimental Mechanics*, 30, 20-25, 1990.

- Skjaerbaek, P. S., Nielsen, S. R. K., and Cakmak, A. S., "Assessment of damage in seismically excited RC-structures from a single measured response", *Proceedings of the 14th International Modal Analysis Conference*, Michigan, U.S.A., 133-139, 1996.

- Skjaerbaek, P. S., Nielsen, S. P. K., and Cakmak, A. S., "Damage localization of severely damaged RC-structures based on measured eigenperiods from a single response", *Proceedings of the 4th International Conference on Computer Aided Assessment and Control*, Southampton, UK, 815-822, 1996.

- Skjarbak, P. S., Nielsen, S. P. K., and Cakmak, A. S., "Assessment of damage in seismically excited RC-structures from a single measured response", *Proceedings of the 14th International Modal Analysis Conference,* Michigan, U.S.A., 133-139, 1996.

- Skjaerbaek, P. S., Nielsen, S. R. K., Kirkegaard, P. H., and Cakmak, A. S., "Damage localization and quantification of earthquake excited RC-frames", *Earthquake Engineering and Structural Dynamics*, 27, 903-916, 1998.

- Sohn, H., and Law, K. H., "A Bayesian probabilistic approach for structure damage detection", *Earthquake Engineering and Structural Dynamics*, 26, 1259-1281, 1997.

- Sophia H., and Garrett, D. J., "Identification of stiffness reduction using natural frequencies", *Journal of Engineering Mechanics, ASCE*, 121, 1106-1113, 1995.

- Spillman, W., Huston, D., Fuhr, P., and Lord, J., "Neural network damage detection in a bridge element", *SPIE Smart Sensing, Processing, and Instrumentation,* 1918, 288-295, 1993.

- Spyrakos, C., Chen, H. L., Stephens, J., and Govidaraj, V., "Evaluating structural deterioration using dynamic response characterization", *Proceedings of Intelligent Structures,* Elsevier Applied Science, 137-154, 1990.

- Stefano, A. D. E., Sabia, D., and Sabia, L., "Probabilistic neural networks for seismic damage mechanisms prediction", *Earthquake Engineering and Structural Dynamics*, 28, 807-821, 1999.

- Stephens, J. E., and Yao, J. T. P., "Damage assessment using response measurements", *Journal of Structural Engineering, ASCE,* 113, 787-801, 1987.

- Stephens, J. E., "A damage function using structural response measurements", *Structure Safety Journal,* 5, 22-39, 1985.

● Straser, E. G., and Kiremidjian, A. S., "Monitoring and evaluating civil structures using measured vibration", *Proceedings of the 14th International Modal Analysis Conference*, Michigan, U.S.A., 84-90, 1996.

● Stubbs, N., and Garcia, G., "Application of pattern recognition to damage localization", *Microcomputers in Civil Engineering*, 11, 395-409, 1996.

● Subrahmonia, A. R., Bhave, S. S., and Khan, M. N., "Condition monitoring of some industrial floors through vibration studies", *Proceedings of Fatigue and Fracture in Steel and Concrete Structures, Madras*, India, 1111-1121, 1991.

● Suh, M. W., Shim, M. B., and Kim, M. Y., "Crack identification using hybrid neuro-genetic technique", *Journal of Sound and Vibration,* 238, 617-635, 2000.

● Swamidas, A. S. J., and Chen, Y., "Monitoring crack growth through change of modal parameters", *Journal of Sound and Vibration*, 186, 325-343, 1995.

● Takuji, H., "Experimental verification for damage detection strategies of multistory buildings based on vibration monitoring", *Proceedings of SPIE*, Vol. 5057, 106-117, 2003.

● Tamura, Y., and Suganuma, S. Y., "Evaluation of amplitude-dependent damping and natural frequency of buildings during strong winds", *Journal of Wind Engineering and Industrial Aerodynamics*, 59, 115-130, 1996.

● Tasker, F., Bosse, A., and Fisher, S., "Real-time modal parameter estimation using subspace methods: theory", *Mechanical System and Signal Processing*, 12, 797-808, 1998.

● Topole, K. G., and Stubbs, N., "Non-destructive damage evaluation of a structure from limited modal parameters", *Earthquake Engineering and Structural Dynamics*, 24, 1427-1436, 1995.

● Vanik, M.W., Beck, J.L. and Au S.K., "Bayesian Probabilistic Approach to Structural Health Monitoring", *Journal of Engineering Mechanics* 126(7): 738-745, 2000.

● Wu, X., Ghaboussi, J., and Garrett, J. H., "Use of neural network in detection of structural damage", *Computers and Structures,* 42, 649-659, 1992.

● Xia, Y., and Hao, H., "Measurement selection for vibration-based structural damage

identification", *Journal of Sound and Vibration*, 236, 89-104, 2000.

- Xu, B., Wu, Z.S. and Yokoyama, K., "Response Time Series Based Structural Parametric Assessment Approach with Neural Networks", *Proceedings of the First International Conference on Structural Health Monitoring and Intelligent Infrastructure*, Tokyo, Japan, Vol.1: 601-609, 2003.

- Xu, B. and Chen, G., "Acceleration-Based Identification of Structural Parameters with Neural Networks", *Proceedings of the 5th International Workshop on Structural Health Monitoring*, Stanford Univ., Stanford, CA: 1073-1080, 2005.

- Zhang, D.W. and Li, Y.M., "A general method of element----equation arrangement", *Structure & Environment Engineering,* 6: 9-15, 1989.

AUTHOR'S BIOGRAPHY

Yuyin Qian was born in Shanghai, China in 1977. She obtained a B.S. and M.S. in Engineering Mechanics from Tongji University in 2000 and 2003. Qian then came to Japan to pursue her graduate study. She received a second M.S. in System Design Engineering in 2005 from Keio University, and is expected to receive her Ph.D. in System Design Engineering from Keio University in 2008.

LIST OF PUBLICATIONS

Journal Papers:

1. Qian, Y., Mita, A. "Structural damage identification using Parzen window approach and neural networks", *Structural Control and Health Monitoring*, Vo. 14, Issue 4, 576-590, (2007.6).

2. Xue, S., Mita A., Qian, Y., Xie, L., Zheng, H. "Application of a Grey Control System Model to Structural Damage Identification", *Smart Materials & Structures,* Vol. 14, No. 3, 125-129, (2005.6).

3. Qian, Y., Mita, A. "Acceleration-based damage indicators for building structures using neural network emulators", *Structural Control and Health Monitoring*, (accepted, published on-line).

4. Qian, Y., Mita, A. "Acceleration-based damage identification techniques under restricted number of sensors for building structures", *Smart Structures and Systems*, (in review).

Conference Papers:

1. Qian, Y., Mita, A. "Acceleration-Based Damage Evaluation of Building Structures with Neural Networks and Particle Swarm Optimization", *Proceedings of The 3rd International Conference on Structural Health Monitoring of Intelligent Infrastructure*, Vancouver, Canada (2007.11).

2. <u>Qian, Y.</u>, Mita, A. "Two-Phase Damage Evaluation Approach for Buildings under Earthquakes", *Summaries of Technical Papers of Annual Meeting of Architectural Institute of Japan*, Fukuoka, Japan (2007.8).

3. <u>Qian, Y.</u>, Mita, A. " Condition assessment of buildings using acceleration data for life cycle predictions", *Proceedings of World Forum on Smart Material & Smart Structures Technology*, Chongqing & Nangjing, China, (2007.5).

4. <u>Qian, Y.</u>, Mita, A. "Time Series-Based Damage Evaluation Algorithm with Application to Building Structures", *Proceedings of Asia-Pacific Workshop on SHM*, Yokohama, Japan, (2006.12).

5. <u>Qian, Y.</u>, Mita, A. "Acceleration-based Evaluation of Building Structures with Neural Networks," *Summaries of Technical Papers of Annual Meeting of Architectural Institute of Japan*, Yokohama, Japan (2006.8).

6. <u>Qian, Y.</u>, Mita, A., Clayton, E. H., Dyke, S. J. "Experimental Study on Localization and Quantification of Structural Damage Using ZigBee Motes", *Proceedings of Third European Workshop Structural Health Monitoring*, 5-7 July 2006, Granada, Spain, 405-412, (2006.7).

7. Clayton, E. H., <u>Qian, Y.</u>, Orjih, O., Dyke, S. J., Mita, A., Lu, C. "Off-the-Shelf Modal Analysis: Structural Health Monitoring with Motes Monitoring", *Proceedings of the 24th International Modal Analysis Conference (IMAC XXIV).* , Saint Louis, MO, USA, (2006.2).

8. Mita, A., <u>Qian, Y.</u> "Qualitative and Quantitative Damage Detection Algorithm for Structures Using Pattern Classification and Sensitivity Analysis", *Proceedings of the Second International Conference on SHM of Intelligent Infrastructure*, 16-18 November 2005, Shenzhen, China, 201-206 (invited paper), (2005.11).

9. <u>Qian, Y.</u>, Mita, A. "Damage Identification of Structures Based on Pattern Classification using Limited Number of Sensors", *Proceedings of the 5th International*

Workshop on Structural Health Monitoring, Stanford University, CA, USA, 1033-1040, (2005.09).

10. <u>Qian, Y.</u>, Mita, A. "Data Selection, Condensation and Recognition Processes for Damage Identification of Structures Using Limited Number of Sensors", *Summaries of Technical Papers of Annual Meeting of Architectural Institute of Japan*, Osaka, Japan (2005.8)

11. <u>Qian, Y.</u>, Mita, A., Suzuki, T. "Risk-Based Design and Maintenance of Civil and Building Structures", *Proceedings of Third International Conference on Earthquake Engineering, New Frontiers and Research Transformation*, Nanjing, China, 330-333, (2004.10).

12. <u>Qian, Y.</u>, Xue, S., Zheng, H., Xie, L., Mita A. "Application of Grey Relational Analysis to Structural Damage Identification", *Proceedings of First International Conference on Structural Health Monitoring and Intelligent Infrastructure*, Tokyo, Japan, 641-644, (2003.11).

13. Zheng, H., Xue, S., <u>Qian, Y.</u>, Xie, L., Mita A. "Structural Damage Identification by Neural Networks and Modal Analysis," *Proceedings of First International Conference on Structural Health Monitoring and Intelligent Infrastructure*, Tokyo, Japan, 635-639, (2003.11).